Removal of H_2S and SO_2 by $CaCO_3$-Based Sorbents at High Pressures

Final Report

August 1995–July 2000

Prepared by:

Prof. Stratis V. Sotirchos

September 2000

Work Performed under Grant No.: DE-FG22-95PC95217

Performed for:

U.S. Dept. of Energy
University Coal Research Program
Pittsburgh Energy Technology Center
Pittsburgh, Pennsylvania

Performed at:

University of Rochester
Dept. of Chemical Engineering
Rochester, NY 14627

EXECUTIVE SUMMARY

The mechanism of the removal of SO_2 and H_2S by $CaCO_3$-based sorbents in pressurized fluidized-bed coal combustors (PFBC) and high pressure gasifiers was investigated in this project. Reactivity evolution experiments were carried out in thermogravimetric apparatuses both under simulated high pressure conditions and at high pressures. Experiments at high pressure were conducted in a high pressure thermogravimetric arrangement that was set up and developed under this project. Two calcitic solids of high calcium carbonate content (over 97%) were employed in the experiments: a fine-grained distributed by Greer Limestone Co. (Greer Limestone) and a solid supplied in the form of large calcitic crystals (Iceland Spar). The decision to work with these solids was mainly based on the fact that they have been employed in several past studies of sulfation, sulfidation, and calcination in our laboratory, and therefore, a large volume of data on their performance under different conditions was available for comparison purposes. In addition to the experimental studies, work was also done on the development of rigorous mathematical models for the description of the occurrence of simultaneous processes (e.g., calcination and sulfation and carbonation and sulfation) in the interior of porous solids and for the simulation of the evolution of the pore structure of porous solids that undergo chemical transformation in their interior.

A number of processes were investigated in our experiments in addition to the reaction of $CaCO_3$ solids with SO_2 or H_2S under high pressure (noncalcining) conditions. Specifically, we investigated: i) the simultaneous occurrence of the calcination and sulfation (reaction with SO_2) of limestones, ii) the simultaneous occurrence of the calcination and sulfidation (reaction with H_2S) of limestones, iii) the simultaneous occurrence of the carbonation and sulfation of calcined limestones, and iv) the sulfidation of limestones in the presence of small amounts of oxygen.

Our high pressure experiments on the sulfation and sulfidation of limestones under noncalcining conditions revealed that the effects of pressure on the behavior of these processes are mainly manifested through its effects on the concentration of the sulfuration species (SO_2 or H_2S).

Experiments at different pressures but corresponding to the same concentration of SO_2 or H_2S gave weight vs. time curves that showed very small differences from each other. This was construed as an indication that the pressure of reaction did not affect the structure of the product layer formed around the shrinking core of the unreacted material and that transport in that layer took place in a mode that was not influenced by the total pressure. Some experiments were also carried out on the effects of pressure on the reaction of calcined $CaCO_3$ with SO_2 or H_2S, and conclusions similar to those reached for the indirect reactions were derived.

The experiments on the simultaneous occurrence of the calcination and sulfuration (sulfidation or sulfation) reactions – this is what is actually taking place in a combustor or gasifier operating under calcining conditions when calcium carbonate particles are injected in it – showed that the behavior of the simultaneous calcination and sulfuration process can be markedly different from that inferred from the results of sequential calcination and sulfuration experiments. Simultaneous occurrence of calcination and sulfation has adverse effects on the effective capacity of limestone for SO_2 removal, which intensify as the particle size increases or the rate of calcination decreases. In general, the differences between the weight vs. time curve measured in the simultaneous process and that constructed on the basis of the results of the independent (sequential) experiments become larger as the rates of the processes become comparable, that is, as the rate of calcination is decreased. Similar observations were made in the study of the sulfidation and calcination processes. However, since in that case, the difference between the volume of the solid product and the volume of solid reactant is not large enough to cause complete pore closure before complete conversion of CaO to CaS is reached, the simultaneous occurrence of sulfidation and calcination does not affect the conversion level reached at very large times. Interesting conclusions were also reached from the study of the simultaneous occurrence of the carbonation and sulfation reactions, a situation that may be encountered as calcined particles move into areas of a combustor where the concentration of CO_2 is above the equilibrium value. It was found that the interference of the carbonation reaction with the sulfation reaction can lower the effective capacity of a $CaCO_3$ sorbent for SO_2 removal.

The incentive for carrying out sulfidation experiments in the presence of oxygen was provided by the observation that some sulfidation experiments that were conducted as oxygen was accidentally leaking into the feed mixture of the reactor showed completely different behavior from that obtained in the absence of oxygen. Sulfidation experiments were carried out following calcination or simultaneously with that process, and the concentration of oxygen that was introduced in the H_2S-containing stream that was fed to the reactor ranged from 0.2 to 2.5%. The obtained results showed that the behavior of the sulfidation of limestone depended strongly, in both a qualitative and a quantitative sense, on the level of the oxygen concentration in the feed. For small oxygen concentrations, the weight gained by the calcined sample during sulfidation in a N_2-H_2S atmosphere went through a maximum, whereas for oxygen concentrations above 0.5-0.6%, it increased continuously. A constant weight value was reached at large reaction times in both cases. The value of the weight gain at the maximum increased with increasing concentration of oxygen in the feed, and the same behavior was manifested by the constant value reached at large times. When a maximum was present in the weight gain vs. time curve, the constant value was lower than that expected for complete sulfidation of the solid. On the other hand, for oxygen concentration around 2-3%, the particles reached weight gains that corresponded to complete conversion of CaO to $CaSO_4$ even though the maximum allowable conversion for complete pore plugging by $CaSO_4$ is about 50%. A maximum in the variation of the weight of the sample during sulfidation in the presence of oxygen was observed only for small particle sizes, small samples, and temperatures above 750 ^oC, and in some cases, the reduction in the weight corresponded to complete disappearance of the solid from the pan. This led us to conclude that the CaS-$CaSO_4$ solid-solid reaction, the most probable cause of the reduction of the weight of the sample, must be proceeding through the formation of a volatile intermediate. This very interesting phenomenon should be investigated further.

A mathematical model for simultaneous decomposition and solid product formation reactions was developed for the most general case where the particles are nonisothermal, the interaction of the mass transport fluxes of the components of the gaseous mixture is important, and the rate of the decomposition reaction can be limited by its intrinsic kinetics or the transport of its

gaseous products away the reaction interface. Thus, the model can be applied to the study of and gas-solid reaction with solid product formation that accompanies a decomposition reaction. Since the process of sulfur gases removal by CaO involves formation of a solid product that occupies more space than the solid reactant it replaces, a stochastic simulation scheme was formulated for studying inaccessible pore volume formation in pore structures represented as assemblages of solid grains. It combines a gradual increase of the size of the grain that represent the porous structure with a random walk scheme, the latter used to determine whether a randomly chosen point in the unit cell of the two-phase structure lies in the particle phase or in the connected or in the isolated part of the matrix phase. The use of the algorithm was demonstrated by performing computations on structures of freely overlapping, unidirectional cylinders, and results were obtained both for the volume fractions and the specific surface areas of the accessible and inaccessible parts of the pore phase.

TABLE OF CONTENTS

LIST OF FIGURES

1. BACKGROUND INFORMATION

In a fluidized-bed combustor, a bed of combustible (coal) and noncombustible material is fluidized using air blown upward. Using dolomite or limestone as the noncombustible material, it is possible to have fuel combustion and flue gas desulfurization taking place simultaneously in the combustion vessel. If operation occurs under atmospheric pressure, the average partial pressure of carbon dioxide in the combustor (typically, 10-15% of the total pressure) is considerably lower than the equilibrium CO_2 pressure for decomposition of limestone ($CaCO_3$) or dolomite ($CaCO_3MgCO_3$) at the temperatures usually encountered in FBC units (800-950 ^oC). In the high temperature environment of the AFBC unit, the limestone or dolomite particles undergo calcination, yielding a highly porous product (CaO or MgO), which reacts with the sulfur dioxide produced during coal combustion forming, mainly, calcium or magnesium sulfate. The sulfates occupy more space than the oxides they replace, and as a result, the pores of the calcine are completely plugged with solid product before complete conversion takes place. (The conversion for complete pore plugging is about 50% for the calcine of a stone consisting of $CaCO_3$ only.) Pores of different size are plugged at different conversion levels, and it is thus possible to have formation of inaccessible pore space in the interior of the particles when the small feeder pores of clusters of large pore are filled with solid product (Zarkanitis and Sotirchos, 1989). Moreover, under conditions of strong internal diffusional limitations, complete pore closure may first take place at the external surface of the particles while there is still open pore space left in the interior. For these reasons, ultimate conversions much lower than those predicted by the stoichiometry of the reaction for complete plugging of the internal pore space (less than 30-40%) are seen in AFBC units.

The reaction of calcined limestones (primarily) and dolomites with SO_2 has been the subject of extensive investigation. In accordance with the above remarks, the experimental evidence in most of the studies of the literature indicates strong effects of the pore size distribution on the overall reactivity of the calcined solids (Borgwardt and Harvey, 1972; Wen and Ishida, 1973; Hartman and Coughlin, 1974, 1976; Ulerich et al., 1977; Vogel et al., 1977; Hasler et al., 1984; Simons and Garman, 1986; Yu, 1987; Gullett and Bruce, 1987; Zarkanitis and

Sotirchos, 1989; Zarkanitis, 1991). Unfortunately, the immense volume of information that has been accumulated over the years on the reaction of calcined limestones and dolomites with SO_2 is not applicable to SO_2 emissions control by limestones and dolomites under PFBC conditions. PFBC units normally operate under a pressure of 16 atmospheres, and for an average CO_2 content of 15%, this implies that the partial pressure of CO_2 in the reactor is 2.4 atm. Thermodynamic calculations show that the temperature for $CaCO_3$ calcination in the presence of 2.4 atm of CO_2 must be larger than 980 ^oC, that is, well above the temperature range (750-950 ^oC) encountered in a PFBC unit. Nevertheless, even though formation of a highly porous material with a high specific surface area cannot take place under PFBC conditions, favorable desulfurization is known to occur in PFBC units (Bulewicz and Kandefer, 1986; Murthy et al., 1979). For dolomites, the situation is somewhat different since half-calcination (formation of an MgO-$CaCO_3$ product) is possible under 2.4 atm of CO_2. Even in this case, however, if the absorption of SO_2 occurred only in the pore space of the half-calcined solid, the utilization of the calcium content of dolomites should be much smaller than what is seen in practice under PFBC conditions.

The reaction of $CaCO_3$ with SO_2 may involve various reaction steps (Van Houte et al., 1981):

$$CaCO_3 + SO_2 \rightarrow CaSO_3 + CO_2 \quad (1)$$

$$CaSO_3 + 1/2\ O_2 \rightarrow CaSO_4 \quad (2)$$

$$CaSO_3 + 1/2\ SO_2 \rightarrow CaSO_4 + 1/2\ S \quad (3)$$

$CaSO_3$ decomposes at temperatures higher than 650 ^oC, and therefore, under typical operating conditions in a PFBC unit, the overall reaction may be written as:

$$CaCO_3 + SO_2 + 1/2\ O_2 \rightarrow CaSO_4 + CO_2 \quad (4)$$

For dolomites, one should also address the question of the reaction of MgO with SO_2.

If the partial pressure of CO_2 within the bed varies, calcination of $CaCO_3$ may take place in regions where CO_2 pressures lower than the equilibrium pressure are prevailing. The calcination of $CaCO_3$ will yield a partially calcined product, the extent of calcination depending on the residence time of the solid in the bw CO_2 concentration region. CaO formed in the solid will react with the SO_2 present in the bed in the same fashion as in the case of AFBC units:

$$CaCO_3 \rightarrow CaO + CO_2 \quad (5)$$

$$CaO + SO_2 + 1/2\ O_2 \rightarrow CaSO_4 \quad (6)$$

If the partially calcined solid moves into regions rich in CO_2, where reaction (5) is favored to proceed from right to left, carbonation, i.e., recovery of $CaCO_3$, will take place, with reaction (4) competing with reaction (5) for CaO. Decomposition of $CaCO_3$ may also take place even if there is no variation of the CO_2 pressure in the reactor. Large variations in the temperature profile (100-140 ^oC) within the combustor unit have been reported by Smith et al. (1982). Therefore, if the solid particles move into regions where the temperature of the reactor is above the temperature at which $CaCO_3$ is stable, at the average partial pressure of CO_2 in the reactor, decomposition of $CaCO_3$ will occur. However, only small amounts of CaO have been found in the reactor by Ljungstrom and Lindqvist (1982), suggesting that direct sulfation of limestones (eq. (4)) is the main reaction occurring in the combustor. Similarly, PFBC data from Exxon (Hoke et al., 1977) with uncalcined Grove limestone showed that most of the unreacted Ca in the bed for CO_2 partial pressures above the equilibrium value existed in the form of $CaCO_3$.

Studies of SO_2 removal at high pressures have been carried out both with carbonates and precalcined solids (Newby et al., 1980; Ulerich et al., 1982; Dennis and Hayhurst, 1984, 1987; Bulewicz et al., 1986). However, because of the aforementioned complexities, with the exception of the general conclusion that favorable desulfurization is possible under PFBC conditions, there is not much agreement in the literature on the effects of the various parameters

on the process. Dennis and Hayhurst (1984, 1987), for example, found that the reaction rate of precalcined limestones in a fluidized-bed reactor decreases with an increase in the operating pressure, both in the absence and presence of CO_2. Working with a laboratory-size PFBC, Bulewicz et al. (1986) observed an increase in the sorption capacity of Ca-based sorbents (chalk, limestone, and dolomite) with an increase in pressure up to 2 atm, but further increase in pressure caused a reduction in the sorption capacity of all samples. Similar observations were made by Jansson et al. (1982). PFBC studies at Exxon (Hoke et al., 1977) showed better sulfur retention for precalcined limestones, but Stantan et al. (1982) observed no improvement in sorbent utilization by precalcination. Stantan et al. also reported that under weakly noncalcining conditions, a feed of uncalcined limestone gave better sulfur retention than what kinetic studies performed in a thermogravimetric apparatus predicted.

A situation similar to that prevailing in PFBC units is encountered in desulfurization in gasifier at high pressures. Fixed-bed and fluidized-bed gasifiers typically operate around 850 ^{o}C with a temperature at the exit of around 500-800 ^{o}C. The pressure of operation is in most cases in the 200-300 psi range, and at an average pressure of 250 psi, it turns out that the CO_2 partial pressure in the reactor is about 1.8 and 4.3 atm for air blown and oxygen blown gasifiers, respectively (based on a typical CO_2 content (mole/mole) of 11% and 26%, respectively (Grindley et al., 1985). Almost all observations made for SO_2 removal in PFBC reactors apply to H_2S removal in high pressure gasifiers but with reactions (7) and (8) taking place (primarily) in a gasifier instead of (4) and (6):

$$CaCO_3 + H_2S \rightarrow CaS + CO_2 + H_2O \qquad (7)$$

$$CaO + H_2S \rightarrow CaS + H_2O \qquad (8)$$

Like in the case of sulfation, the main difference between the direct and indirect reactions is that a highly porous solid is involved in the indirect process while that participating in the direct reaction is essentially nonporous. In view of this difference, the information that is presently

available on the sulfidation of limestone-derived calcines (e.g., see Borgwardt et al. (1984) and Efthimiadis and Sotirchos (1992)) and sulfidation of half-calcined dolomites (e.g., see Ruth et al. (1972) and Yen et al. (1981)) from studies in thermogravimetric analysis (TGA) systems and other types of reactors is inapplicable to the direct reaction of limestones with H_2S. Few fundamental studies have been presented in the literature on the direct reaction of limestones with H_2S, and most of those have been carried out under low pressures (Borgwardt and Roache, 1984) or under conditions where both sulfidation reactions ((7) and (8)) could take place (Attar and Dupuis, 1979).

The direct sulfation or sulfidation of calcium carbonate-containing sorbents can be studied under atmospheric pressure provided that there is enough CO_2 in the reactor to prevent decomposition of the carbonate (simulated PFBC or high pressure gasification conditions). Tullin and Ljungstrom (1989) performed sulfation experiments in a thermogravimetric analyzer (TGA) under conditions inhibiting calcination of $CaCO_3$ and found that the sulfation rate of uncalcined $CaCO_3$ was comparable with the sulfation rate of calcined material; they thus concluded that desulfurization in PFBC's is achieved by direct sulfation of limestones. Large amounts of sample and small particles (around 150 mg and 10-90 μm) were used by those authors in their experiments, and thus extracting any quantitative information is practically impossible (because of strong interparticle diffusional limitations). A similar procedure was employed by Snow et al. (1988) and Hajaligol et al. (1988), who also observed that the direct sulfation of $CaCO_3$ can reach for some precursors higher conversions than the sulfation of the calcines (CaO). High concentrations of CO_2 (70% CO2 by volume) were also used by Borgwardt and Roache (1984) to study the direct reaction of limestone particles with H_2S at atmospheric pressure in a differential reactor. They employed a limestone precursor (Fredonia limestone) of relatively high porosity (about 8%), and thus, they were able to explain the behavior of the conversion-time trajectories for large particles (diameter greater than 15 μm) along the lines of the overall mechanism for the sulfidation of limestone-derived calcines (reaction (8)).

A detailed investigation of the direct sulfation of limestones with SO_2 and H_2S under simulated high pressure conditions was carried out by our research group (Krishnan and Sotirchos, 1993a,b,1994) using three limestone specimens of high CaCO3 content. In accordance with the observations of Tullin and Ljungstrom (1989), Snow et al. (1988), and Hajaligol et al. (1988), our sulfation results (Krishnan and Sotirchos, 1993a,1994) showed that the direct reaction of calcium carbonate with SO_2, believed to be the dominant reaction in a PFBC, is qualitatively different from the reaction of limestone calcines. A similar conclusion was reached for the limestone-H_2S reaction (Krishnan and Sotirchos, 1994). These results reinforced our early conclusion that the accumulated knowledge in the literature from the extensive study of the reaction of calcined limestones and dolomites with SO_2 or H_2S cannot be used to derive any reliable conclusions for flue or coal gas desulfurization under high pressure conditions. Nevertheless, with the exception of the studies conducted under simulated high pressure conditions on a few limestones, no fundamental studies have been carried out in the literature on the reaction of limestones and dolomites with SO_2 or H_2S under true high pressure conditions (i.e., at high pressures and in the presence of CO_2). Moreover, even though the experimental data under simulated high pressure conditions have been extremely helpful in elucidating some of the phenomena encountered in the direct sulfation or sulfidation of limestones, it is questionable whether these results are directly applicable to reaction under true PFBC or high pressure gasification conditions, especially for solids with significant dolomitic content.

Based on the above observations, a research program was proposed for the investigation of the mechanism of SO_2 and H_2S removal by limestones and dolomites at high pressures. It was proposed to carry out reactivity evolution experiments using thermogravimetric and, if needed, fixed-bed and fluidized-bed reactor (high pressure) arrangements. Thermogravimetric experiments would be carried out under simulated high pressure conditions at atmospheric pressure using atmospheric and high pressure systems. The pore structure of fresh, heat-treated, and half-calcined solids (dolomites) would be analyzed using a variety of methods. Our work would focus on limestones and dolomites whose reaction with SO_2 or H_2S under atmospheric conditions had been in detail investigated by either us or other research groups. The obtained

experimental data would be analyzed using various theoretical tools developed by my research group for studying gas-solid reactions, and would be used as basis for the development of predictive single particle models for use in design models of combustors or gasifiers.

2. WORK DONE AND DISCUSSION

2.1. Simultaneous Calcination and Sulfation Studies

The subject of most studies, both theoretical and experimental, on limestone sulfation or sulfidation is the investigation of the sulfation behavior of samples which have been calcined completely in the absence of sulfur compounds. This is also the case with the studies that have been carried out by my research group on limestone calcination and sulfidation (Zarkanitis and Sotirchos, 1989; Efthimiadis and Sotirchos, 1992; Sotirchos and Zarkanitis, 1992). However, when desulfurization is carried out in a combustor or a gasifier in situ through limestone addition, both calcination and sulfation or sulfidation are carried out simultaneously. The argument that is usually made in justifying how experimental results obtained from sequential calcination and sulfuration (sulfation or sulfidation) experiments can be used to determine the performance of actual desulfurization systems in which these processes occur simultaneously is that calcination is so faster than sulfuration that in the time needed to achieve complete calcination the conversion of the calcined material to sulfide or sulfate is extremely low. However, the time needed to completely plug the pores at the external surface of the particles (during sulfation) or reach complete conversion (during sulfidation) is independent of the particle size, whereas the time needed for complete calcination increases strongly with increasing particle size. Therefore, the interaction between the calcination and sulfuration processes is expected to intensify as the particle size increases. Moreover, at high partial pressures of CO_2, as it is the case in high pressure reactors, the calcination of limestone – provided that it is thermodynamically possible – is expected to occur with rate much lower than that in the absence of CO_2. Therefore, it is possible the interaction of calcination and sulfuration to lead to sorbent performance in an actual unit much different from that revealed by sequential calcination and sulfuration experiments.

In order to examine the validity of the assumption of minimal interaction of calcination and sulfation during sulfur removal in a combustor, we investigated experimentally the simultaneous calcination and sulfation of limestones at atmospheric pressure using two limestone specimens. Experiments were carried out without CO_2 added in the reactant stream – except that resulting from the decomposition of calcium carbonate – in order to be able to compare our results with sequential calcination and sulfidation experiments that had been carried out under the same conditions in past studies using the same sorbents. The samples we used were: a limestone of very high $CaCO_3$ content distributed by Greer limestone Co. (Greer Limestone) and a calcite (Iceland Spar) distributed by Wards Inc. Chemical analysis of the solids showed that the calcium carbonate content was 99.19% in the Iceland spar and 97.89% in the Greer limestone. Detailed chemical analyses of the three solids are given elsewhere (Krishnan, 1993).

Simultaneous calcination and sulfation experiments were carried out in a thermogravimetric analysis (TGA) system operating at 1 atm. In order to avoid having significant interparticle diffusional limitations, a small amount of solid (1.4-4 mg) was used for reactivity experiments. Gas flow rates of 200 ml/min under standard conditions were used in all of the experiments. The effect of particle size on conversion vs. time results was studied by carrying out experiments with particles in two size ranges (53-62 and 297-350 μm) for each of the three solids. The temperature effect was also studied by performing experiments at two different temperatures, 750 and 850 ^oC. A gas mixture consisting of 3,000 ppm SO2, 12% O2, and the balance N_2 was used as reactant stream. Simultaneous calcination and sulfation experiments were started by heating the limestone sample to the reaction temperature under a stream of 70% CO_2 and the balance N_2 to prevent occurrence of decomposition, and switching to the SO_2-O_2-N_2 stream once the reaction temperature was reached.

Some of the results we obtained in our experiments are presented in Figure 1.1-1.8. The results are presented as the weight gain added to the initial weight of the limestone before calcination, that is, as $(1+\Delta W / W_0)$ vs. time, where W_0 is the initial weight of the sample (after heat treatment but before calcination). This is done because the simultaneous occurrence of the two

reactions does not permit us to determine which part of the total weight change is due to each process. In the same figures, we also present the weight change ratio vs. time curves that were determined in past studies for the same limestones (Sotirchos and Zarkanitis, 1992) for calcination and sulfation carried out independently of each other and the composite curves that are obtained by assuming that the interaction of the two processes as they occur simultaneously is unimportant.

We see from the results of Figures 1.1-1.8 that the total weight change vs. time curve for simultaneous occurrence of calcination and sulfation behaves qualitatively in the same way as the composite curve that is constructed using results from independent calcination and sulfation experiments, but there is not much quantitative agreement between the two curves in each case. Significant differences are observed even for particles with size in the range 53-62 μm, and this observation points to the conclusion that it is not possible to determine the performance of a limestone for in situ SO_2 removal from results obtained from sequential calcination and sulfation experiments. Both in the simultaneous (actual) and in the sequential (artificial) processes, the total weight of the sample decreases initially at a high rate, but after some time, it starts to increase, with the rate of increase being noticeably higher for the composite process. The weight change (drop) at the minimum is much larger in the sequential process. Since the decrease of the weight is due to the loss of CO_2 during calcination, one is led to conclude that the conversion of calcium oxide to sulfate impedes the progress of calcination in the simultaneous process. This effect must be a reflection of the reduction of the average pore size in the calcined shell of the particles by the occurrence of the sulfation reaction, which, as we pointed out before, forms a solid product that is bulkier than the solid reactant it replaces. The decreasing average pore size increases the diffusional limitations that CO_2 experiences as it is transported through the decomposed layer and thus slows down the calcination reaction.

In the case of the Greer limestone particles (Figures 1.1-1.4), the weight loss in the sequential process becomes eventually smaller than that in the simultaneous process, indicating that larger quantities of sulfur are removed per unit of weight of limestone in the former. For the Iceland

spar, the sequential process shows larger weight loss than the simultaneous process at all times, but this does not mean that the sulfur uptake is larger in the latter. The analysis of the sulfation data of Greer limestone and Iceland spar (Sotirchos and Zarkanitis, 1992) showed that the mass transport limitations in the interior of the calcined particles are much higher in the case of Iceland spar. This is why much smaller weight changes are observed in the sulfation of Iceland spar calcines (compare Figures 1.5-1.8 with Figures 1.1-1.4). (Different reaction temperature was used for each of the two solids, but changing the reaction temperature from 750 to 850 ^{o}C does not lead to very large changes in the uptake vs. time curves.) Because of the smaller diffusion coefficient in the product layer, the calcination of Iceland spar particles requires more time to be completed than that of Greer limestone particles. As the calcined layer is sulfated and the effective diffusivity of CO_2 is decreased, the rate of calcination decreases faster than in the absence of the sulfation reaction, practically ceasing when the pores at the external surface becomes plugged with solid product. A significant fraction of the carbonate remains unreacted, and as a result, the simultaneous process curves stay above those of the sequential process at all times. Some unreacted material must also remain in the Greer limestone particles, and therefore, the difference between the sulfur uptake in the sequential process and that in the simultaneous process for this solid must be much larger than what the weight change vs. time curves of Figures 1.1-1.4 suggest.

The comparison of Figures 1.1-1.4 with Figures 1.5-1.8 reveals that the calcination of the Iceland spar particles takes much longer than that of the Greer limestone particles. This difference is a consequence both of higher mass transport limitations in the interior of the Iceland spar particles. From the comparison of the results for different temperatures, it is concluded that lower reaction temperatures lead to lower calcination rates and larger differences between the sequential and simultaneous processes. For the same limestone precursor, a reduction in the temperature increases the duration of the calcination process because it decreases the intrinsic rate of the calcination reaction and, as the analysis of the sulfation results showed (Sotirchos and Zarkanitis, 1992), the diffusion coefficient in the calcined layer. On the other hand, the reaction temperature does not influence significantly the intrinsic rate of sulfation, and thus, the time

needed to plug the pores at the external surface with solid product remains about the same. Because of these two effects, a reduction in the reaction temperature increases the time of interaction between the calcination and sulfation reactions in the simultaneous process, leading to increased differences between the total weight change curves of the sequential and the simultaneous processes.

The comparison of samples of different particle size reacted at the same conditions shows that an increase in the particle size decreases the rates of all processes and leads to larger, in a relative sense, differences between the sequential and simultaneous processes. The first effect is due to the existence of intraparticle diffusional limitations in the interior of the reacting particles, which tend to intensify with increasing particle size. On the other hand, the differences between the sequential and simultaneous processes increase with increasing particle size because – as when the temperature is decreased – the slowing down of the calcination reaction lengthens the time interval over which interaction of sulfation and calcination takes place. An increase in the particle size has a dramatic effect on the overall rate of sulfation of the calcine but it does not affect the intrinsic rate of the sulfation reaction and, therefore, the conversion vs. time curve at the external surface of the particles.

2.2. Simultaneous Calcination and Sulfidation Studies

The experiments on the simultaneous calcination and sulfation experiments that were carried out during the first six-month period of this project revealed the existence of significant quantitative differences between the behavior seen in this process and that observed when calcination and sulfation are carried out sequentially. From the variation with time of the difference in weight change between the simultaneous and sequential processes, it was concluded that under simultaneous calcination and sulfation conditions, calcination is not completed and much smaller amounts of sulfur are absorbed by the solid. Since it is the simultaneous process that is encountered in practical applications, this led us to conclude that it may not be possible to obtain quantitative information on the performance of a limestone in an actual desulfurization process directly from studies of the sequential process.

When limestone is used for H_2S removal, it is introduced in the gasifier in uncalcined form, but the approach used in most studies of limestone sulfidation has been to study the sulfidation reaction of completely calcined samples, that is, to investigate the calcination and sulfidation reactions sequentially. This approach has also been followed in a study of limestone sulfidation that was carried out in our laboratory (Efthimiadis and Sotirchos, 1992). In view of the conclusions reached from the study of the simultaneous calcination and sulfation of limestones, it was decided to carry out a comprehensive investigation of the behavior of limestones during simultaneous calcination and sulfidation and compare the results with those obtained at the same conditions when calcination and sulfidation are carried out sequentially.

Experiments were carried out at atmospheric pressure in a TGA system using two limestone specimens we used in the studies described in the preceding section. As before, in order to avoid having significant interparticle diffusional limitations, a small amount of solid (1.4-4 mg) was used for reactivity experiments. Gas flow rates of 200 ml/min under standard conditions were used in all of the experiments. The effect of particle size on conversion vs. time results was studied by carrying out experiments with particles in two size ranges (53-62 and 297-350 μm) for each of the three solids. The temperature effect was also studied by performing experiments at two different temperatures, 750 and 850 °C. A gas mixture consisting of 7,000 ppm H_2S in N_2 was used as reactant stream. Simultaneous calcination and sulfidation experiments were started by heating the limestone sample to the reaction temperature under a stream of 70% CO_2 and the balance N_2 to prevent occurrence of decomposition, and switching to the H_2S-N_2 stream once the reaction temperature was reached.

Some of the results we obtained in our experiments are presented in Figures 2.1-2.8. The results are again presented as the weight gain added to the initial weight of the limestone before calcination, that is, as $(1+\Delta W / W_0)$ vs. time, where W_0 is the initial weight of the sample (after heat treatment but before calcination). In the same figures, we also present the weight vs. time curves that were obtained from sequential calcination and sulfidation experiments. Efthimiadis

and Sotirchos (1992) presented results on the sequential calcination and sulfidation of the limestone samples we used in our experiments, but since they did not cover all the operating conditions we used in the present study and employed a different thermogravimetric arrangement (e.g., the reactant mixture entered their reactor from below, whereas in our system it inters through the top), we decided to carry out sequential calcination and sulfidation experiments for all combinations of operating conditions we examined. For the same experimental conditions, the results of our sequential experiments were in good agreement with those reported by Efthimiadis and Sotirchos (1992).

The composite curve that is shown in each figure is constructed by adding the weight change observed during calcination and that measured during sulfidation of the calcine. It therefore describes the weight vs. time curve that is expected to be observed in the simultaneous process if the progress of each reaction is independent of that of the other. Significant differences are seen to exist between the weight vs. time curve for the simultaneous process and the corresponding curve (composite curve) for sequential calcination and sulfidation in several cases, and they are more pronounced for the large particle size. It is interesting to note that even though the sulfidation of calcium oxide is accompanied by a weight increase, both sample lose weight faster at 850 ^{o}C during the initial stages of the reaction when calcination and sulfidation are carried out simultaneously. After a minimum is reached in the total weight gain vs. time curve, the simultaneous process exhibits a relatively faster rate of weight increase. For the small particle size (53-62 mum), the two processes appear to reach complete conversion to CaS for relatively small values of reaction time, with the simultaneous process reacting completely at slightly lower times. (For complete calcination followed by complete sulfidation, a sample of pure $CaCO_3$ should attain a value of $(1+\Delta W / W_0)$ equal to 0.72.) If it is assumed that complete calcination takes place for the large particle size in the simultaneous process – a reasonable assumption considering that it exhibits a much lower minimum than the sequential process – the results of Figure 2.2 indicate that the simultaneous process reaches complete conversion after about 30 min of reaction time, whereas within the same time interval the conversion reached in the sequential process is about 65%. A similar observation holds for the large Iceland spar

particles at 850 °C (see Figure 2.4). The most important quantitative difference between the large Iceland Spar particles at 850 °C from their Greer Limestone counterparts is that they are characterized by lower reaction rates (rates of weight change).

Figures 2.1, 2.3, 2.5, and 2.7 show weight vs. time curves obtained at 750 °C for the sequential and simultaneous processes for the two samples. The trends displayed by the same cases of the two solids are similar, the main difference being that in the experiments with Greer limestone particles faster weight changes were observed. In contrast to the behavior of the results obtained at 850 °C, the weight vs. time curves of Figures 2.1, 2.3, 2.5, and 2.7 show that both the calcination and the sulfidation reactions proceed with lower overall rates in the simultaneous process. For the small particle size of Iceland Spar (see Figure 2.7), the sample weight in the simultaneous process reaches a minimum at a time value that is by a factor of 3 larger than the corresponding time in the sequential process. The minimum corresponds to the point where the weight increase because of sulfidation offsets the decrease that results from calcination. If it is assumed that the minimum corresponds to the point where most of the $CaCO_3$ is calcined, the results of Figure 2.7 suggest that it takes at least three times longer for the calcination of the precursor to be completed in the simultaneous process. For the large size Iceland spar particles of Figure 2.5, the calcination and sulfidation rates in the simultaneous process are so slow that within the 30 min window shown in the figure, no minimum is observed in the variation of the weight of the sample with time.

The results of Figures 2.5 and 2.7 are consistent with the behavior that is expected on the basis of the physical and chemical phenomena that occur in the simultaneous and sequential calcination-sulfidation processes. When calcination is carried out in the presence of H_2S (simultaneous process), the calcium oxide that is formed from the decomposition process reacts with H_2S forming CaS. CaS occupies about 50% more space than CaO, and as a result, the converted layer (CaO and CaS) that surrounds the core of uncalcined $CaCO_3$ is characterized by lower porosity and, hence, higher diffusional limitations than the CaO layer that surrounds the unreacted core of particles that undergo calcination in the absence of H_2S. The higher resistance

for diffusion in the product layer leads to lower rates of CO_2 transport away from the calcined-uncalcined solid interface, where calcination takes place, and slows down the calcination process. On the other hand, since sulfidation in the simultaneous process does not start with a porous structure existing everywhere within the particle, there is less surface area available for reaction, and this leads to lower overall sulfidation rates.

The above discussion assumes that the pore structure of the reacting particles evolves during sulfidation in the same way in the sequential process and in the simultaneous process. The higher calcination and sulfidation rates that are observed for the simultaneous process at 850 °C suggest that this is not the case when the reaction is carried out at this temperature. These higher rates of reaction can only be explained if the sulfided material that is formed during the simultaneous process presents much smaller resistance to gaseous diffusion than the layer formed in the sequential process. In their study of the direct sulfidation (i.e., under noncalcining conditions) of the same limestones Krishnan and Sotirchos (1994) observed sintering of calcium sulfide at temperatures as low as 650 °C. Therefore, it is possible that the sintering of calcium sulfide leads to different pore structures in the simultaneous and sequential processes.

2.3. Sulfidation of Limestones in the Presence of Small Amounts of Oxygen

The incentive for carrying out sulfidation experiments in the presence of oxygen was provided by the observation that some sulfidation experiments that were conducted as oxygen was accidentally leaking into the feed mixture of the reactor showed completely different behavior from that obtained in the absence of oxygen. Experiments were carried out in a thermogravimetric analysis system that we developed for studying gas-solid reactions at atmospheric or subambient pressures using the two $CaCO_3$ solids (Greer Limestone and Iceland Spar) that we employed in the experiments of the preceding sections. We employed two particle size ranges (53-62 and 297-350 μm), two temperatures (750 and 850 ^oC), and a stream of 7,000 ppm H_2S in N_2, in which we added small amounts of O_2. Sulfidation was carried out simultaneously or sequentially with calcination.

Results are shown in Figure 3.1-3.12 for the Greer Limestone sample and 3.13-3.18 for the Iceland Spar sample. To make the graphs directly comparable with those presented in previous reports, the results are presented as the weight gain added to the initial weight of the limestone before calcination, that is, as $(1+\Delta W / W_0)$ vs. time, where W_0 is the initial weight of the sample (after heat treatment but before calcination).

The results for the large Greer Limestone particles (Figures 3.1-3.3) show that as the concentration of oxygen in the reactive mixture increases, the total weight reached by the sample after some reaction time also increases, reaching for 2% concentration of oxygen values that are well above the weight gain for the conversion of CaO to CaS, which for the sulfidation process corresponds to $(1+\Delta W / W_0)$ equal to 1.16. The weight gain for large values of time is above this value even for small concentrations of oxygen in the feed. The additional weight is most probably due to the oxidation of CaS to $CaSO_4$ by the oxygen added to the feed, and the comparison of Figures 3.2 and 3.3 suggests that this process reaches higher conversions as the temperature of reaction increases.

For small Greer Limestone particles, a maximum is observed in the variation of the weight of the sample with the extent of sulfidation if the concentration of oxygen is below 0.5-0.8% (Figures 3.4-3.6 and 3.8). When sulfidation is carried out at the same time as calcination, the maximum occurs after the initial drop in the weight that is caused by the occurrence of calcination, a much faster process than sulfidation. For concentrations above 0.5-0.8%, the weight of the sample increases continuously with time, and as in the case of large particles, the weight gain at large values of reaction is above that corresponding to complete conversion of CaO to CaS (Figures 3.7 and 3.9-3.12). However, in the case of the small particles, the observed weight gain is considerably larger, and for relatively large concentrations of oxygen (2%), it corresponds to almost complete conversion of CaO to $CaSO_4$. The concentration of oxygen above which a maximum is observed in the variation of the weight gain with time increases with increasing temperature of reaction (compare Figures 3.4 and 3.6), and this is also the case for the

concentration oxygen above which monotonic variation of weight with time is observed – after the initial drop in the weight in the case of simultaneous calcination and sulfidation (compare Figures 3.7 and 3.8).

The behavior of the Iceland Spar particles (Figures 3.13-3.18) is qualitatively similar to that of the Greer Limestone particles. A maximum in the variation of the weight with time is exhibited only for small particles, but whenever this happens (Figures 3.17 and 3.18), it is less pronounced than in the cases with Greer Limestone particles. For concentrations of oxygen above 0.5-0.8%, the weight of the sample increases monotonically and attains values above that for complete conversion of CaO to CaS, but much lower than that for complete conversion to $CaSO_4$, even for the 53-623 μm particles. Another difference between the Greer limestone and Iceland Spar samples is that at 750 ^oC, the simultaneous calcination and sulfidation curve differs substantially – especially at low reaction times and for the large particle size – from the composite curve for the sequential process. This is caused by the fact that at this temperature, the rate of calcination becomes comparable to that of sulfidation, and thus, there is significant interference between these two reactions.

The weight change of the sample at large reaction times when a maximum is present in the weight gain vs. time curve is in several cases lower that the value that is expected for complete sulfidation of the solid. Complete sulfidation takes place when the reaction is carried in the absence of oxygen. This suggests that part of the sulfide could be converted back to oxide, most probably through the solid-solid reaction of CaS with $CaSO_4$ formed from the oxidation of CaS. Since the solid sample is continuously exposed to H_2S, the leveling off of the weight gain to values at which CaO must be present indicates that CaO formed from the solid-solid reaction of CaS and $CaSO_4$ – if this is the reason for the appearance of a maximum – should exhibit very low reactivity with H_2S.

For oxygen concentrations above 0.5-0.8%, the rate of $CaSO_4$ formation from the oxidation of CaS is apparently much higher than that of CaO formation from the solid-solid reaction of CaS

and $CaSO_4$, and as a result, the weight of the sample increases continuously in the course of the reaction. It was pointed out that for the small Greer Limestone particles, the weight gain reached by the sample for oxygen concentration around 2% corresponds to complete conversion of CaO to $CaSO_4$. This is a surprising result, since if the particle size does not change, the maximum conversion that can be reached for complete pore filling with $CaSO_4$ is about 50%. We are thus led to conclude that when the calcined limestone particles react with H_2S in the presence of oxygen, they react as unconsolidated structures, and thus, their size changes (increases) in the course of the reaction.

Experiments with different sample sizes revealed that the maximum in the variation of the weight of the sample with time became more pronounced as the size of the sample was decreased. This observation, in conjunction with the observation that more pronounced maxima are encountered in the case of Greer limestone, i.e., the material that exhibits much smaller resistance for transport in the pore space of its calcine (Sotirchos and Zarkanitis, 1992), suggests that the decrease in the weight of the sample must be caused by formation of a volatile product that escapes from the pore space of the materials. The formation of a volatile product can also explain why the weight of the sample decreases monotonically after a maximum is formed since, as we mentioned above, if the presence of the maximum were caused by the formation of CaO in the CaS-$CaSO_4$ solid-solid reaction, one would expect this species to react with the H_2S that is continuously sent through the reactor.

Some experiments on the effects of the presence of oxygen on sulfidation were also carried out using CaO samples with very small effective particle size, and the results obtained from them offered further support to the volatile intermediate explanation that we presented above. Specifically, we conducted experiments using CaO samples obtained through decomposition of calcium-enriched bio-oil, a material obtained by reacting bio-oil, the product of the flash pyrolysis of wood, with calcium hydroxide. The CaO material that results from the decomposition of calcium-enriched bio-oil typically has very high porosity, and as a result, the intraparticle diffusional limitations in the interior of the formed particles – or flakes when the

starting material in a thin coating on the pan – are extremely low. Behavior similar to that exhibited by the small Greer Limestone particles was observed, but the maximum in the variation of the weight with time was much more pronounced. Some results are shown in Figures 3.19 and 3.20. In some cases (see Figure 3.20), the reduction of the weight corresponded to complete disappearance of the sample of the pan, and this was verified by visual examination of the pan at the end of the experiment.

The results of Figures 3.1-3.18 clearly show that in the presence of small amounts of oxygen, completely different behavior of the limestone particles from that revealed by simultaneous or sequential calcination and sulfidation experiments is obtained. Since oxygen is present in some regions of a gasification reaction, it is believed that this phenomenon should be investigated further at conditions that are more representative of the operation of a typical gasification unit in which H_2S control is achieved through limestone injection.

2.4. Effects of Pressure on the Direct Sulfation of Limestones

The effects of various operating and process parameters on the direct reaction of limestones with SO_2 in the presence of oxygen and CO_2, the latter at concentration high enough to prevent the decomposition of $CaCO_3$ to CaO. The two calcitic solids of high calcium carbonate content (over 97%) that were employed in the experiments that we described in the preceding sections were used. Experiments were carried out in a high pressure, thermogravimetric analysis system that we developed under this project. In the initial configuration of the system, we used a microfurnace arrangement to heat the sample, but we encountered several problems in the operation of the system. We overcame these problems by redesigning the heating arrangement. Specifically, we used as a furnace tube the quartz process tube in which the pan containing the sample was suspended and heat it directly by winding heating wire around it over a length of about 10 cm. The pan was placed at about the middle of this heating zone. The heated length was wrapped with high temperature insulating material, and the whole arrangement was placed into a stainless steel hangdown tube. The reactive mixture was sent through the quartz tube, and the space between the stainless steel tube and the quartz tube was purged continuously using an

inert gaseous stream. The process stream and the purge steam merged at the exit of the quartz tube just before the outlet port of the high pressure hangdown tube. The hangdown tube was cooled using water flowing through a copper tubing coil over its part that surrounded the heated length of the quartz tube. For safety reasons, it was decided to limit the pressure of operation to less than 5 atm.

Results were obtained on the effects of the concentration of SO_2, particle size, temperature, and pressure. All these variables were found to have very strong effects of the behavior of the process, and the observations that were made from these results were in agreement with those from past studies at atmospheric pressure under noncalcining conditions using the same solids. Representative results are shown in Figures 4.1 and 4.3 for the Greer Limestone sample and Figures 4.2 and 4.4 for the Iceland Spar sample. In all cases shown in these figures, the mixture flowing through the reactor consisted of 70% CO_2 and 30% air containing 0.5% or 2% SO_2.

It is seen in Figures 4.1-4.4 that for both solids and all particle sizes and temperatures we examined, the conversion vs. time curves for 1,500 ppm SO_2 at 4 atm follow the same trend as the two curves that were obtained at atmospheric pressure for 1,500 and 6,000 ppm SO_2 at the same conditions. The particles reacting with 1,500 ppm SO_2 at 4 atm exhibit lower reaction rates than the particles reacting at 1 atm with 1,500 ppm or 6,000 ppm SO_2, but at high reaction times their rates are very similar to those with 6,000 ppm SO_2. Since the concentration of SO_2 in the {6,000 ppm, 1 atm} and {1,500 ppm, 4 atm} cases is the same, the last observation leads us to infer that this variable is the key parameter that determines the rate of the reaction between limestone and SO_2 under noncalcining conditions for a given reaction temperature and a given particle size. The lower reactivities at small reaction times may be the result of the larger amounts of solid that we employed in the high pressure experiments in order to reduce the relative noise in the signal of the microbalance; specifically, we used samples of about 10-20 mg on the average vs. 1-2 mg for experiments at atmospheric pressure.

The atmospheric pressure results that were obtained in our experiments were in agreement with those obtained by Krishnan and Sotirchos (1993) in past studies using the same solids but a different thermogravimetric reactor. The analysis of those data using a shrinking core model for gas-solid reactions with position-dependent diffusivity of SO_2 through the product layer (variable diffusivity shrinking core model) showed that the initial ($t = 0$) differences between the Iceland Spar and the Greer Limestone samples were caused by the different value of the rate constant of the $CaCO_3$-SO_2 reaction. The same conclusion was also reached from the analysis of the results we obtained in this study. A rate equation of the form $R_s = k_s c_{SO_2}^n$ was assumed, and the order of the reaction, *n*, was found to be equal to 0.4. This is the reason for which the relative differences in the initial slopes of the cases with 1,500 and 6,000 ppm SO_2 mole fraction for the same values of the other operating parameters are not as large as the differences in the SO_2 concentration.

The strong effect of particle size on the conversion vs. time results is a consequence of the presence of strong diffusional limitations in the product layer. On the other hand, the effects of the temperature reflect its effects on both the reaction rate constant and the product layer diffusivity. The analysis of the experimental data with the variable diffusivity shrinking core model gave an average value for the activation energy of about 120 kJ/mol for the rate constant and of about 200 kJ/mol for the product layer diffusivity. This indicates that the effect of temperature on the diffusional limitations in the product layer is much stronger than that on the rate of the reaction. The product layer diffusivity was found to be a strong function of the distance from the external surface of the particles, of the type of limestone, and of the concentration of SO_2 in the product layer.

The Greer Limestone sample had about one order of magnitude higher effective diffusivity through the product layer than the Iceland Spar sample at the same conditions, and this is the main reason for the much lower reactivity of the latter at all operating conditions (compare Figures 4.1 and 4.3 with Figures 4.2 and 4.4). The product layer diffusivity decreased with

increasing distance from the external surface of the particles, and the concentration of SO_2 was found to have a strong negative effect on its value at all positions. On the average, the product layer diffusivity for 1,500 ppm SO_2 at 1 atm was by about a factor of 2 higher than that for 6,000 ppm SO_2 at 1 atm or 1,500 ppm SO2 at 4 atm. The strong negative effect of the concentration of SO_2 on the product layer diffusivity is the reason for which the overall rate of the reaction (slope of the weight vs. time curve) at a given level of conversion and a given set of operating parameters does not vary proportionally to the concentration of SO_2 in the surrounding gas phase after the initial stages of the reaction when transport through the solid product shell becomes the controlling mechanism of the whole process. (It can be easily shown using correlations of the literature for the Sherwood number that the diffusional limitations from the gas phase to the particles are negligible.)

The solid product of the direct sulfation process ($CaSO_4$) occupies about 24% more solid than the solid it replaces ($CaCO_3$), and as a result, the size of the reacting $CaCO_3$ particles – which in general show very little porosity – must increase with the extent of the conversion of the solid. However, for this to happen, it is necessary to have rearrangement of the solid grains that comprise the solid product that surrounds the unreacted core to provide space for the new solid that is forming at the solid product-solid reactant interface. As the reaction proceeds, the newly formed solid product 'pushes' against a progressively thicker layer of already formed solid product in order to accommodate itself into the reacting particle. Thus, one expects the product layer to become denser as the distance from the external surface of the particle increases, and this is exactly what the decreasing value of product layer diffusivity with the distance suggests. As the concentration of SO_2 in the gas phase is increased, the rate of formation of $CaSO_4$ increases as well, and this provides less time to the grains that comprise the product shell to rearrange themselves to make space for the added solid volume at the interface. This leads to denser solid product and, hence, to lower values of effective diffusivity.

The observation that the behavior of the direct sulfation process is controlled mainly by the concentration of SO_2 in the product layer indicates that the information that is available in the

literature on this reaction can be used at pressures different from those used in the experiments in which this information was acquired. Preliminary experiments on the direct sulfidation reaction of limestones have shown that the above also holds for that process as well. The examination of the effects of the pressure on the direct sulfidation of limestones will be the focus of the experiments we plan to carry out in the next reporting period.

2.5. Effects of Pressure on the Direct Sulfidation of Limestones

The investigation of the effects of various operating and process parameters on the direct sulfidation of limestones, that is, their reaction with H_2S in the presence of CO_2 at concentrations large enough to prevent the decomposition of $CaCO_3$ to CaO, was carried in an analogous manner as that of their direct sulfation. The two calcitic solids of high calcium carbonate content (over 97%) that were employed in the experiments that we described in past reports were also employed in these studies: a fine-grained limestone (Greer Limestone) and a solid supplied in the form of large single crystals (Iceland Spar).

Experiments were carried out in a high pressure, thermogravimetric analysis system that we developed under this study. Results were obtained on the effects of the concentration of H_2S, particle size, temperature, and pressure. The results showed that all these operating conditions and parameters had very strong effects on the behavior of the process. The type of limestone also had a very strong influence on the reaction rate; specifically, the Iceland Spar sample presented much lower reactivity than the Greer Limestone material at the same conditions.

Figure 5.1 presents experimental results on the effects of particle size, pressure, and concentration at 750 ^oC on the conversion vs. time behavior of Greer Limestone, and Figure 5.2 presents the corresponding results for Iceland Spar. Qualitatively similar results were obtained at other temperatures. In all cases shown in these two figures, the solid samples were exposed during reaction to a mixtures consisting of 70% CO_2 and 30% N_2 containing 0.5% or 1% H_2S.

The concentrations of H_2S in the two pairs of H_2S mole fraction and pressure that are used in Figures 5.1 and 5.2 ({3,000 ppm H_2S, 1 atm} and {1,500 ppm H_2S, 4 atm}) differ by a factor of 2, and for this reason, the reaction time shown in the figures for the case with the larger concentration corresponds to the real time multiplied by a factor of 2. It is seen in both figures that the conversion vs. time curves of the two curves are very close to each other, and this indicates that the rates of the various subprocesses that are encountered in the overall direct sulfidation process of the particles depend linearly on the concentration of H_2S.

The following subprocesses are involved in the sulfidation process: the sulfidation reaction at the unreacted solid-reacted solid interface, the transport of the reactant (H_2S) from the gas phase to the external surface of the particles, and the transport of the sulfiding species (H_2S or some other ionic species) from the external surface to the reaction interface. The rate of mass transport from the gas phase to the external surface of the particles spends linearly on the concentration of H_2S, but even if that were not the case, it would not have any effect on the behavior of the overall process since – as it can be easily verified using correlations of the literature for the Sherwood number of spherical particles – the corresponding resistance for mass transport is negligible. The initial overall reaction rates are only influenced by the intrinsic rate of the chemical reaction, and the analysis of the acquired data led to the result that the rate of the reaction is of first order with respect to the concentration of H_2S. Since the rate of the overall process was found to change linearly with the concentration of H_2S, one concludes in view of the above results, that the rate of mass transport through the solid product layer depends linearly on the concentration of H_2S. This in turn implies that if this rate is expressed in terms of the concentration of H_2S, the diffusion coefficient in the solid product layer should be independent of that variable.

A shrinking core model with diffusion coefficient depending only on the temperature of operation and having the same value at all positions within the solid product shell was used to model the sulfidation process. The predictions of the mathematical model are shown in Figures 5.1 and 5.2, and they hold for both cases considered in the figures ({3,000 ppm H_2S, 1 atm} and

{1,500 ppm H_2S, 4 atm}). (In accordance with the remarks made above, the time for the second case was multiplied by a factor of 2.) Very good agreement is seen to exist between the model results and the experimental data. The reaction rate constant of the Greer Limestone sample was found to be by about a factor of 2 greater than that of Iceland spar, and both samples exhibited rather low activation energy of similar value, much lower than that of the direct sulfation reaction (about 16 vs. 120 kJ/mol). The product layer diffusivity for Greer Limestone was by a factor of 6-8 larger than that for Iceland Spar, and this was the main reason for the large differences in the sulfidation rates of same size particles of the two solids at the same conditions. The activation energy for the product layer diffusivity varied from about 100 kJ/mol for Iceland Spar to about 150 kJ/mol for Greer Limestone.

The results on the effects of particle size, temperature, and concentration of H_2S on the direct sulfidation of limestones were in agreement with those obtained in a past investigation of the process at atmospheric pressure (Krishnan and Sotirchos, 1994). Considering that the effects of pressure on the process were found to be manifested only through its effects on the concentration of H_2S, this is a very interesting finding because it suggests that the information of the literature on the direct-limestone reaction at atmospheric pressure can be used to derive conclusions on their performance at high pressures.

2.6. Simultaneous Carbonation and Sulfation of Calcined Limestones

An experimental investigation was carried out of the interaction of the carbonation ($CaO-CO_2$ reaction) and sulfation ($CaO-SO_2$ reaction in the presence of oxygen) reactions during exposure of calcined calcitic solids to an environment containing SO_2, O_2, and CO_2, the last of these species at concentrations above the equilibrium value for equilibration of the calcination reaction (decomposition of $CaCO_3$). The two calcitic solids of high calcium carbonate content (over 97%) that were employed in the experiments that we described in past reports were also employed in these studies. It was decided to study the simultaneous occurrence of the calcination and sulfation reactions because, as it was pointed out in the introductory section of this report, if the partially or fully calcined solid moves into regions rich in CO_2, where reaction

(5) is favored to proceed in the direction of carbonation, that is, from right to left, the sulfation reaction (reaction (4)) will be competing with that reaction for CaO.

Experiments were carried out using two particle sizes (53-62 and 297-350 μm) and two temperatures (750 and 850 ^{o}C) for each calcitic solid. The obtained results for the 8 cases that correspond to these parameters are shown in Figures 6.1-6.4 for Greer Limestone and 6.5-6.8 for Iceland Spar. In each figure, we present weight vs. time results for i) sulfation, ii) calcination, iii) carbonation, and iv) simultaneous occurrence of carbonation and sulfation. The results are presented as the weight gain added to the initial weight of the limestone before calcination, that is, as $(1+\Delta W / W_0)$ vs. time, where W_0 is the initial weight of the sample (after heat treatment but before calcination). The gas mixture used for sulfation contained 3,000 ppm SO_2, the mixture used for sulfation 70% CO_2, and that used for the simultaneous process 3,000 ppm SO_2 and 70% CO_2.

The comparison of the results of Figures 6.1-6.4 with those for the corresponding cases of Figures 6.5-6.8 indicates that all processes occur much faster for the Greer Limestone sample. This was seen to be the case in all other processes we studied for these two solids in other studies and past reports of this project, and it is chiefly due to the much higher resistance for mass transport in the pore space of the calcine of Iceland Spar and in the solid product layer that is formed (sulfide or sulfate) when this solid is reacted.

For both solids, the conversion reached during carbonation is well below 100%, and in all cases it is lower than 70%. (For 100% conversion, $1+\Delta W / W_0$ should reach of a value of about 1.44.) Conversions close to 70% are exhibited by the small Greer Limestone particles at both temperatures, but the conversions of the large particles of this solid are not much lower. The small Iceland spar samples reach conversions comparable to those seen for their Greer Limestone counterparts, but the large particles reach conversions lower than 50%.

The rate of the carbonation reaction is considerably higher at the smaller temperature (750 ^{o}C). This can be explained if the reaction is assumed to be proceeding in a shrinking core fashion and to be controlled by mass transport through the reacted shell. In such a case, the driving force for mass transport through the reacted shell is the difference of the concentration of CO_2 in the gas phase from its equilibrium concentration at the reaction interface. Since the equilibrium concentration decreases with decreasing temperature, this driving force increases in the same direction, thereby causing an increase of the rate of mass transport through the reacted shell and, hence, of the rate of carbonation.

From the comparison of the weight vs. time curves of the simultaneous process with the weight vs. time curves that would be obtained if the weight changes during sulfation and carbonation were assumed to be additive, one concludes that the effects of the interference of the processes of carbonation and sulfidation area much stronger in the case of Iceland Spar. In all cases of this solid, the results suggest that the uptake of SO_2 is much lower when the sulfation reaction occurs simultaneously with carbonation. For the large Iceland Spar particles (see Figures 6.7 and 6.8), the results indicate – if it is assumed that the carbonation reaction is the first to reach completion – that the extent of the sulfation reaction under simultaneous carbonation conditions is negligible,. This conclusion was verified by exposing particles simultaneously sulfated and carbonated under the conditions of Figures 6.7 and 6.8 to a calcining environment. It was observed that the particles reached a weight level that corresponded to the weight of the solid produced after complete calcination (CaO).

The results of Figures 6.1-6.8 clearly show that there can be strong interference between the sulfation and the carbonation reactions of calcined limestones. This interference tends to lead to reduced efficiencies for SO_2 removal. When the conditions that prevail in a combustor are calcining on the average, one expects the limestone particles to go through a sequence of successive calcination and carbonation steps as they move out of calcining regions into carbonating regions. A few experiments were carried out on the calcination of the carbonated material. It was found that the subsequent calcination steps are much faster than the initial

process (the calcination of the as received solid). In view of this, one may argue that the formation of $CaCO_3$ may not affect strongly the performance of the sorbent particles under the above conditions in a combustor since the material formed during carbonation would decompose rapidly. However, since the carbonation process is also very fast, this cycle of sequential calcinations and carbonations to cause formation of calcium sulfate to take place only in very thin shell close to the external surface of the particles. Since the formation of calcium sulfate causes pore blockage, this could eventually lead to severely limited sorbent efficiencies for SO_2 removal.

2.7. A General Mathematical Model for Simultaneous Decomposition and Solid Product Formation Reactions

The physical picture that we used as basis in the development of the model is shown in Figure 7.1 for the case of simultaneous calcination and sulfation of limestones. To simplify the illustration, the particle is assumed to be of slab geometry. The figure shows a limestone (primarily $CaCO_3$) particle at some time after the initiation of its simultaneous calcination (decomposition) and sulfation (solid product formation) reactions. Calcination is assumed to occur at a sharp interface separating the unreacted material ($CaCO_3$) and a reacted shell. The reacted shell is porous since the product of the decomposition reaction (CaO) occupies less space per mole (about half less) than the reactant ($CaCO_3$) it replaces. The material that is adjacent to the interface on the side of the reacted shell consists only of CaO since it has just been formed and has not had the opportunity to react with SO_2. On the other hand, the CaO material that is at the external surface has been exposed to SO_2 since the beginning of the process, and as a result, its conversion to $CaSO_4$ has progressed to a significant extent. Since the concentration of SO_2 at the external surface is higher than that at the unreacted core (because of intraparticle diffusional limitations) and the temperature at the core is lower than that at the external surface (because of intraparticle heat transport limitations and the endothermic nature of the decomposition reaction), the conversion of CaO to $CaSO_4$ is higher at the external surface and decreases towards the unreacted core.

$CaSO_4$ occupies more space than the reactant it replaces (CaO), and therefore, the porosity of the converted layer varies with the local extent of sulfation, decreasing from the unreacted core to the external surface. The molar volume of $CaSO_4$ is by about 30% larger than that of $CaCO_3$, and thus, complete pore plugging occurs when only 50% of CaO is converted to $CaSO_4$). Because of the nonuniform porosity profile, complete pore closure may take place at the external surface of the particles while there is open pore space available in the interior or before all $CaCO_3$ is decomposed. When this happens, further reaction in the interior of the particles practically ceases since it becomes impossible for the product gas of the decomposition reaction (CO_2 for calcination) to escape from the particle and the reactant gases of the solid product formation reaction (SO_2 and O_2 for sulfation) to enter it.

It follows from the preceding discussion that the simultaneous decomposition and solid product formation process involves the following subprocesses: the decomposition reaction, the solid product formation reaction, transport of the components of a gaseous mixture in the pore space of the decomposed layer, diffusion of the gaseous reactants and products that participate in the solid product formation reaction (SO_2 and O_2) through the product layer ($CaSO_4$) that surrounds the pores of the decomposed layer, evolution of the pore structure of the decomposed layer, and heat transport in the intraparticle space. The presentation of the equations that describe the mathematical is beyond the scope of this report. Here, we will only outline the main features of the models used for the various subprocesses.

The decomposition reaction is described using reversible kinetics (of zero order in the forward direction), consistent with its thermodynamic equilibrium. Because of the reversibility of this reaction, it is possible, depending on the resistance for transport of the product gas of decomposition (CO_2 for calcination) through the converted layer, its rate to be determined by the rate of transport of that gas away from the reaction interface. The dusty-gas model (Jackson, 1977; Mason and Malinauskas, 1983) is used to describe the interaction of the transport fluxes of the gaseous species in the decomposed layer. The only assumption used in modeling the processes of structure evolution and transport of the reactant gases through the

product layer of the pores is that the structure of the porous layer (CaO) that is formed from the decomposition reaction evolves in time only because of the solid product formation reaction, that is, sintering effects are not taking place or, if they are taking place, are not important. It is possible to relax this assumption but at the expense of increasing the complexity of the model. The structure of the decomposed material is represented using a pore network model based on finite length pore segments arranged around the bonds of a lattice, and it is assumed to evolve during formation of a solid product according to the models of Yu (1987) and Sotirchos and Zarkanitis (1992). Finally, the existence of significant temperature gradients is accounted for both in the converted shell and in the unreacted core; of course, in the unreacted core, significant temperature gradients exist only during the initial stages of the process before pseudosteady state is reached.

2.8. Computation of the Evolution of the Structural and Transport Properties of Reacting Porous Solids Using Stochastic Computer Algorithms

A stochastic simulation scheme was formulated for studying matrix volume trapping in structures of growing particles, where growth can occur only on surfaces that serve as boundaries of infinite (accessible) subsets of the matrix phase. This is the case that is encountered in the sulfidation or the sulfation of calcined limestones. The following steps are involved in the method: i) a unit cell is constructed for the starting (mother) structure, and the mother structure is used as basis for the construction of a number of derivative (daughter) structures of uniformly grown particles; ii) a number of points is selected randomly within the unit cell, and these points are used as starting points of random walkers that travel in the matrix space (outside the particles) by suffering diffuse reflections (according to the cosine law) on the particle surfaces; iii) such computations are carried out both for the initial and the derivative structures, and the information that is extracted from these computations is employed to determine, for each uniformly grown structure, which of the randomly selected points in the two-phase medium lie in the particle phase, the accessible part of the matrix, or its inaccessible part; iv) the same determination is made for the real particle structures (that is, with matrix volume trapping accounted for) using a method developed in this study, and this information is further employed to estimate matrix

volume fractions, mean intercept lengths, surface areas, and volume and surface area distributions of matrix phase fragments. In addition, we develop a formula that allows us to determine the variation of the inaccessible matrix volume of the real structures with the extent of particle growth from the variation of the surface areas and volume fractions of the inaccessible and accessible parts of the uniformly grown structures. The obtained results for the real structures are approximate, converging to the exact results as the steps between successive structures approach zero.

The method was applied to structures of randomly overlapping (fully penetrable), unidirectional cylinders. The comparison of the results for real and uniformly grown structures showed that the inaccessible and total matrix volume fractions increase by relatively small amounts when formation of trapped matrix (pore) space is taken into account. Since the inaccessible matrix fragments tend to have much larger surface area per unit volume than the accessible matrix space (by about a factor of 4 at the onset of formation of inaccessible matrix space starts), the total surface area of real structures is slightly larger than that of uniformly grown structures of the same particle size. It is believed that the reason for the existence of small differences between real (with volume trapping accounted for) and uniformly grown structures is that formation of inaccessible matrix space occurs at a significant rate only close to the percolation threshold. In past studies, this was also observed to be the case for structures of multidirectional, randomly overlapping fibers or unidirectional, partially overlapping fibers. It is thus expected that real and uniformly grown structures will exhibit small differences for these cases as well. This is a very important result for since it implies that the information that is available in the literature on the percolation behavior of the above fibrous media for uniform fiber growth can also be employed, without leading to significant errors for practical purposes, for the physically meaningful case where the fibers grow only on their accessible surfaces. This may also be the case for the grain or pore structures that are used to simulate the structure of calcined limestones (Yu, 1987; Sotirchos and Zarkanitis, 1992).

The information on the trajectories of the random walkers as they travel in the pore space suffering collisions on the pore walls can be employed to determine the effective Knudsen diffusion coefficients of gases in the pore structure. If allowance is made for molecule-molecule collisions, effective diffusivities in the bulk and transition diffusion regimes can also be obtained. By allowing the walkers to enter the solid phase, it is also possible to use their trajectories to determine effective thermal conductivities and other transport properties of the porous material. A general stochastic simulation scheme was formulated on the basis of the above ideas for computing the effective transport properties of multiphase media in which the constitutive phases may be anisotropic. Its development was based on similar algorithms that had been formulated in past studies by my research group for computing effective transport properties in multiphase media possessing a single conductive phase (e.g., porous media). Computations were carried out using structures in which the transport problem is amenable to analytical treatment, such as structures consisting of parallel layers and regular arrays of cylinders, in order to validate the developed simulation scheme. Work was also done to determine the variation of the effective thermal conductivity of partially sulfated or sulfided calcined limestones with the extent of reaction. This parameter is needed in modeling the simultaneous calcination and sulfation or sulfidation of limestones since heat transport through the partially converted (sulfated or sulfided) layer may be among the controlling factors of the overall process.

More information on and results from the above computations are given in an article published in J. Chem. Phys. (Sotirchos, S.V., and M.M. Tomadakis, J. Chem. Phys., 109, 4508 (1998).).

3. SUMMARY

A number of chemical reaction processes occurring between limestone particles and the gaseous species present in combustors or gasifiers in which limestone in particle form is injected to achieve removal of sulfur-containing gases were investigated under this project. Specifically, experimental research was carried out on the reaction of $CaCO_3$ solids with SO_2 or H_2S under high pressure (noncalcining) conditions, the simultaneous occurrence of the calcination and sulfation (reaction with SO_2) of limestones, the simultaneous occurrence of the calcination and

sulfidation (reaction with H_2S) of limestones, the simultaneous occurrence of the carbonation and sulfation of calcined limestones, and the sulfidation of limestones in the presence of small amounts of oxygen. Two calcitic solids of high calcium carbonate content (over 97%) were employed in the experiments: a fine-grained distributed by Greer Limestone Co. (Greer Limestone) and a solid supplied in the form of large calcitic crystals (Iceland Spar). In addition to the experimental work, theoretical studies were conducted on the development of rigorous mathematical models for the description of the occurrence of simultaneous processes (e.g., calcination and sulfation and carbonation and sulfation) in the interior of porous solids and for the simulation of the evolution of the pore structure of porous solids that undergo chemical transformation in their interior.

In order to prevent the decomposition of $CaCO_3$, experiments on the direct reaction of SO_2 with limestone were carried out in the presence of CO_2 at levels above the equilibrium pressure of the calcination reaction at the reaction temperature. The reaction was studied in a thermogravimetric analysis system that can operate at pressures above atmospheric. Pressures in the 1-4 atm range were employed. The results revealed strong effects of pressure on the variation of the conversion with time, but experiments with different combinations of mole fraction of SO_2 in the feed and total pressure led us to conclude that these effects were mainly a manifestation of the effects of pressure on the concentration of SO_2. This in turn was interpreted as an indication that the structure of the product layer ($CaSO_4$) that surrounds the unreacted core ($CaCO_3$) of the particles depends only on the concentration of SO_2, and that transport of SO_2 in that layer takes place through mechanisms that are not affected by the total pressure (e.g., Knudsen diffusion and ionic diffusion).

The results on the direct sulfidation of limestones showed that the pressure influenced the behavior of the process mainly through its effects on the concentration of H_2S, and the rate of the reaction was found to be of first order with respect to this variable. The behavior of the process could be described satisfactorily by a shrinking core model with a product layer diffusivity that depended only on the temperature and did not vary with the distance from the

external surface of the particles. The results on the effects of particle size, temperature, limestone sample, and concentration of H_2S were in agreement with those in a past investigation of the direct sulfidation reaction of limestones in our laboratory at atmospheric pressure. Some of the conclusions of our study on the direct sulfidation reaction of limestones were at variance with those reached from the study of the direct reaction of limestones with SO_2 in the previous reporting period, where the reaction rate was found to exhibit order equal to 0.4, a variable diffusivity (decreasing away from the external surface of the particles) had to be employed in the shrinking core model to describe the experimental data, and the product layer diffusivity was a strong function of the concentration of SO_2 in the gas phase.

The experiments on the simultaneous occurrence of the calcination and sulfuration (sulfidation or sulfation) reactions – this is what is actually taking place in a combustor or gasifier operating under calcining conditions when calcium carbonate particles are injected in it – showed that the behavior of the simultaneous calcination and sulfuration process can be markedly different from that inferred from the results of sequential calcination and sulfuration experiments. Simultaneous occurrence of calcination and sulfation has adverse effects on the effective capacity of limestone for SO_2 removal, which intensify as the particle size increases or the rate of calcination decreases. In general, the differences between the weight vs. time curve measured in the simultaneous process and that constructed on the basis of the results of the independent (sequential) experiments become larger as the rates of the processes become comparable, that is, as the rate of calcination is decreased. Similar observations were made in the study of the sulfidation and calcination processes. However, since in that case, the difference between the volume of the solid product and the volume of solid reactant is not large enough to cause complete pore closure before complete conversion of CaO to CaS is reached, the simultaneous occurrence of sulfidation and calcination does not affect the conversion level reached at very large times.

Sulfidation experiments in the presence of oxygen were carried out because in past experiments we had observed that leaks of oxygen into the feed mixture led to completely different results

from those obtained in the absence of oxygen. The behavior of the sulfidation of limestone was found to depend strongly, in both a qualitative and a quantitative sense, on the level of the oxygen concentration in the feed. For small concentration of oxygen, the weight gained by the calcined sample during sulfidation in a N_2-H_2S atmosphere presented a maximum, whereas for concentrations above 0.5-0.8%, it increased continuously, reaching in some cases values that corresponded to complete conversion of CaO to $CaSO_4$. The maximum in the variation of the weight gain with time tended to become more pronounced as the intraparticle diffusional limitations were decreased. The use of different sample sizes showed that the interparticle diffusional limitations had a similar effect, and this led us to the conclusion that the main cause for the presence of a maximum in the variation of the weight of the sample during sulfidation in the presence of oxygen is the formation of a volatile product (possibly Ca) in the CaS-$CaSO_4$ solid-solid reaction.

Experiments were conducted to investigate the interaction of the carbonation (CaO-CO_2 reaction) and sulfation (CaO-SO_2 reaction in the presence of oxygen) that may take place during exposure of calcined calcitic solids to an environment containing SO_2, O_2, and CO_2, the last of these species at concentrations above the equilibrium value for equilibration of the calcination reaction (decomposition of $CaCO_3$).). The results showed that the interference of the carbonation reaction with the sulfation reaction can lower the effective capacity of a $CaCO_3$ sorbent for SO_2 removal. The rate of carbonation was found to decrease with increasing temperature, most probably because of the larger driving force (concentration difference) for the transport of CO_2 to the reaction interface at the lower temperature. For both solids, the carbonation reaction was found to be a very fast process, but the conversions that were reached were well below 100%. From the comparison of the weight vs. time curves of the simultaneous process with the weight vs. time curves of the independent processes, it was concluded that the effects of the interference of the processes of carbonation and sulfidation were much stronger in the case of Iceland Spar.

The mathematical model that we formulated for simultaneous decomposition and solid product formation reactions was developed for the most general case where the particles are nonisothermal, the interaction of the mass transport fluxes of the components of the gaseous mixture is important, and the rate of the decomposition reaction can be limited by its intrinsic kinetics or the transport of its gaseous products away the reaction interface. Thus, the model can be applied to the study of and gas-solid reaction with solid product formation that accompanies a decomposition reaction. Since the process of sulfur gases removal by CaO involves formation of a solid product that occupies more space than the solid reactant it replaces, a stochastic simulation scheme was formulated for studying inaccessible pore volume formation in pore structures represented as assemblages of solid grains. It combines a gradual increase of the size of the grain that represent the porous structure with a random walk scheme, the latter used to determine whether a randomly chosen point in the unit cell of the two-phase structure lies in the particle phase or in the connected or in the isolated part of the matrix phase. The use of the algorithm was demonstrated by performing computations on structures of freely overlapping, unidirectional cylinders, and results were obtained both for the volume fractions and the specific surface areas of the accessible and inaccessible parts of the pore phase.

BIBLIOGRAPHY

Attar, A., and F. Dupuis, Ind. Eng. Chem. Process Des. Dev., 18, 607 (1979).

Borgwardt, R.H. and R.D. Harvey, Environ. Sci. Technol., 6, 350 (1972).

Borgwardt, R.H. and N.F. Roache, Ind. Eng. Chem. Process Des. Dev., 23, 742-748 (1984).

Borgwardt, R.H., N.F. Roache, and K.R. Bruce, Environ. Progress, 3, 129-135 (1984).

Bulewicz, E.M., S. Kandefer, and C. Jurys, J. Inst. Energy, 188 (1986).

Dennis, J.S. and A.N. Hayhurst, Inst. Chem. Eng. Symp. Ser., 87, 61 (1984).

Dennis, J.S. and A.N. Hayhurst, Chem. Eng. Sci., 42, 2361 (1987).

Efthimiadis, E.A., and S.V. Sotirchos, Ind. Eng. Chem. Res., 31, 2311 (1992).

Grindley, T., S.S. Kim, E.E. Gorski, and G. Steinfeld, “Aspects of the Design of a Process Development Unit for High-Temperature Coal Gas Desulfurization," Technical Report, DOE/METC-85/6025, 1985.

Gullett, B.K. and K.R. Bruce, AIChE J., 33, 1719 (1987).

Hajaligol, M.R., J.P. Longwell, and A.F. Sarofim, Ind. Eng. Chem. Res., 27, 2203 (1988).

Hartman, M. and R.W. Coughlin, Ind. Eng. Chem., Process Dec. Dev.,13, 248 (1974).

Hartman, M. and R.W. Coughlin, AIChE J., 22, 490 (1976).

Hasler J.R. et al., “Testing of Limestone Samples from the TVA region as Sulfur Dioxide Sorbents in Atmospheric Fluidized Bed Combustors,” Technical Report, Institute for Mining and Mineral Research, Univ. of Kentucky, 1984.

Hoke, R.C. et al., “Studies of the Pressurized Fluidized-Bed coal Combustion Process,” Technical Report, EPA-600/7-77-107, September 1977.

Jackson, R., *Transport in Porous Catalyst*, Elsevier, New York, 1977.

Jansson, S.A., L.P. O'Connell, and J.E. Stantan, Proc. Int. Conf. Fluid. Bed Combust., 7, 1095 (1982).

Krishnan, S.V., Ph.D. Thesis, University of Rochester, 1993.

Krishnan, S.V. and S.V. Sotirchos, Can. J. Chem. Eng., 71, 244 (1993a).

Krishnan, S.V. and S.V. Sotirchos, Can. J. Chem. Eng., 71, 724 (1993b).

Krishnan, S.V. and S.V. Sotirchos, Ind. Eng. Chem. Res., 33, 1444 (1994).

Ljungstrom, E., and O. Lindqvist, Proc. Int. Conf. Fluid. Bed. Combust., 7, 465 (1982).

Mason, E. A., and A. P. Malinauskas, *Gas Transport in Porous Media: The DustyGas Model*, Elsevier, New York, 1983.

Murthy, K. S., J. E. Howes, and H. Nack, Environ. Sci. Technol., 13, 197 (1979).

Newby, R.A., N.H. Ulerich, and D.L. Keairns, Proc. Int. Conf. Fluid. Bed Combust., 6, 803 (1980).

Ruth, L.A., A.M. Squires, and R.A. Graff, Environ. Sci. Technol. 6, 1009-1014 (1972).

Simons, G.A. and A.R. Garman, AIChE J., 32, 1491 (1986).

Smith, D. et al., Proc. Int. Conf. Fluid. Bed Combust., 7, 439 (1982).

Snow, M. J. H., J. P. Longwell, and A. F. Sarofim, Ind. Eng. Chem. Res. 27, 268 (1988).

Sotirchos, S.V., and S. Zarkanitis, AIChE J., 38, 1536 (1992).

Stantan, J.E., S.N. Barker, R.V. Wardell, N.H. Ulerich, and D.L. Keairns, Proc. Int. Conf. Fluid. Bed Combust., 7, 1064 (1982).

Tullin, C., and E. Ljungstrom, Energy Fuels, 3, 284 (1989).

Ulerich, N.H., R.A. Newby, W.G. Vaux, and D.L. Keairns, Proc. Int. Conf. Fluid. Bed Combust., 7, 121 (1982).

Ulerich, N.H, E.P. O'Neill, and D.L. Keairns, "The Influence of Limestone Calcination on the Utilization of the Sulfur-Sorbent in Atmospheric Pressure Fluid-Bed Combustors," EPRI ER-426, Final Report, 1977.

Van Houte, G., L. Rodrique, M. Genet, and B. Delmon, Environ. Sci. Technol., 15, 327 (1981).

Vogel, G.J. et al., Quarterly Report (January-March 1977), prepared for DOE, Argonne National Laboratory, 1977.

Wen, C.Y., and M. Ishida, Environ. Sci. Technol., 7, 703(1973).

Yen, J.H., K. Li, and F.H. Rogan, Chem. Eng. Comm., 10, 35-60 (1981).

Yu, H.C., Ph.D. Thesis, University of Rochester, 1987.

Zarkanitis S., Ph.D. Thesis, University of Rochester, 1991.

Zarkanitis, S., and S.V. Sotirchos, AIChE J., 35, 821 (1989).

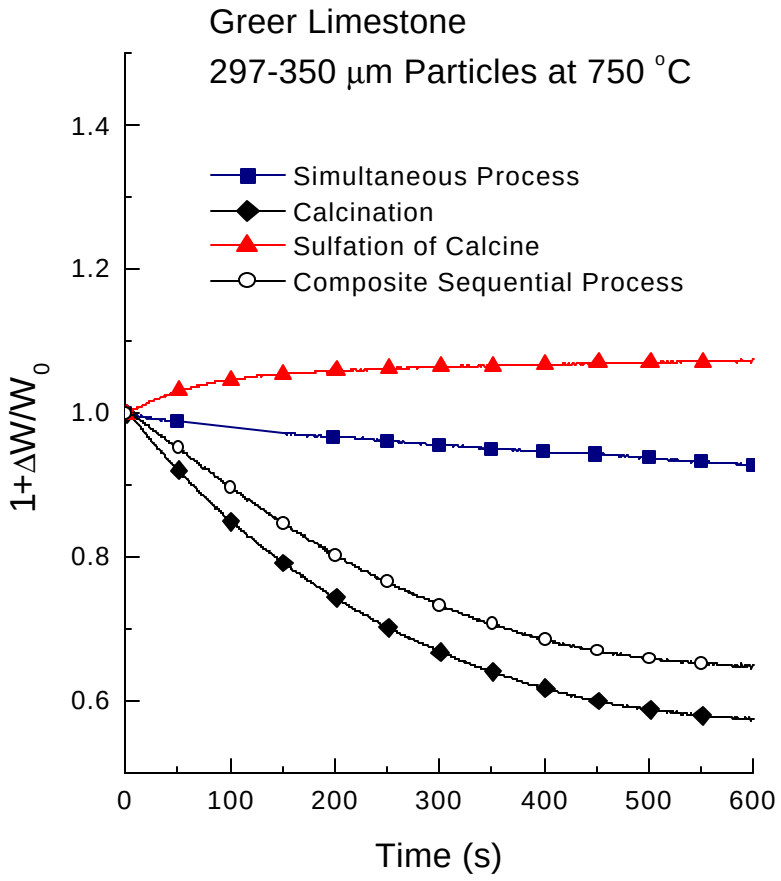

Figure 1.1. Weight vs. time curves during calcination and sulfation of 297-350 μm Greer Limestone particles at 750 °C.

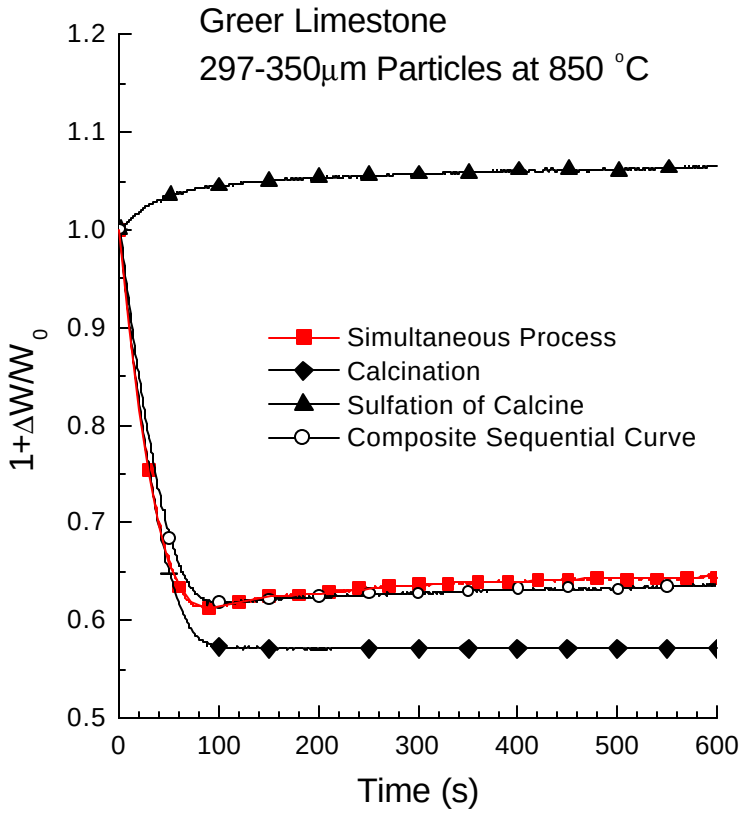

Figure 1.2. Weight vs. time curves during calcination and sulfation of 297-350 μm Greer Limestone particles at 850 °C.

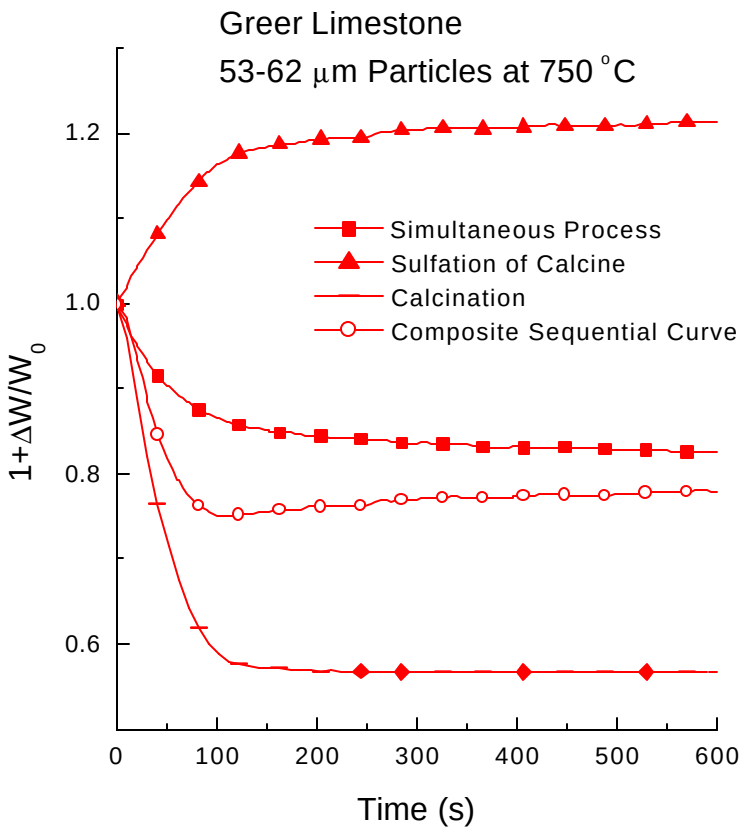

Figure 1.3. Weight vs. time curves during calcination and sulfation of 53-62 μm Greer Limestone particles at 750 °C.

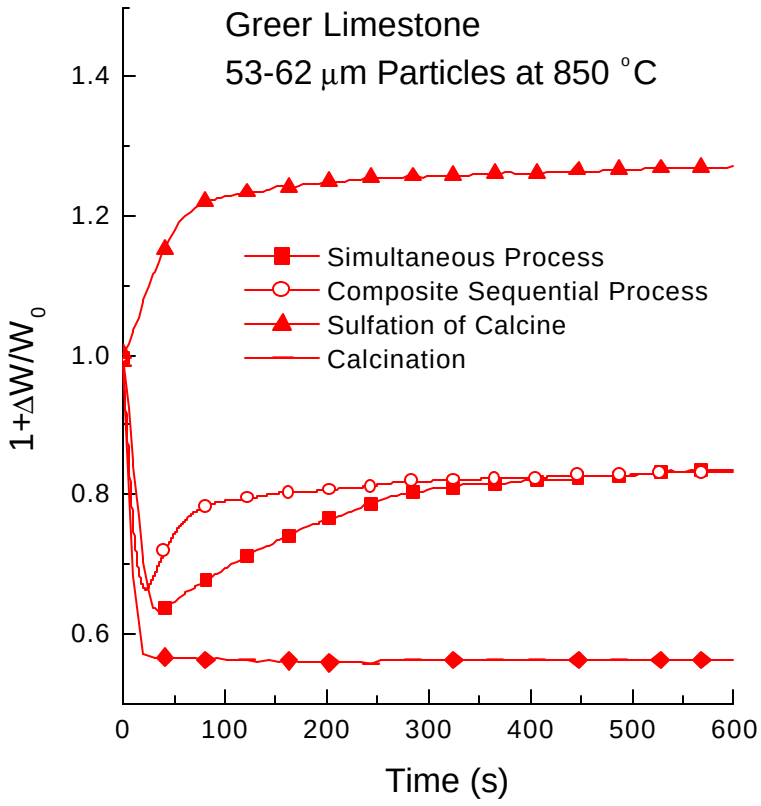

Figure 1.4. Weight vs. time curves during calcination and sulfation of 53-62 μm Greer Limestone particles at 850 °C.

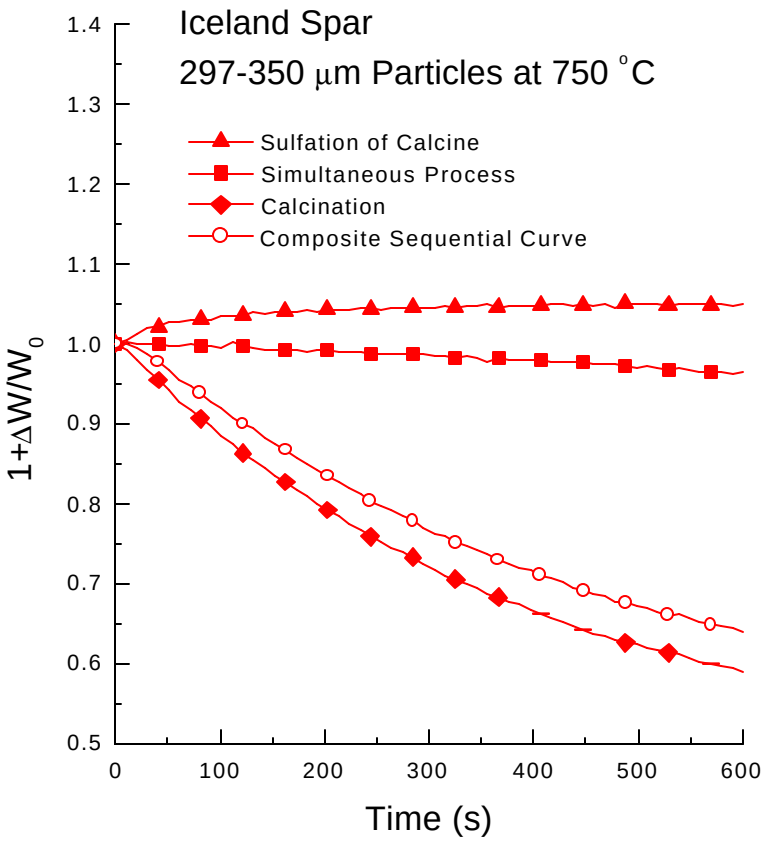

Figure 1.5. Weight vs. time curves during calcination and sulfation of 297-350 μm Iceland Spar particles at 750 °C.

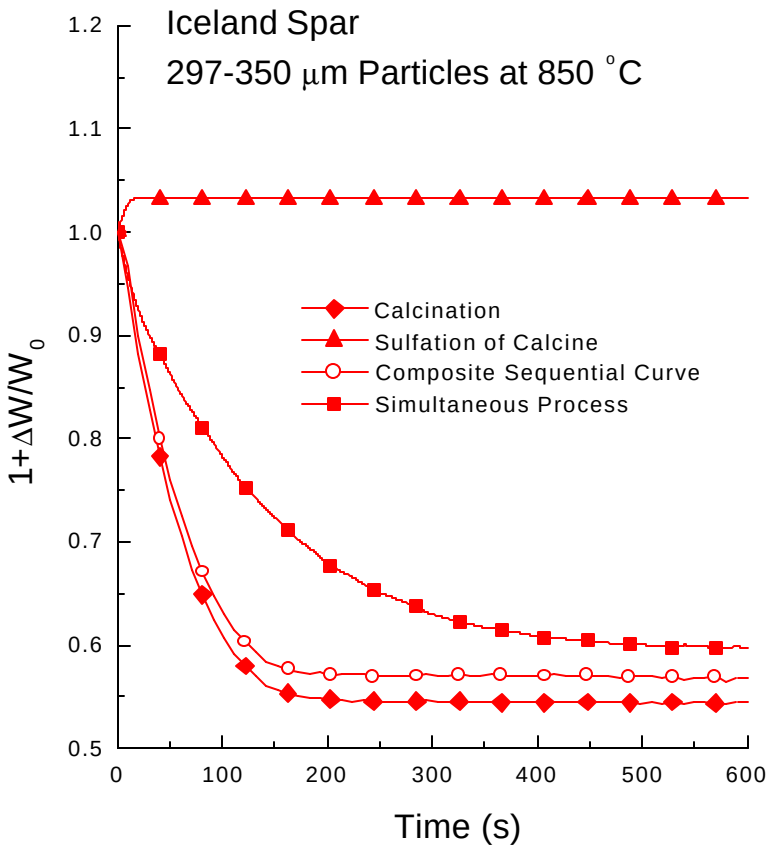

Figure 1.6. Weight vs. time curves during calcination and sulfation of 297-350 μm Iceland Spar particles at 850 °C.

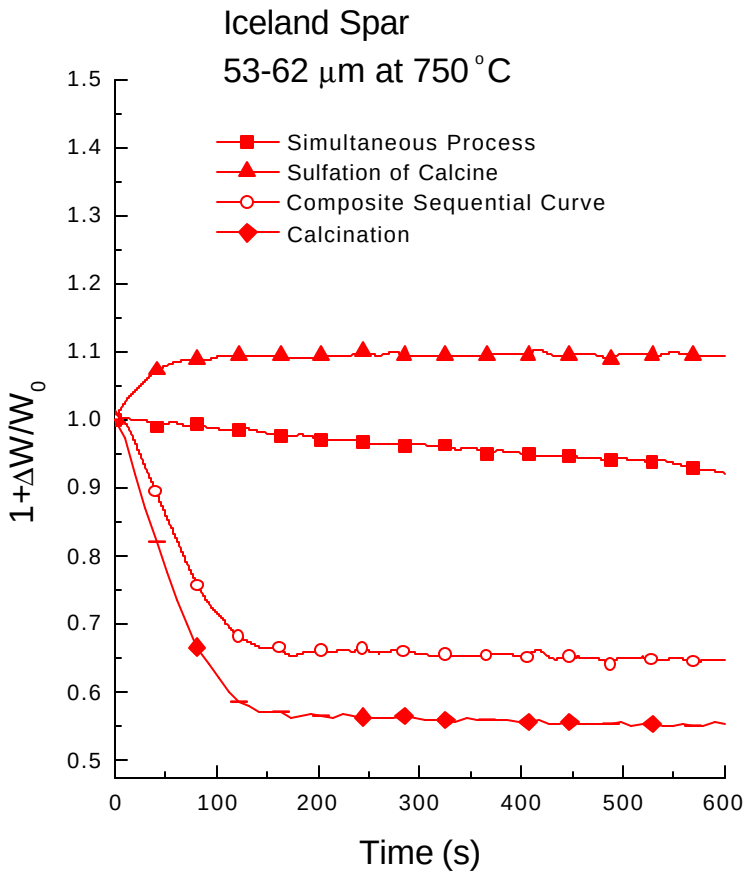

Figure 1.7. Weight vs. time curves during calcination and sulfation of 53-62 μm Iceland Spar particles at 750 °C.

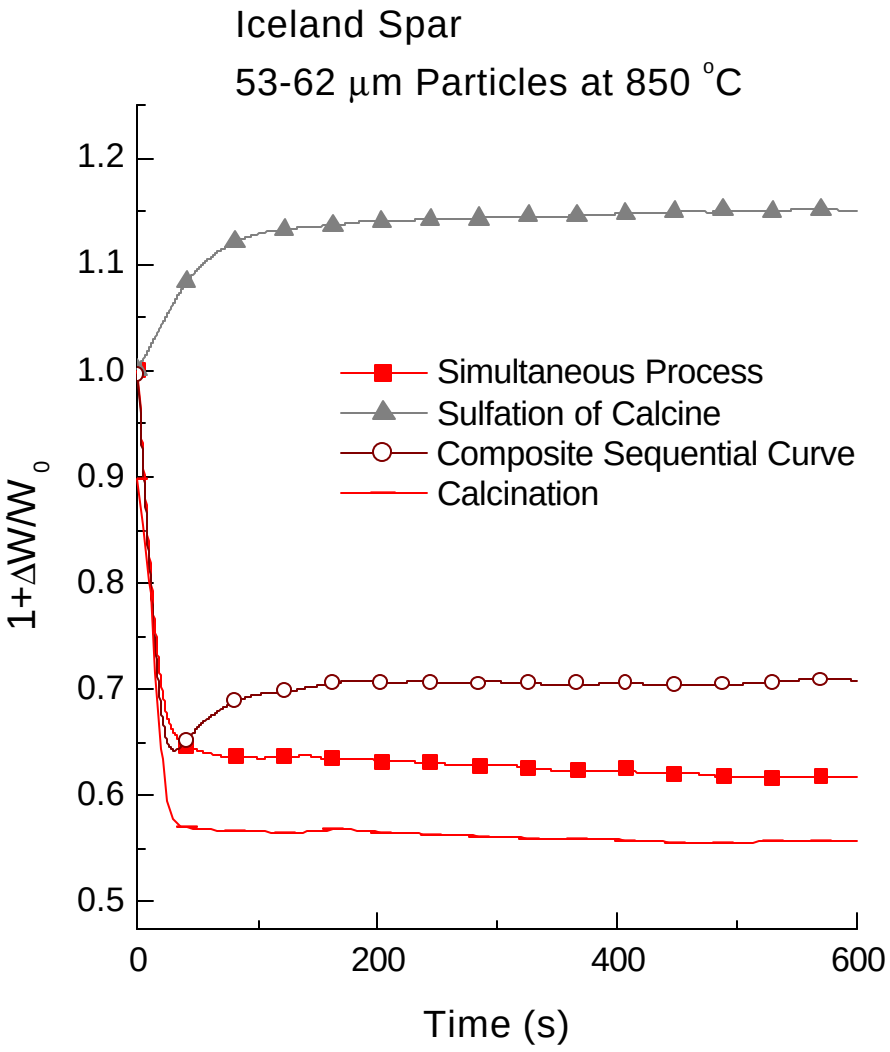

Figure 1.8. Weight vs. time curves during calcination and sulfation of 53-62 μm Iceland Spar particles at 850 °C.

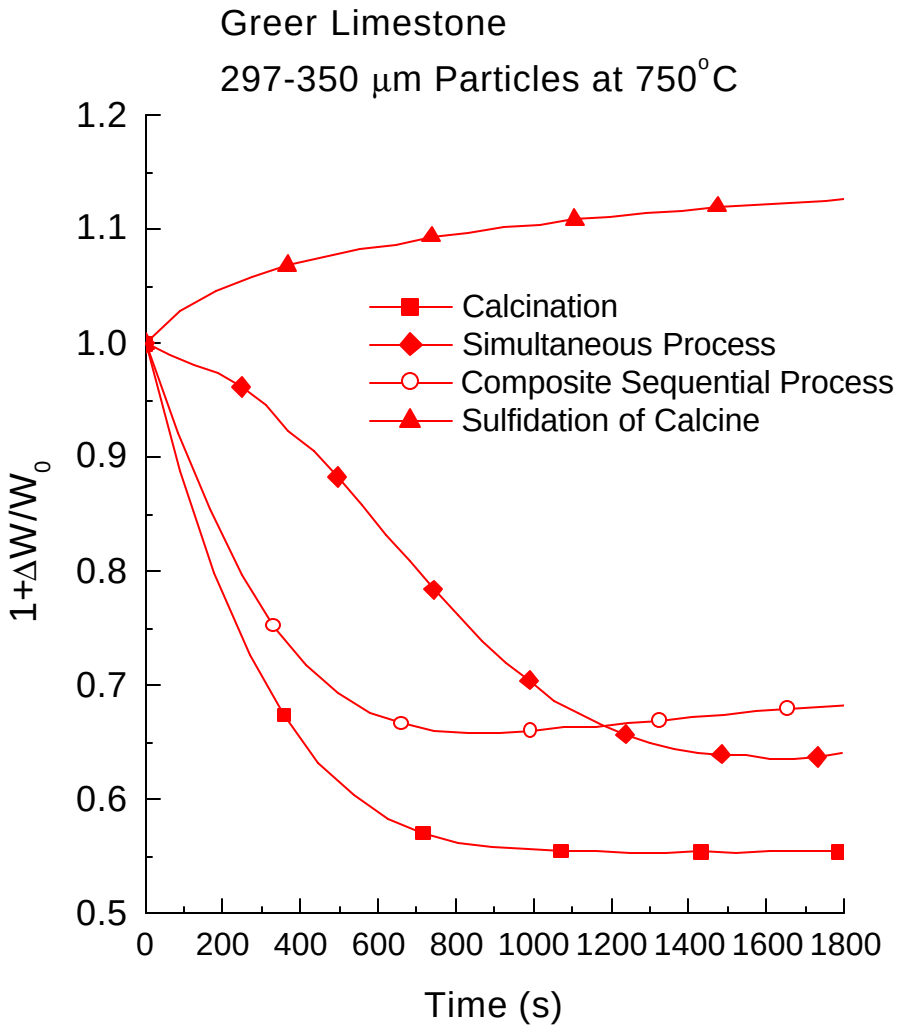

Figure 2.1. Weight vs. time curves during calcination and sulfidation of 297-350 μm Greer Limestone particles at 750 °C.

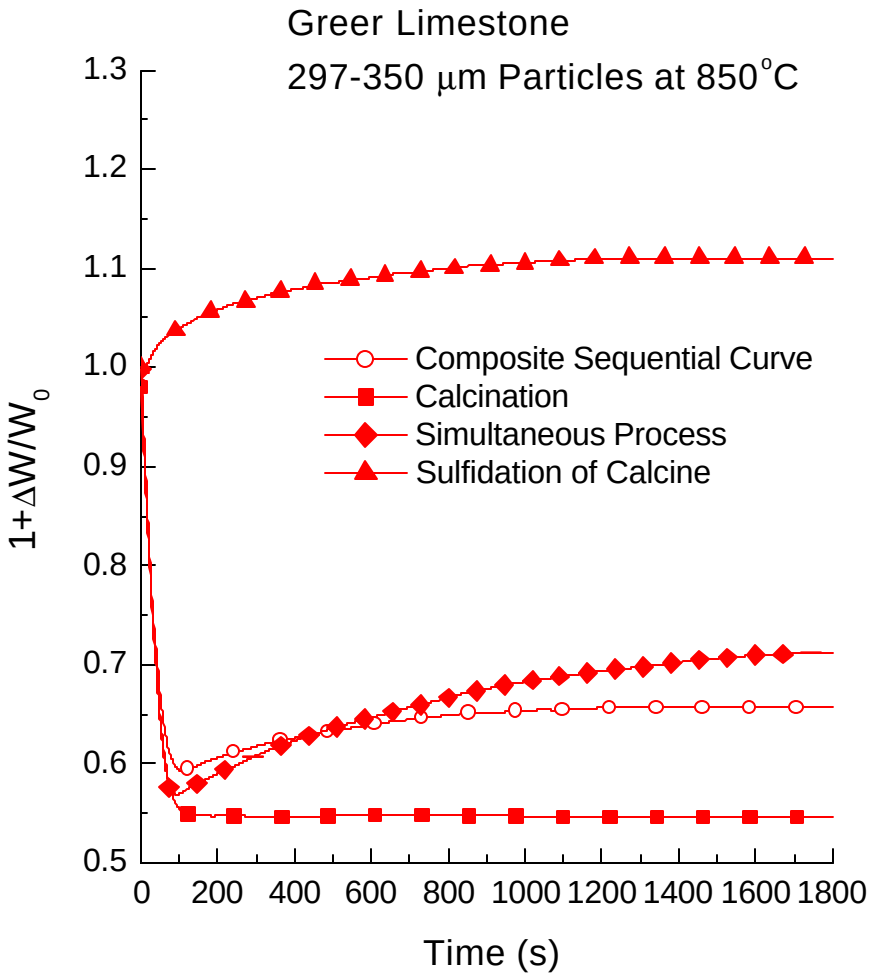

Figure 2.2. Weight vs. time curves during calcination and sulfidation of 297-350 μm Greer Limestone particles at 850 °C.

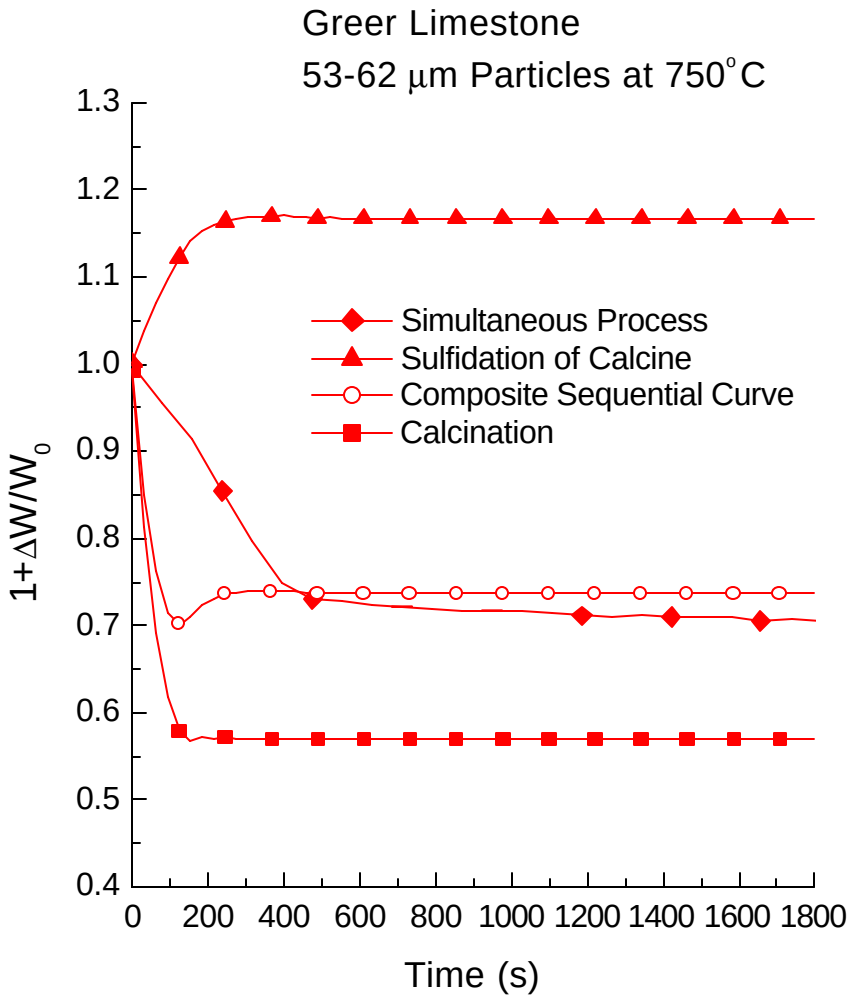

Figure 2.3. Weight vs. time curves during calcination and sulfidation of 53-62 μm Greer Limestone particles at 750 °C.

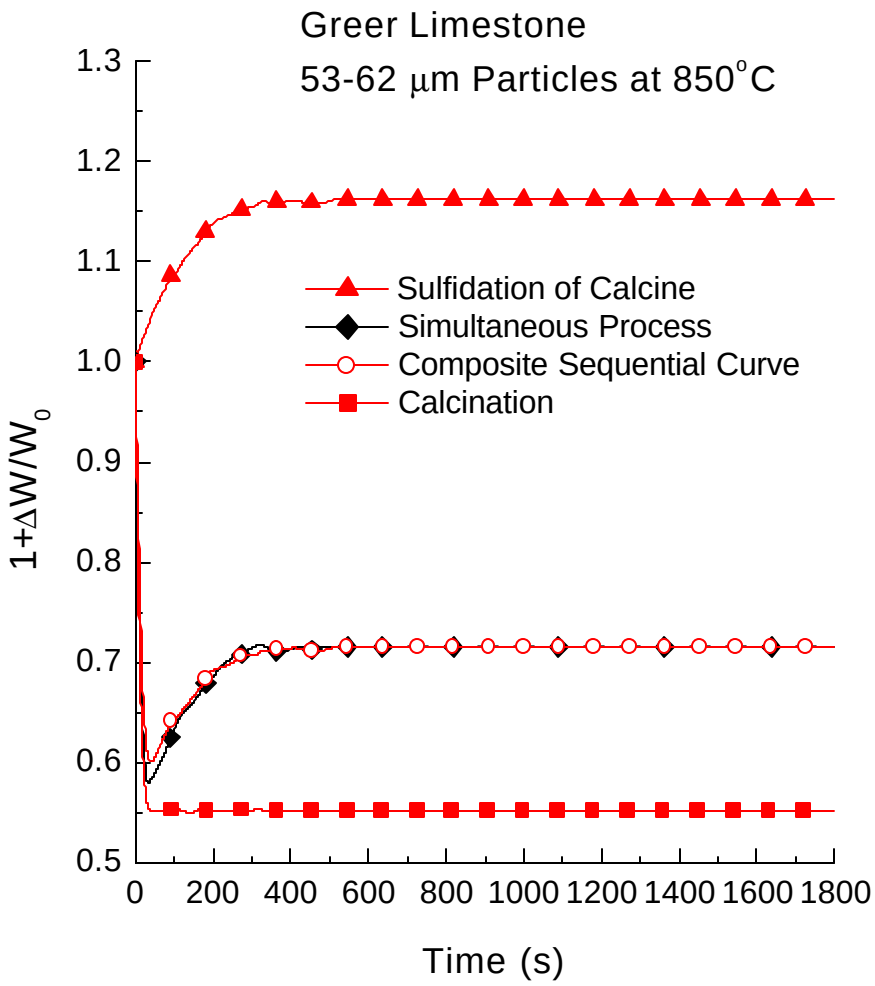

Figure 2.4. Weight vs. time curves during calcination and sulfidation of 53-62 μm Greer Limestone particles at 850 °C.

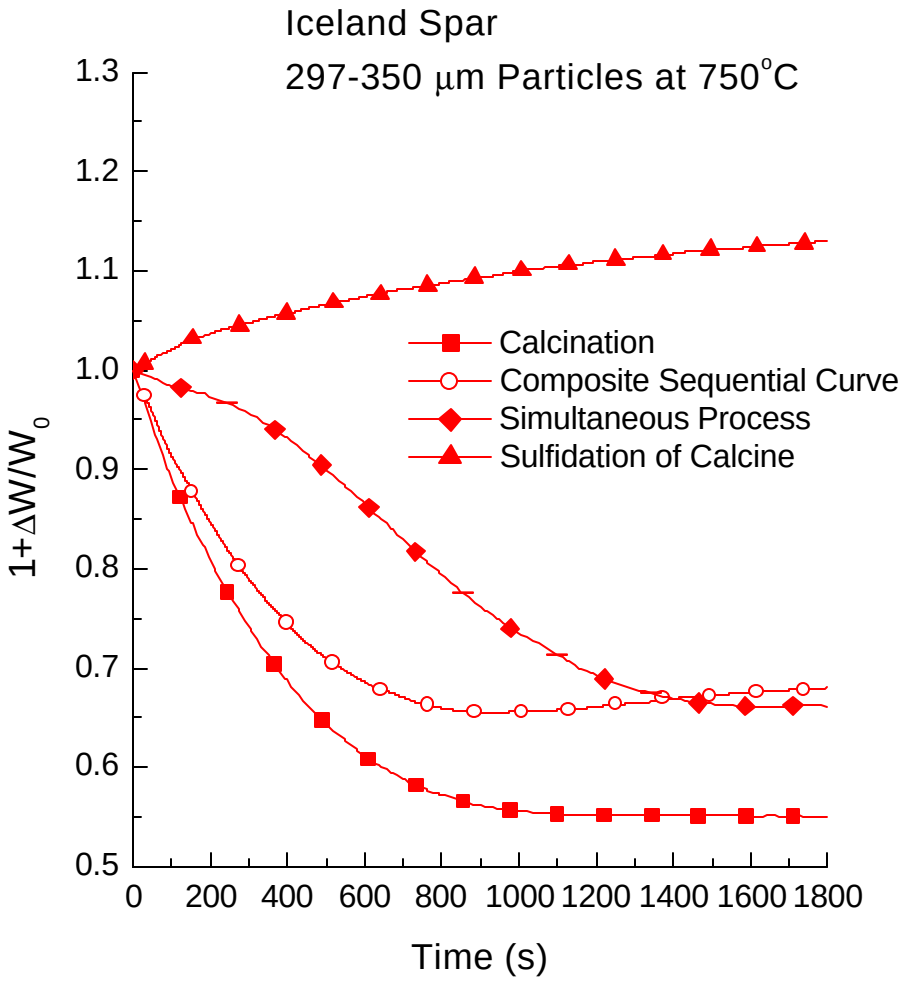

Figure 2.5. Weight vs. time curves during calcination and sulfidation of 297-350 μm Iceland Spar particles at 750 °C.

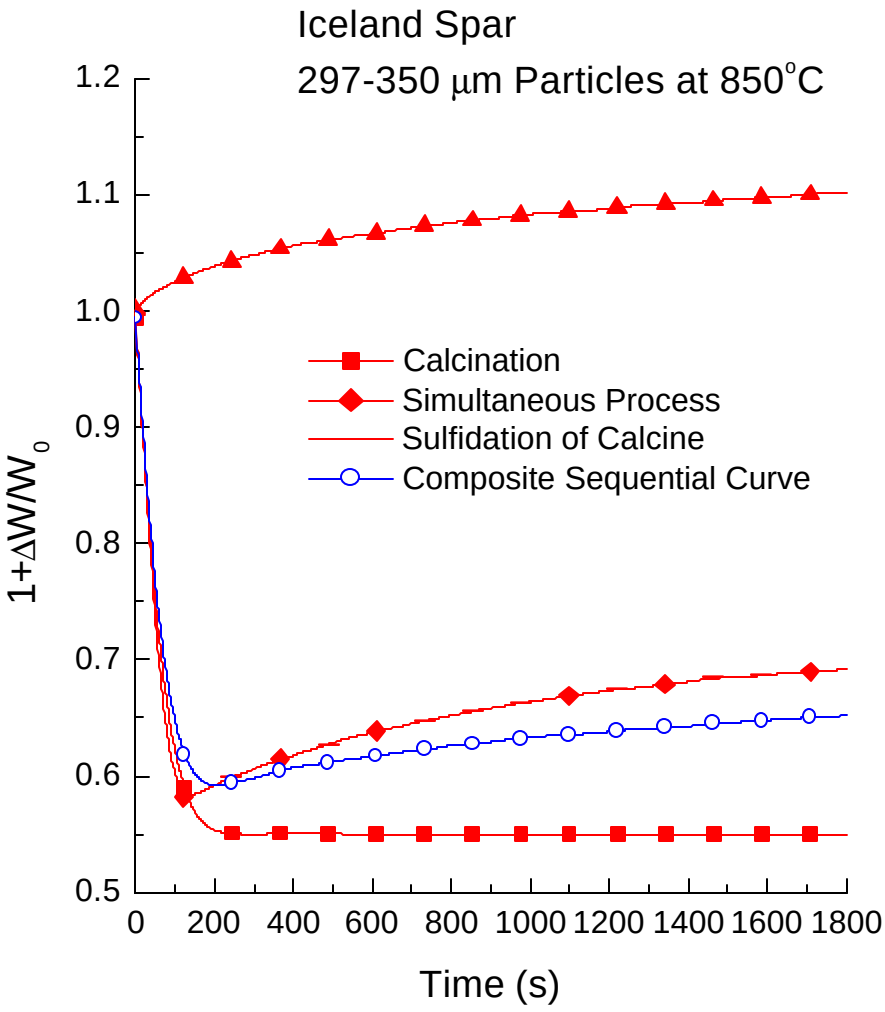

Figure 2.6. Weight vs. time curves during calcination and sulfidation of 297-350 μm Iceland Spar particles at 850 °C.

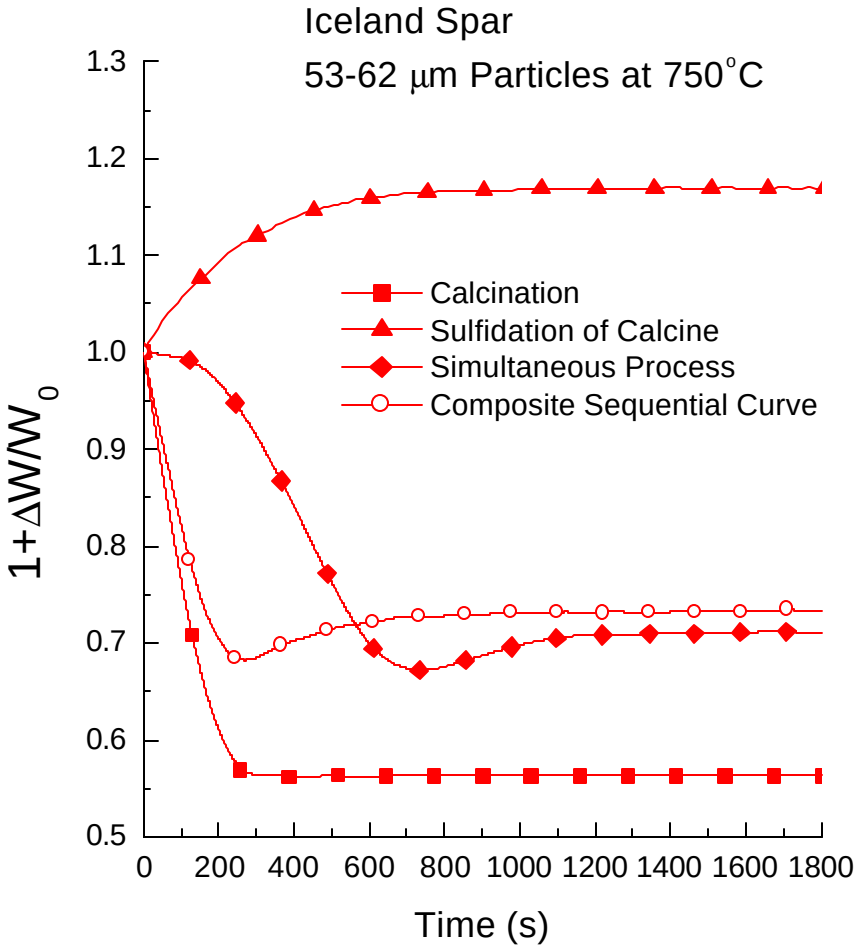

Figure 2.7. Weight vs. time curves during calcination and sulfidation of 53-62 μm Iceland Spar particles at 750 °C.

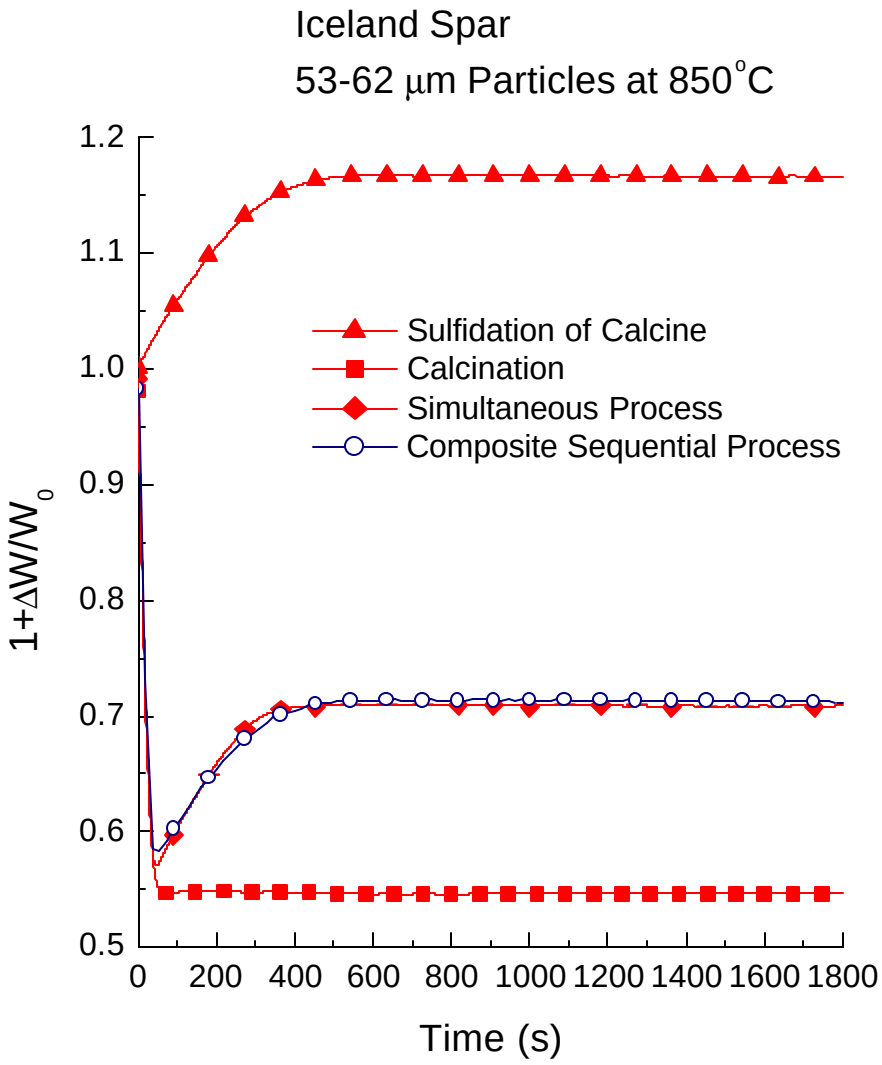

Figure 2.8. Weight vs. time curves during calcination and sulfidation of 53-62 μm Iceland Spar particles at 850 °C.

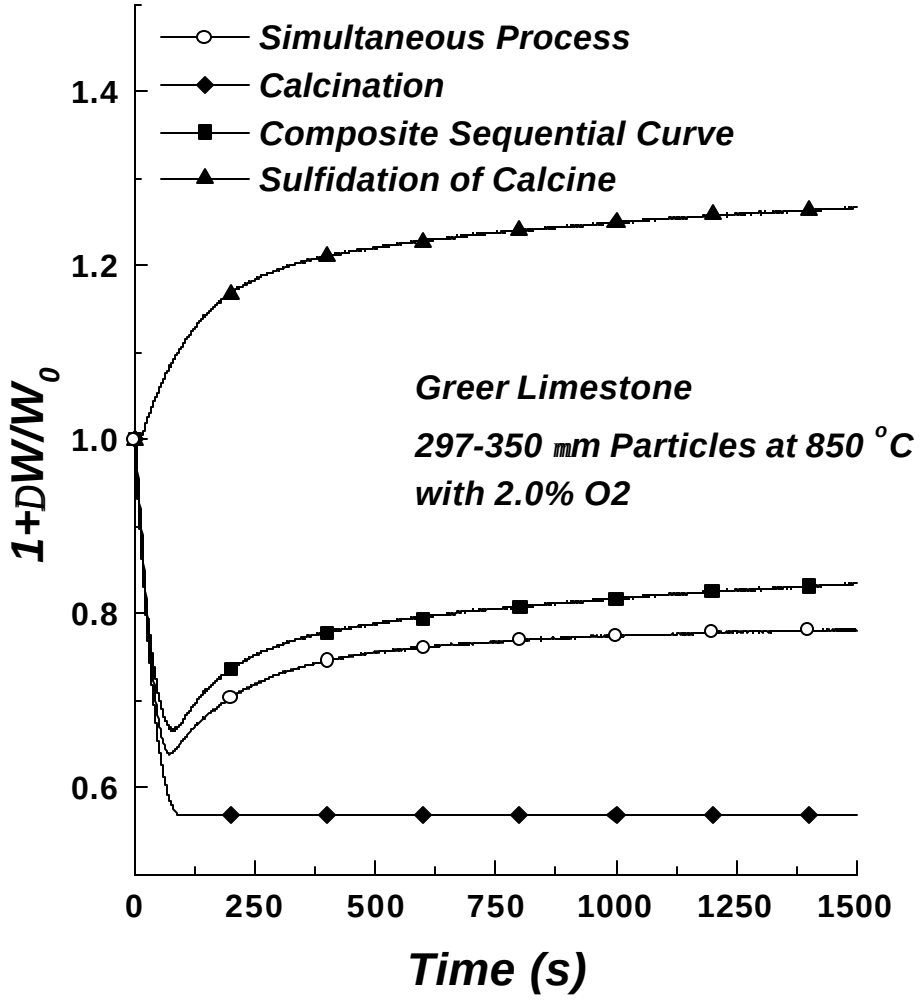

Figure 3.1. Variation of the conversion of Greer Limestone 297-350 μm particles at 850 °C during sulfidation simultaneously or sequentially with calcination in the presence of 2% oxygen in the N_2-H_2S mixture.

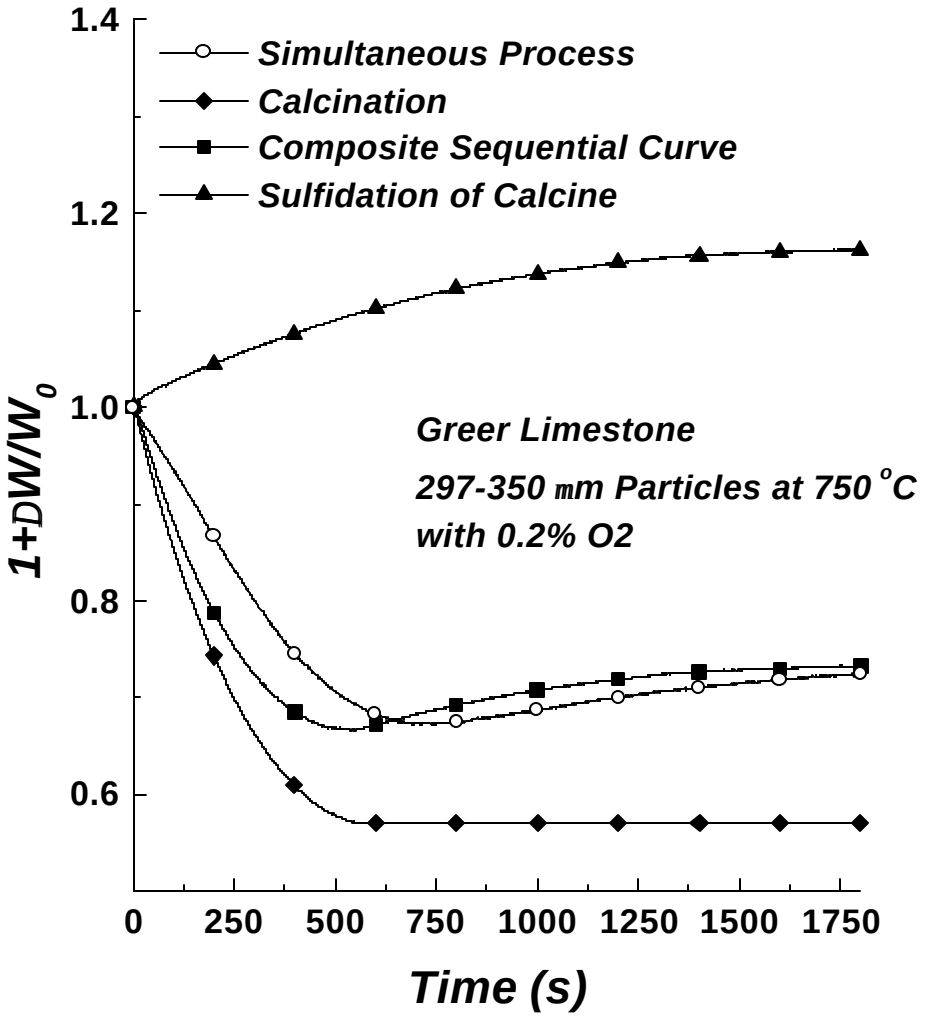

Figure 3.2. Variation of the conversion of Greer Limestone 297-350 μm particles at 750 °C during sulfidation simultaneously or sequentially with calcination in the presence of 0.2% oxygen in the N_2-H_2S mixture.

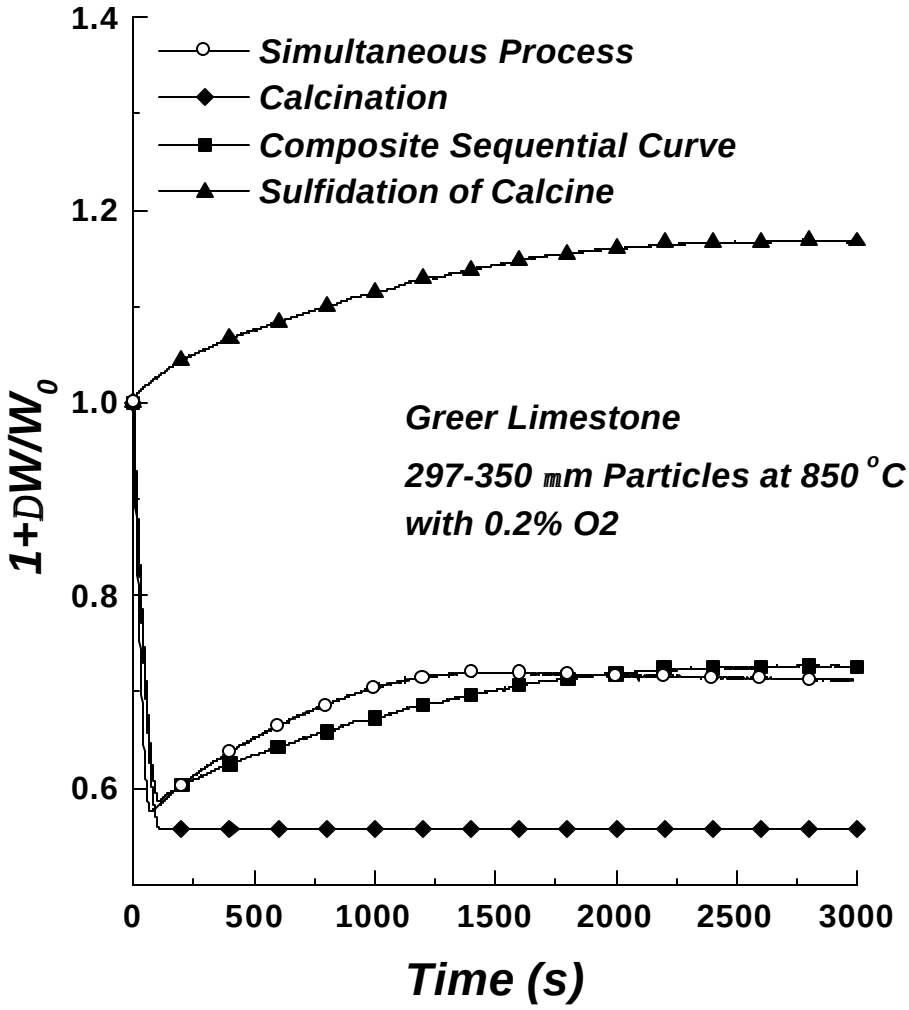

Figure 3.3. Variation of the conversion of Greer Limestone 297-350 μm particles at 850 °C during sulfidation simultaneously or sequentially with calcination in the presence of 0.2% oxygen in the N_2-H_2S mixture.

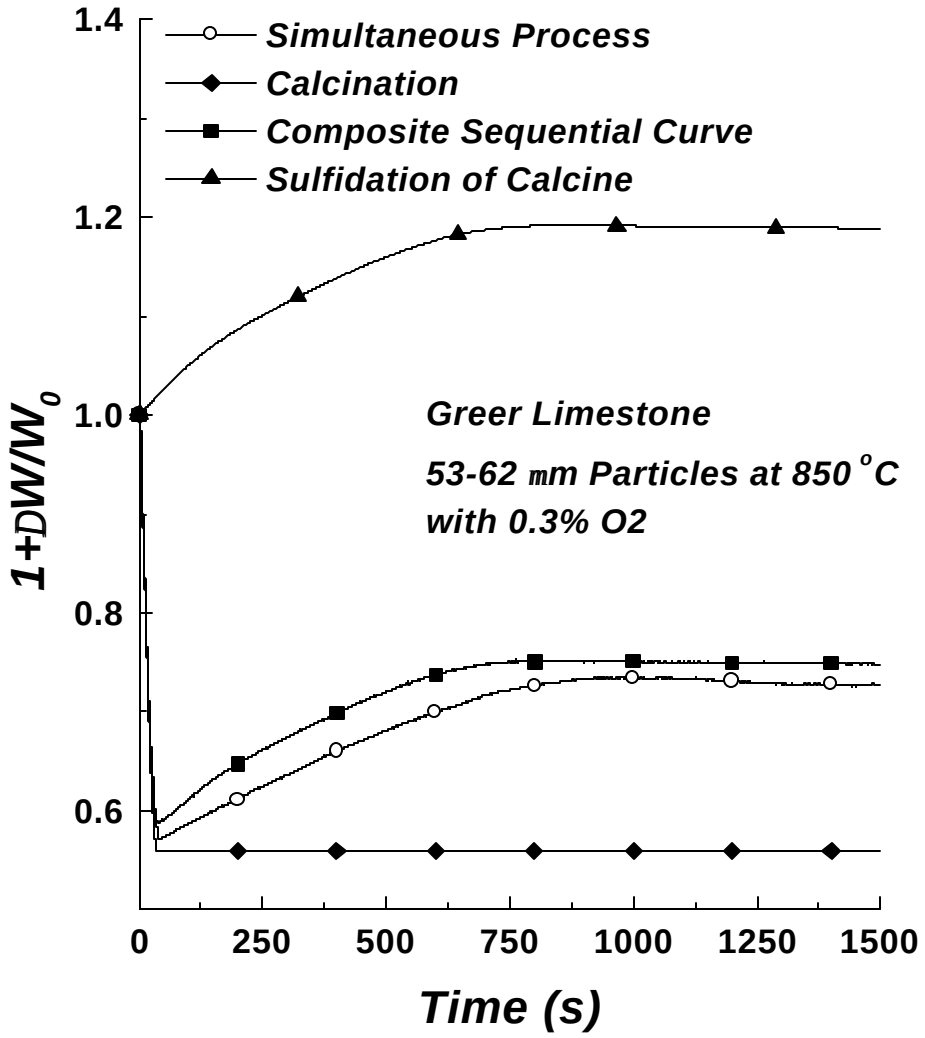

Figure 3.4. Variation of the conversion of Greer Limestone 53-62 μm particles at 850 °C during sulfidation simultaneously or sequentially with calcination in the presence of 0.3% oxygen in the N_2-H_2S mixture.

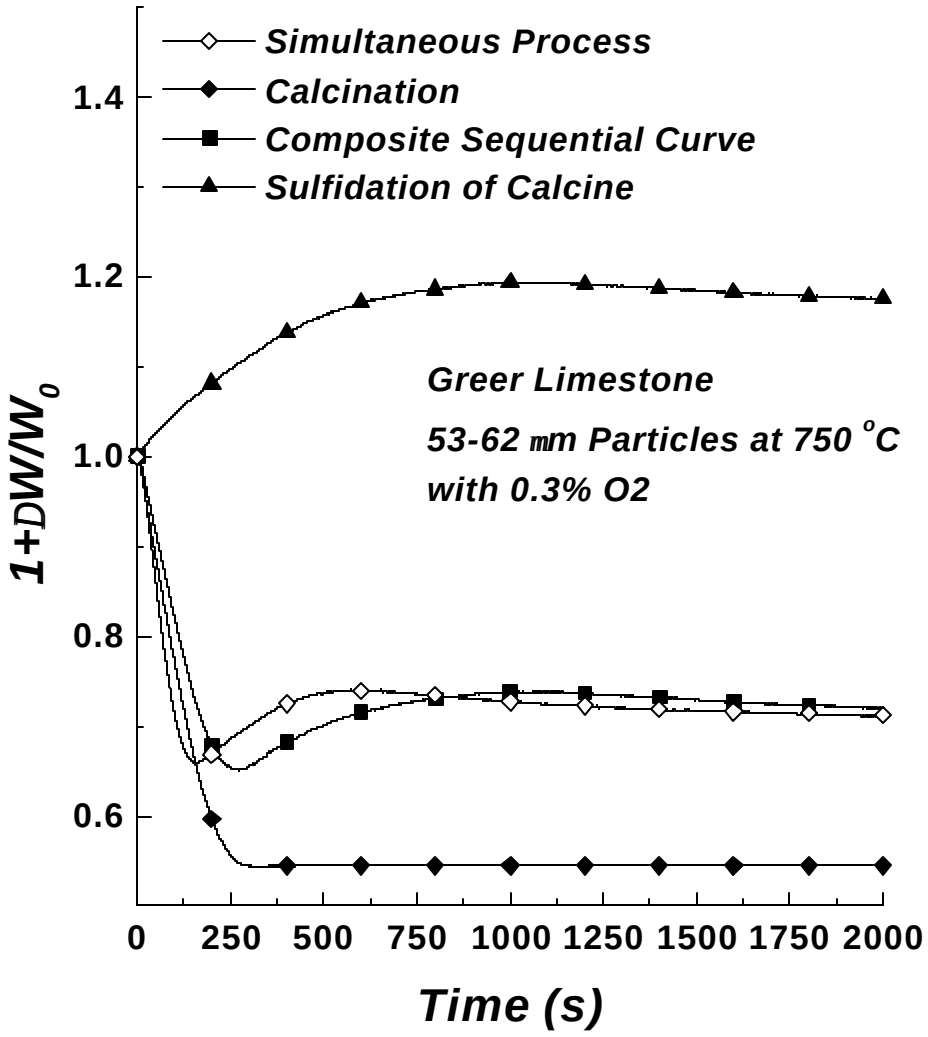

Figure 3.5. Variation of the conversion of Greer Limestone 53-62 μm particles at 750 °C during sulfidation simultaneously or sequentially with calcination in the presence of 0.3% oxygen in the N_2-H_2S mixture.

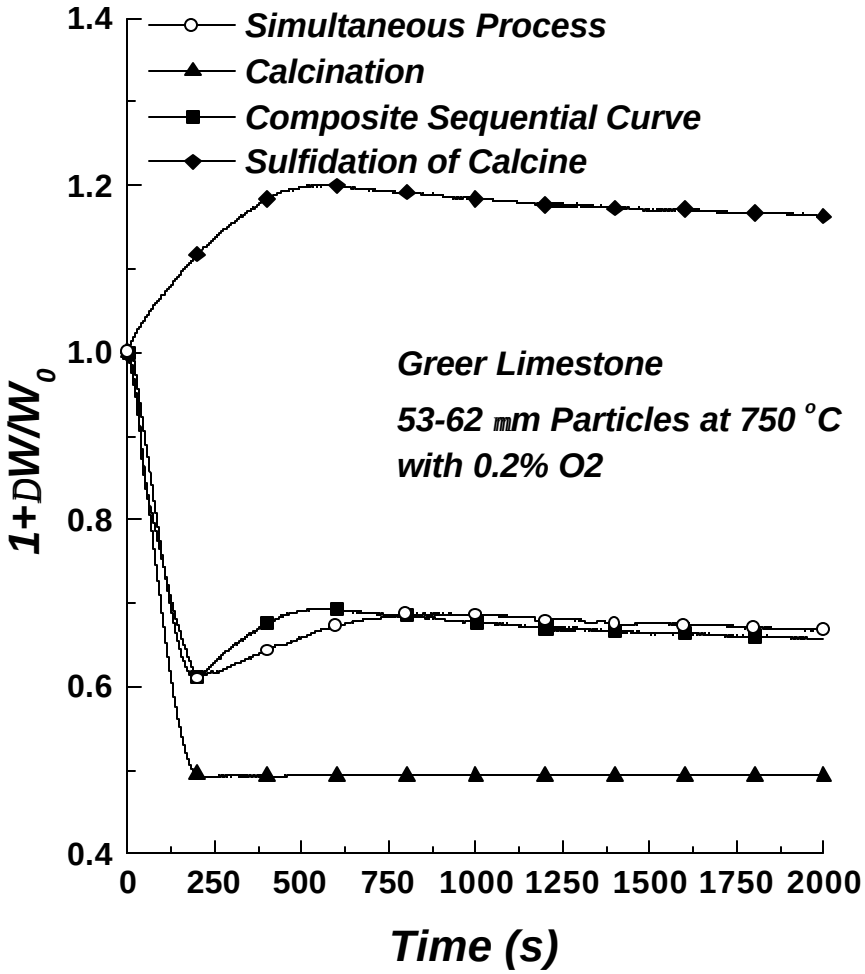

Figure 3.6. Variation of the conversion of Greer Limestone 53-62 μm particles at 750 °C during sulfidation simultaneously or sequentially with calcination in the presence of 0.2% oxygen in the N_2-H_2S mixture.

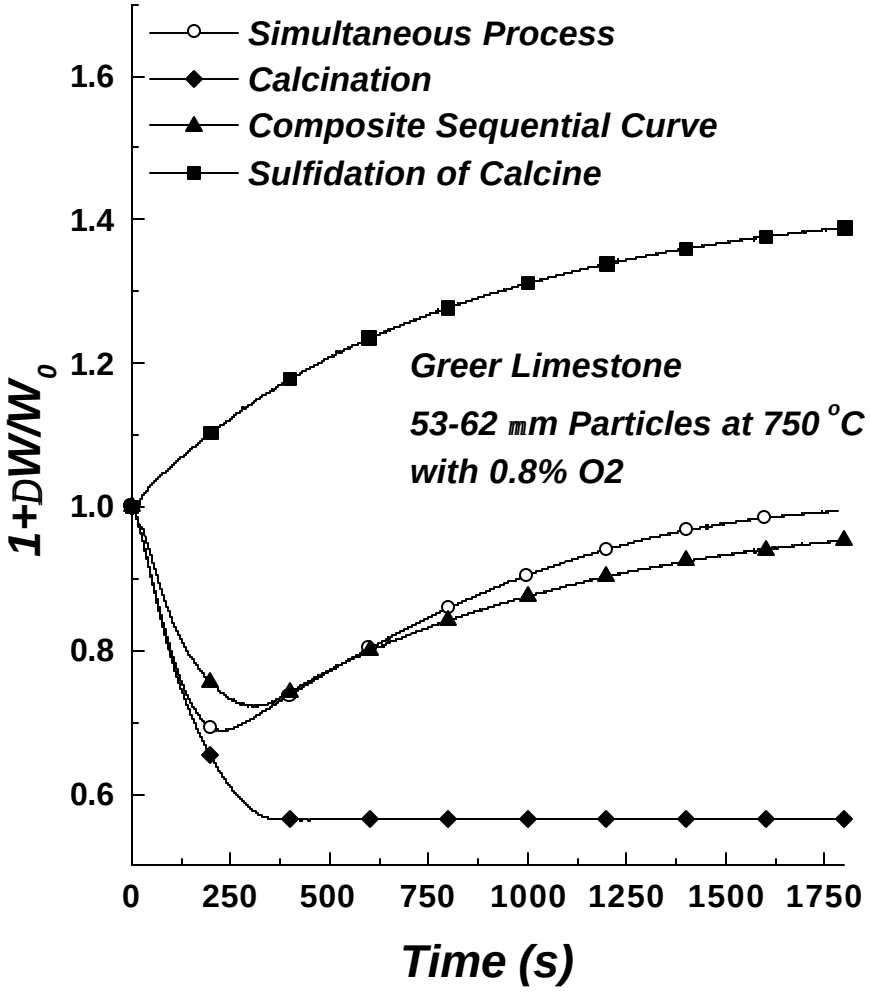

Figure 3.7. Variation of the conversion of Greer Limestone 53-62 μm particles at 750 °C during sulfidation simultaneously or sequentially with calcination in the presence of 0.8% oxygen in the N_2-H_2S mixture.

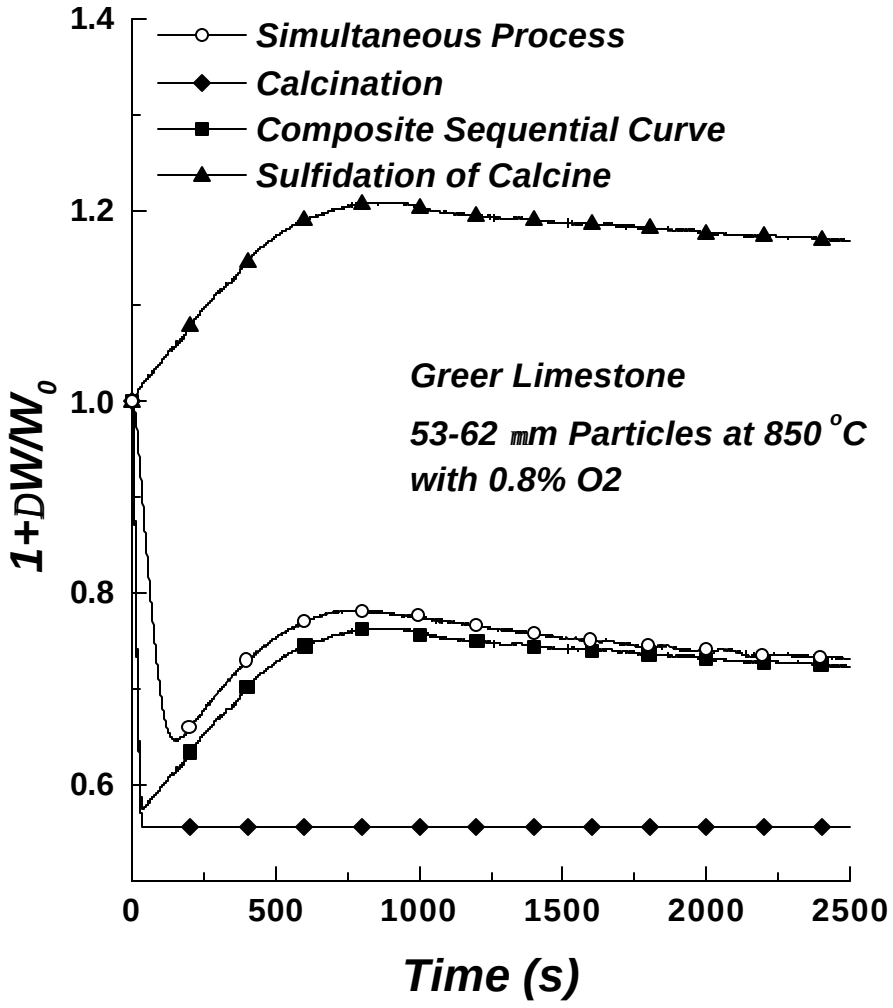

Figure 3.8. Variation of the conversion of Greer Limestone 53-62 μm particles at 850 °C during sulfidation simultaneously or sequentially with calcination in the presence of 0.8% oxygen in the N_2-H_2S mixture.

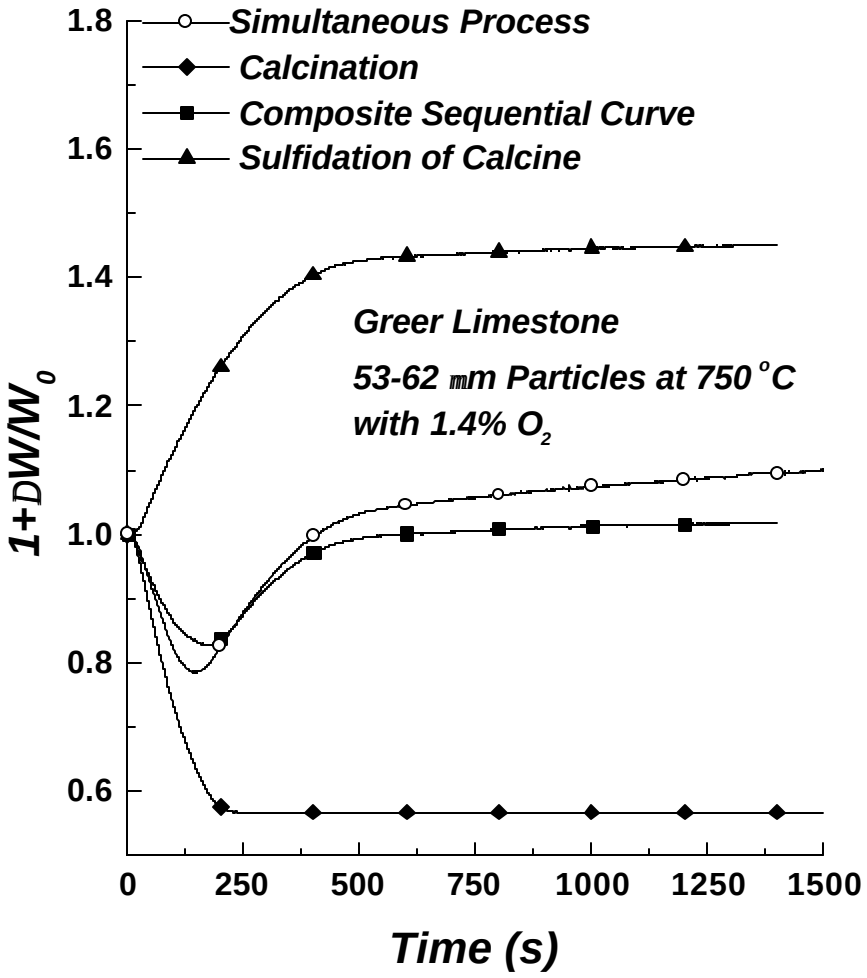

Figure 3.9. Variation of the conversion of Greer Limestone 53-62 μm particles at 750 °C during sulfidation simultaneously or sequentially with calcination in the presence of 1.4% oxygen in the N_2-H_2S mixture.

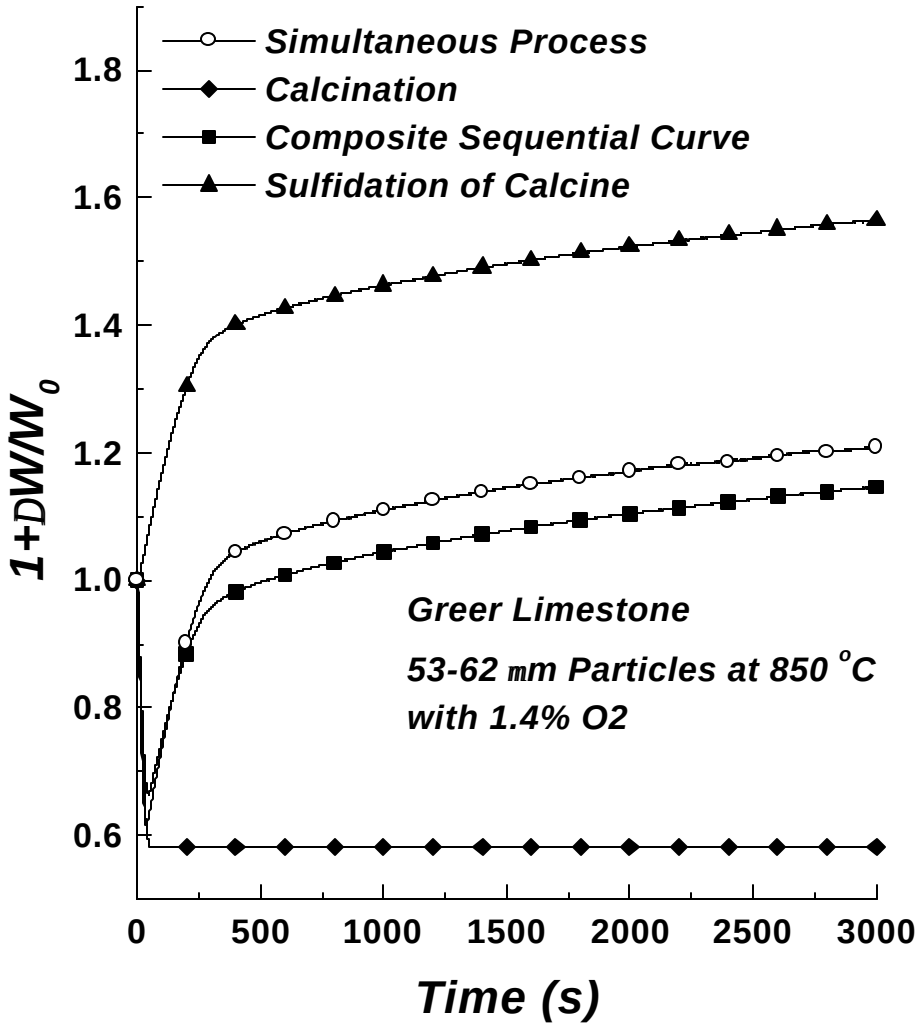

Figure 3.10. Variation of the conversion of Greer Limestone 53-62 μm particles at 850 °C during sulfidation simultaneously or sequentially with calcination in the presence of 1.4% oxygen in the N_2-H_2S mixture.

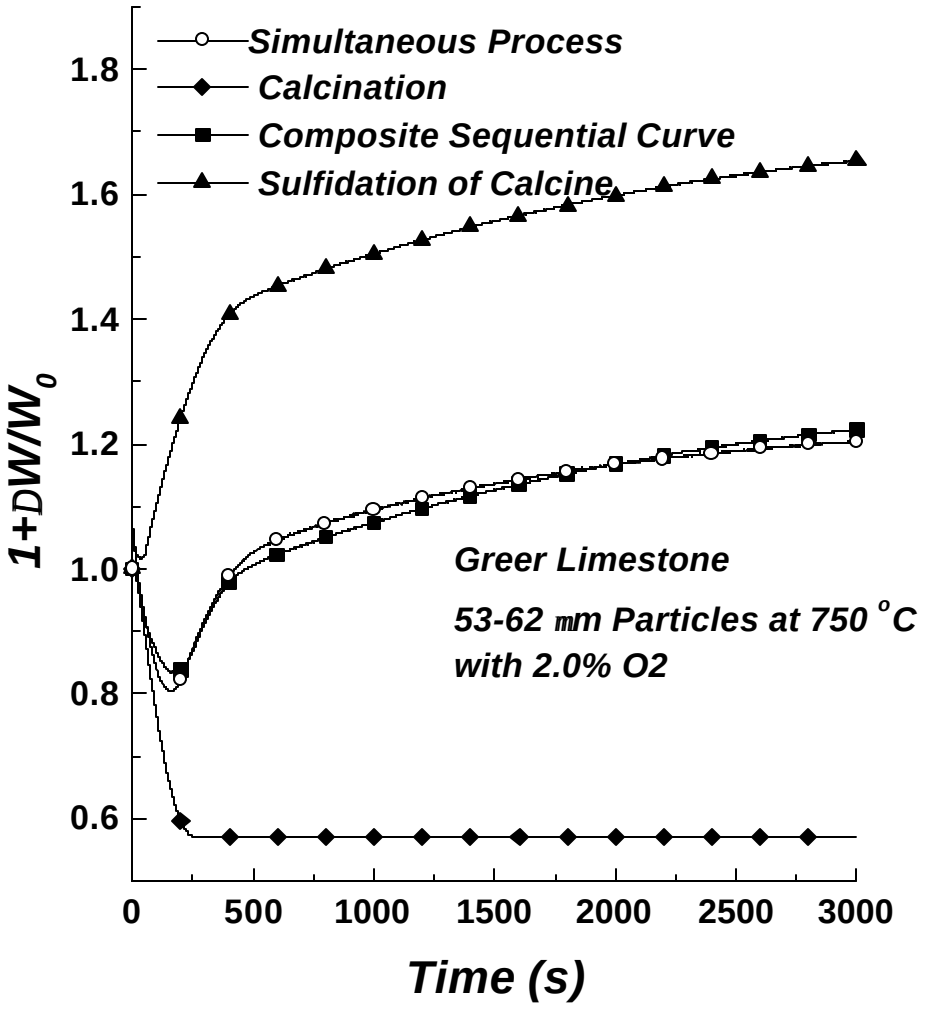

Figure 3.11. Variation of the conversion of Greer Limestone 53-62 μm particles at 750 °C during sulfidation simultaneously or sequentially with calcination in the presence of 2% oxygen in the N_2-H_2S mixture.

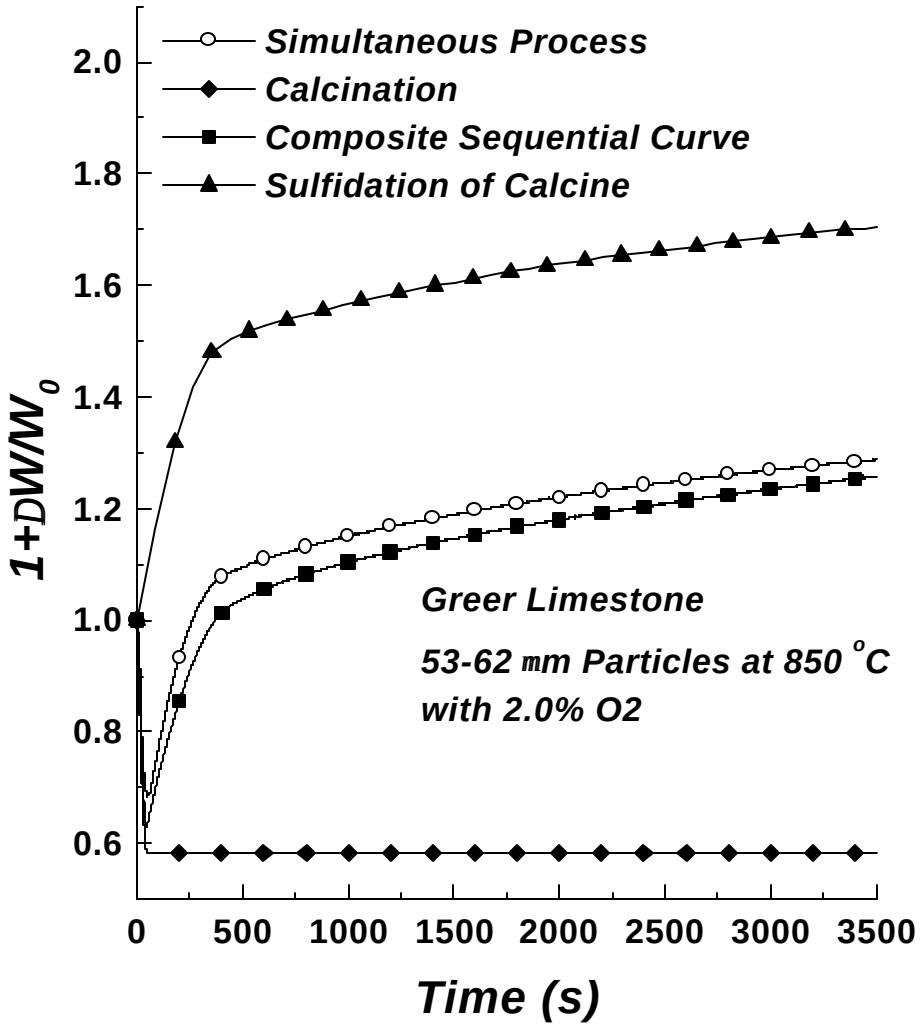

Figure 3.12. Variation of the conversion of Greer Limestone 53-62 μm particles at 850 °C during sulfidation simultaneously or sequentially with calcination in the presence of 2% oxygen in the N_2-H_2S mixture.

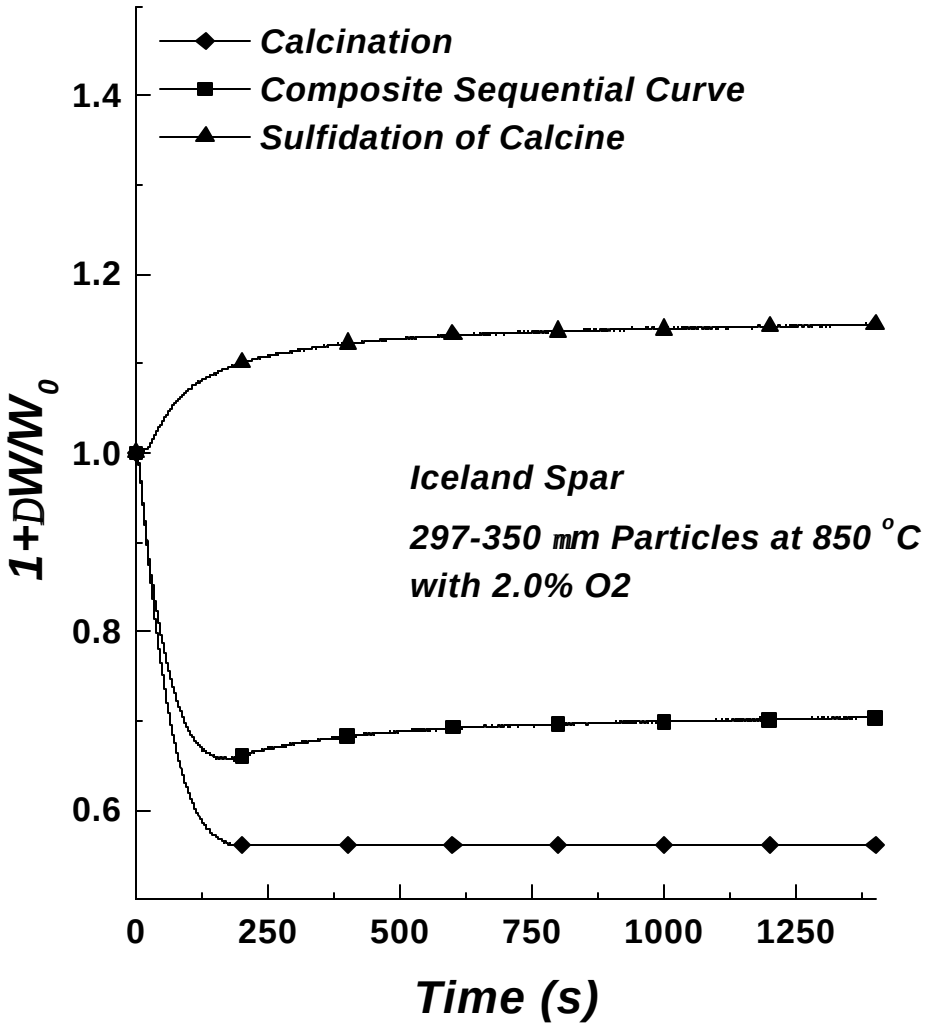

Figure 3.13. Variation of the conversion of Iceland Spar 297-350 μm particles at 850 ^{o}C during sulfidation sequentially with calcination in the presence of 2% oxygen in the N_2-H_2S mixture.

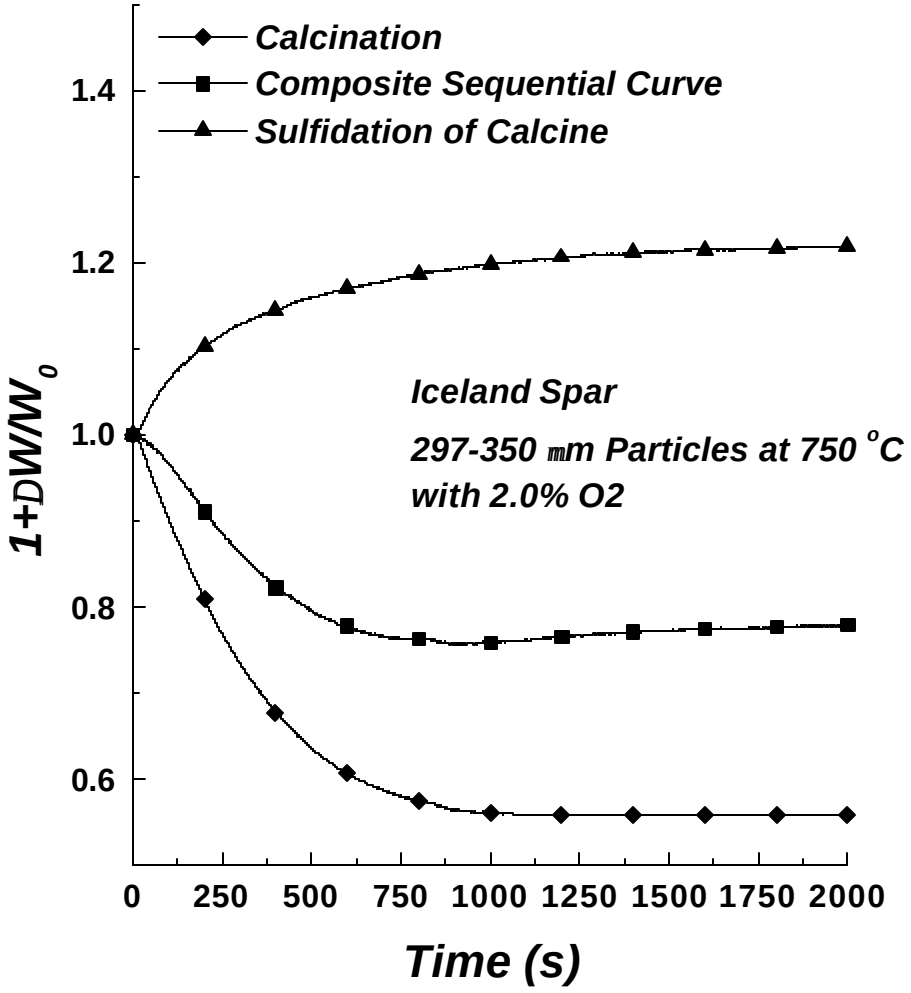

Figure 3.14. Variation of the conversion of Iceland Spar 297-350 μm particles at 750 ^{o}C during sulfidation sequentially with calcination in the presence of 2% oxygen in the N_2-H_2S mixture.

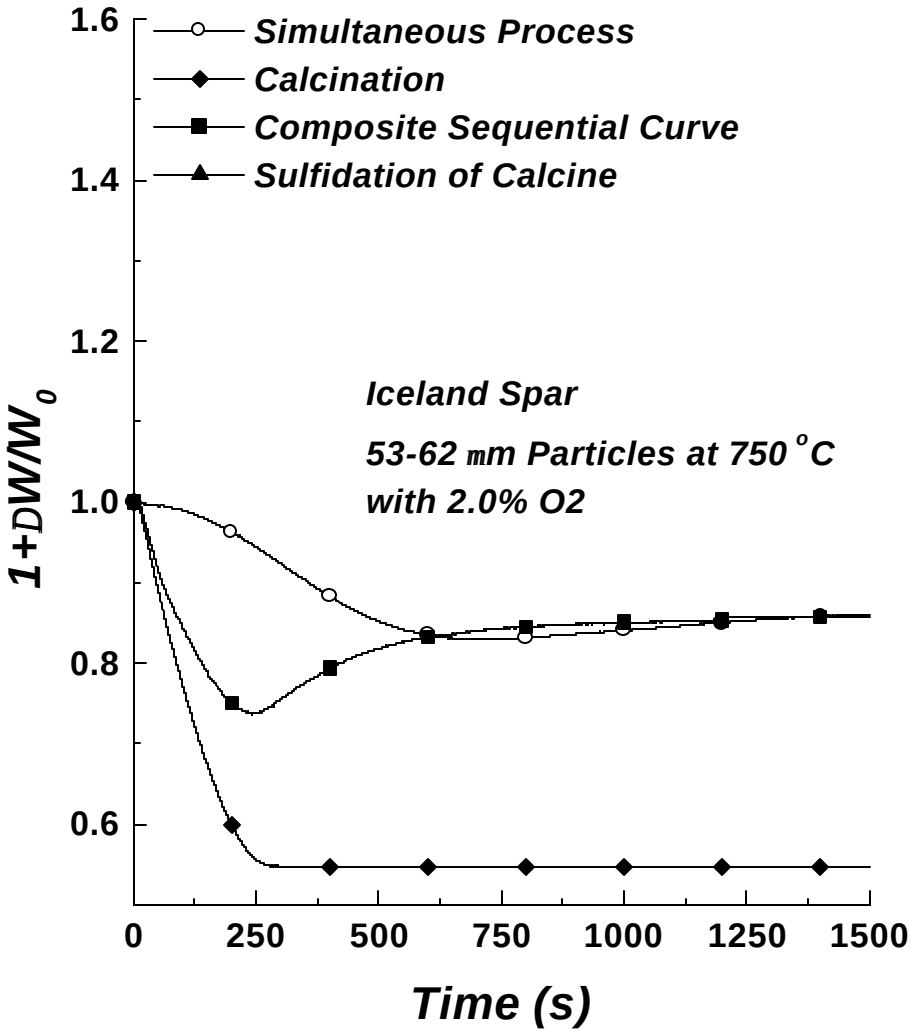

Figure 3.15. Variation of the conversion of Iceland Spar 53-62 μm particles at 750 °C during sulfidation simultaneously or sequentially with calcination in the presence of 2% oxygen in the N_2-H_2S mixture.

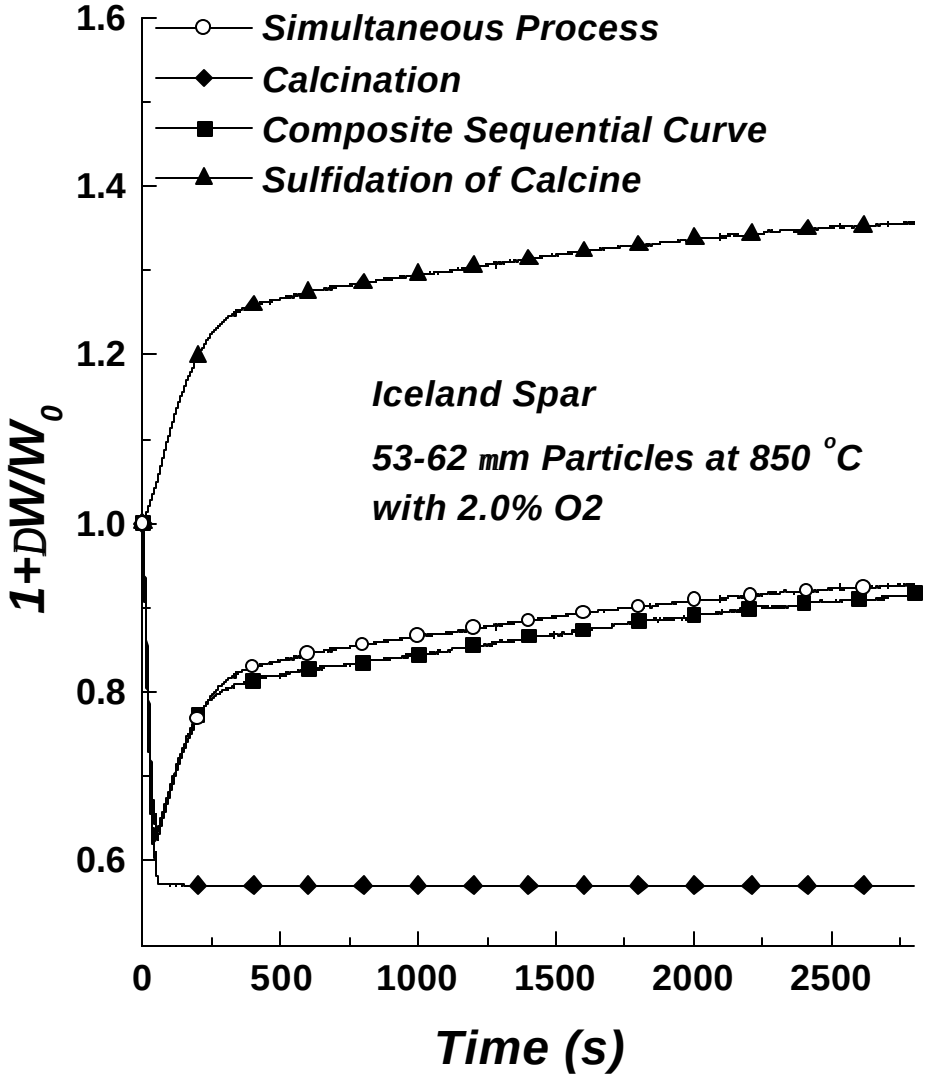

Figure 3.16. Variation of the conversion of Iceland Spar 53-62 μm particles at 850 °C during sulfidation simultaneously or sequentially with calcination in the presence of 2% oxygen in the N_2-H_2S mixture.

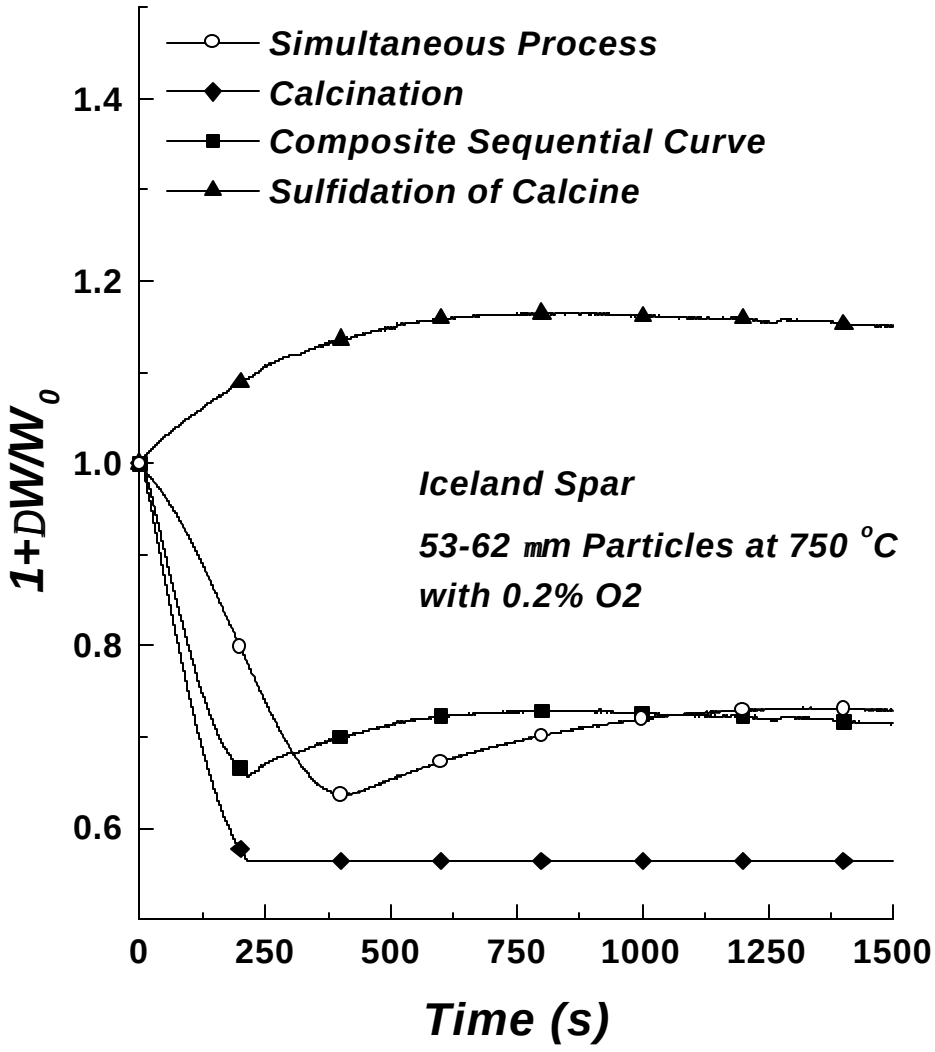

Figure 3.17. Variation of the conversion of Iceland Spar 53-62 μm particles at 750 °C during sulfidation simultaneously or sequentially with calcination in the presence of 0.2% oxygen in the N_2-H_2S mixture.

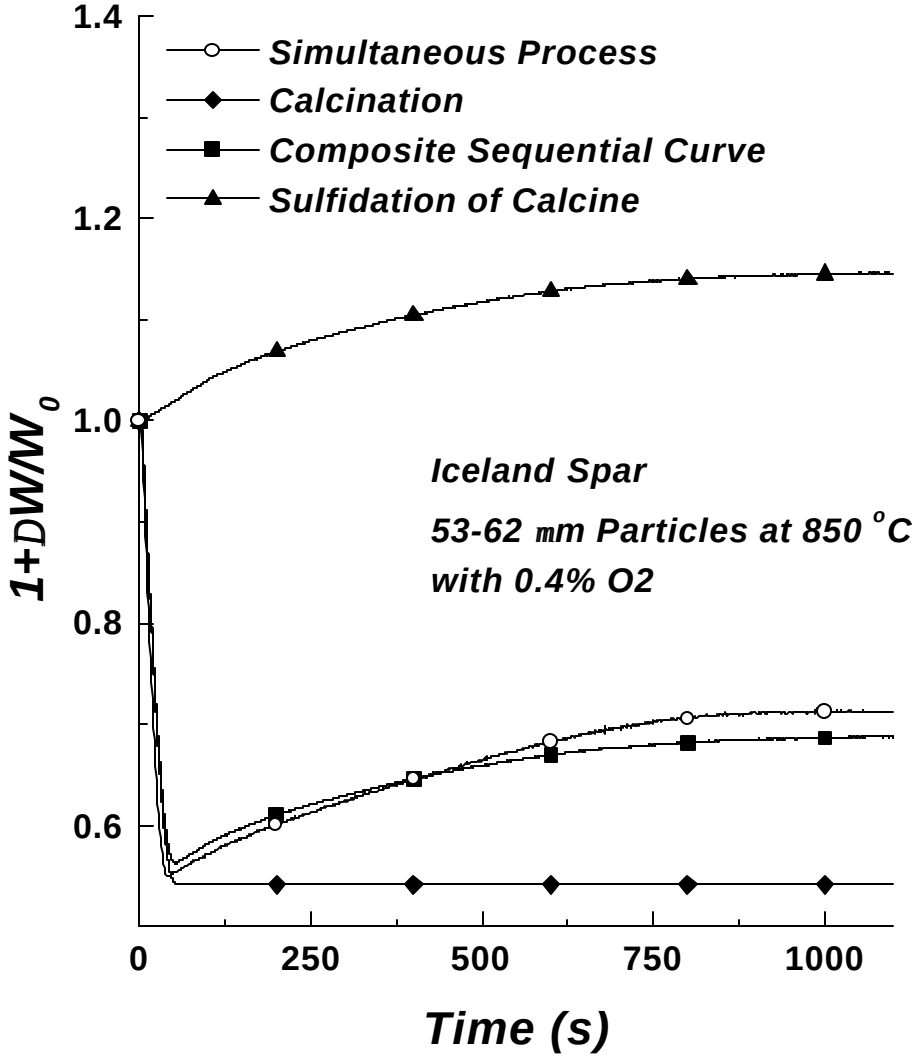

Figure 3.18. Variation of the conversion of Iceland Spar 53-62 μm particles at 850 °C during sulfidation simultaneously or sequentially with calcination in the presence of 0.4% oxygen in the N_2-H_2S mixture.

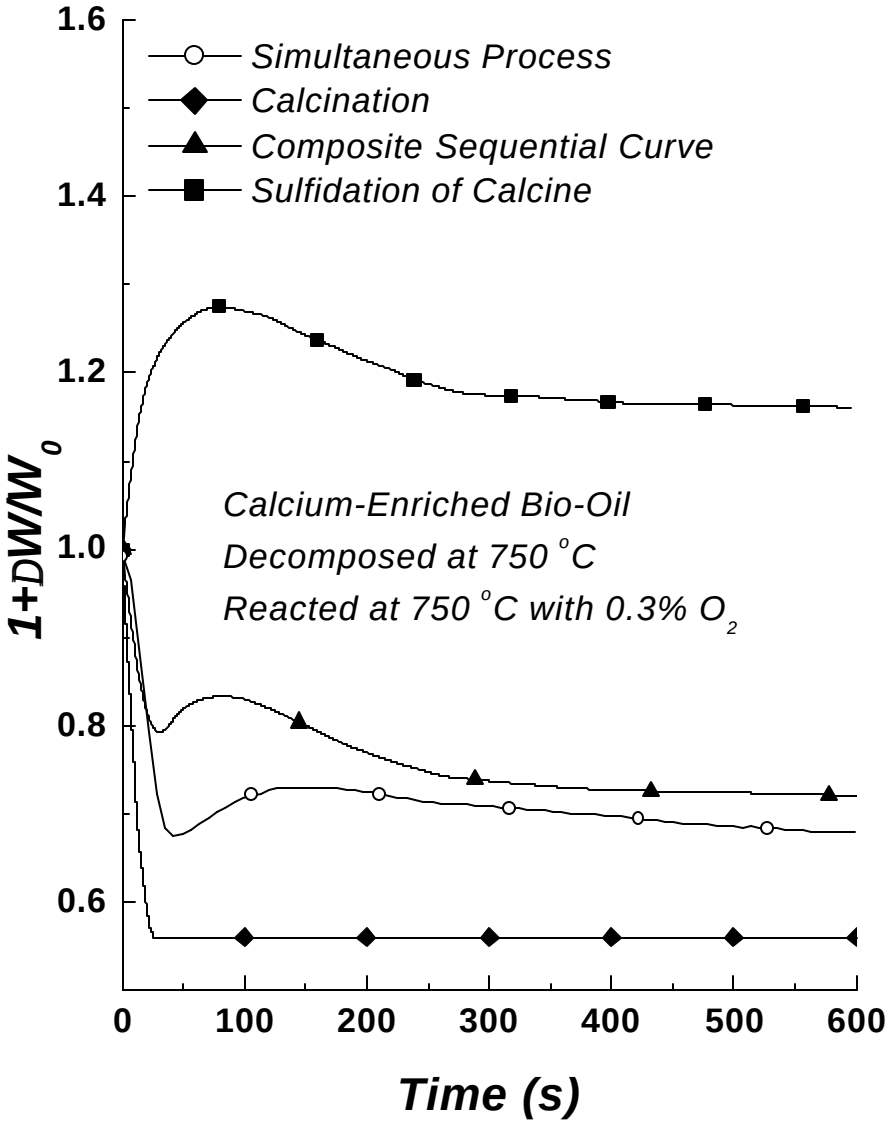

Figure 3.19. Variation of the conversion of calcium carbonate produced through decomposition of calcium-enriched bio-oil at 750 ^{o}C during sulfidation simultaneously or sequentially with calcination in the presence of 0.3% oxygen in the N_2-H_2S mixture.

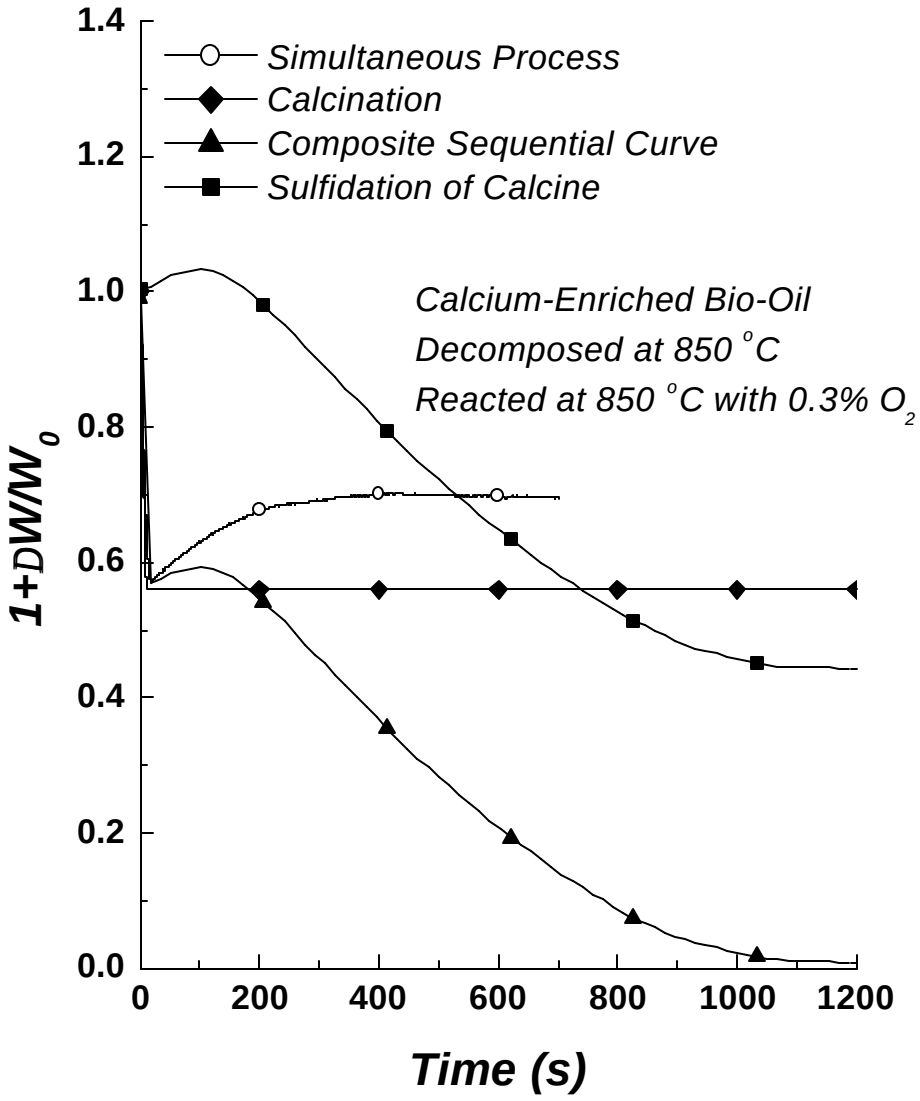

Figure 3.20. Variation of the conversion of calcium carbonate produced through decomposition of calcium-enriched bio-oil at 850 °C during sulfidation simultaneously or sequentially with calcination in the presence of 0.3% oxygen in the N_2-H_2S mixture.

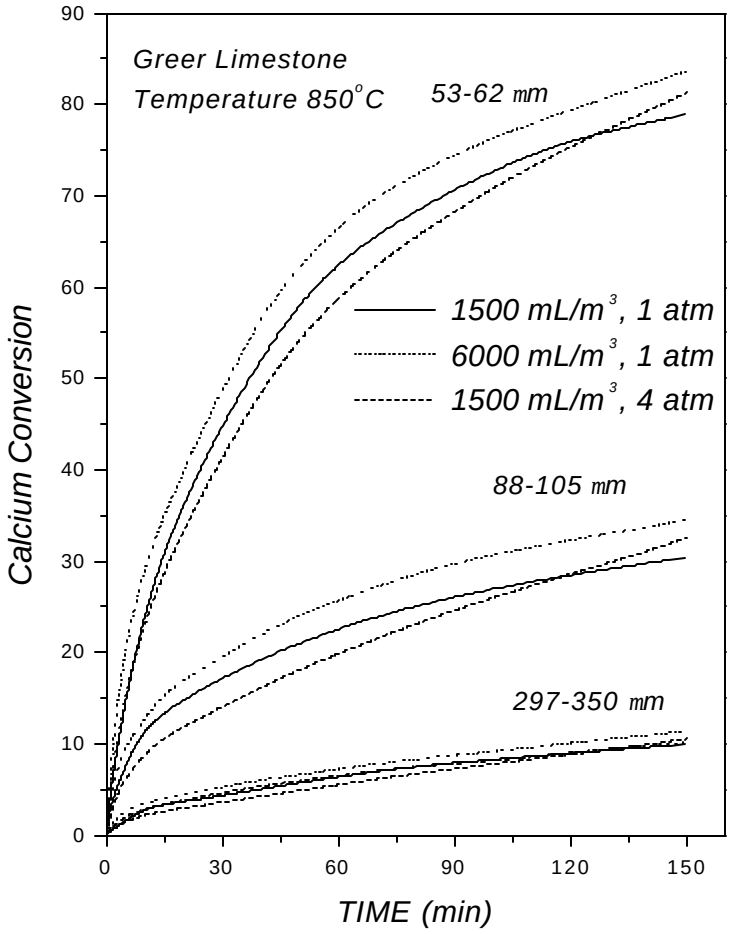

Figure 4.1. Dependence on the variation of the conversion with time for the Greer Limestone sample during direct sulfation at 850 °C on the pressure, the SO_2 concentration, and the particle size.

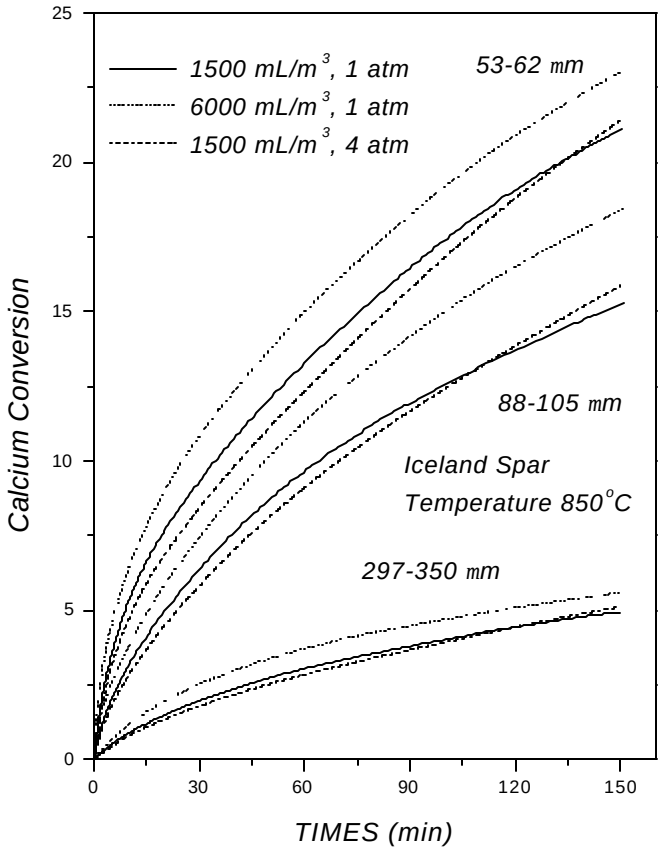

Figure 4.2. Dependence on the variation of the conversion with time for the Iceland Spar sample during direct sulfation at 850 ^{o}C on the pressure, the SO_2 concentration, and the particle size.

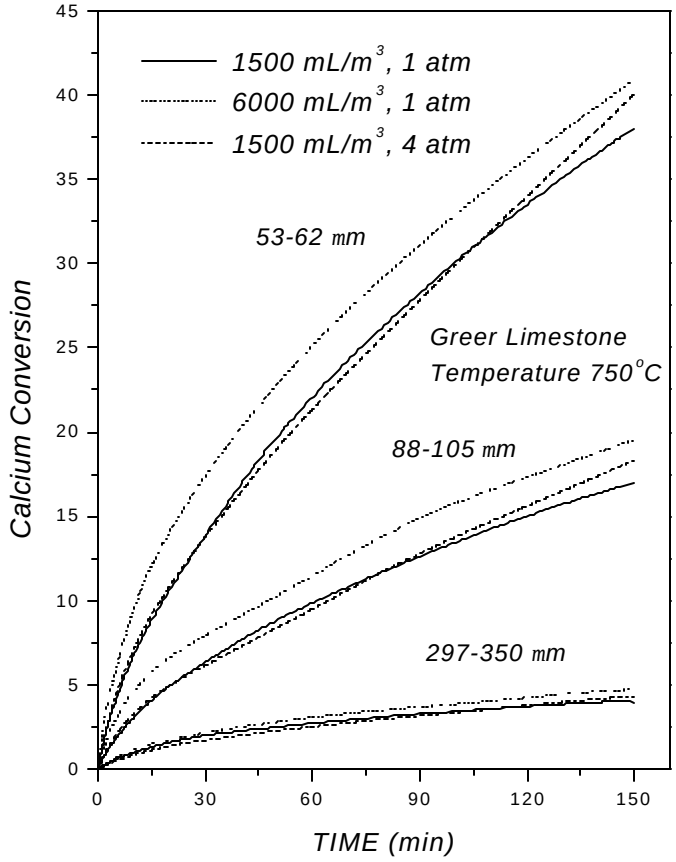

Figure 4.3. Dependence on the variation of the conversion with time for the Greer Limestone sample during direct sulfation at 750 °C on the pressure, the SO_2 concentration, and the particle size.

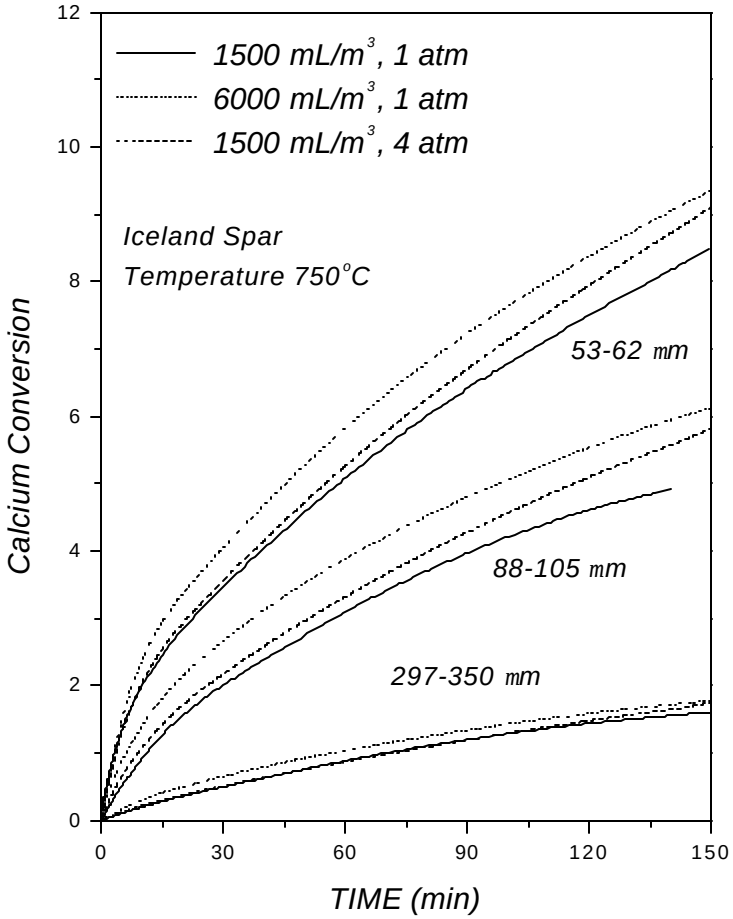

Figure 4.4. Dependence on the variation of the conversion with time for the Iceland Spar sample during direct sulfation at 750 ^{o}C on the pressure, the SO2 concentration, and the particle size.

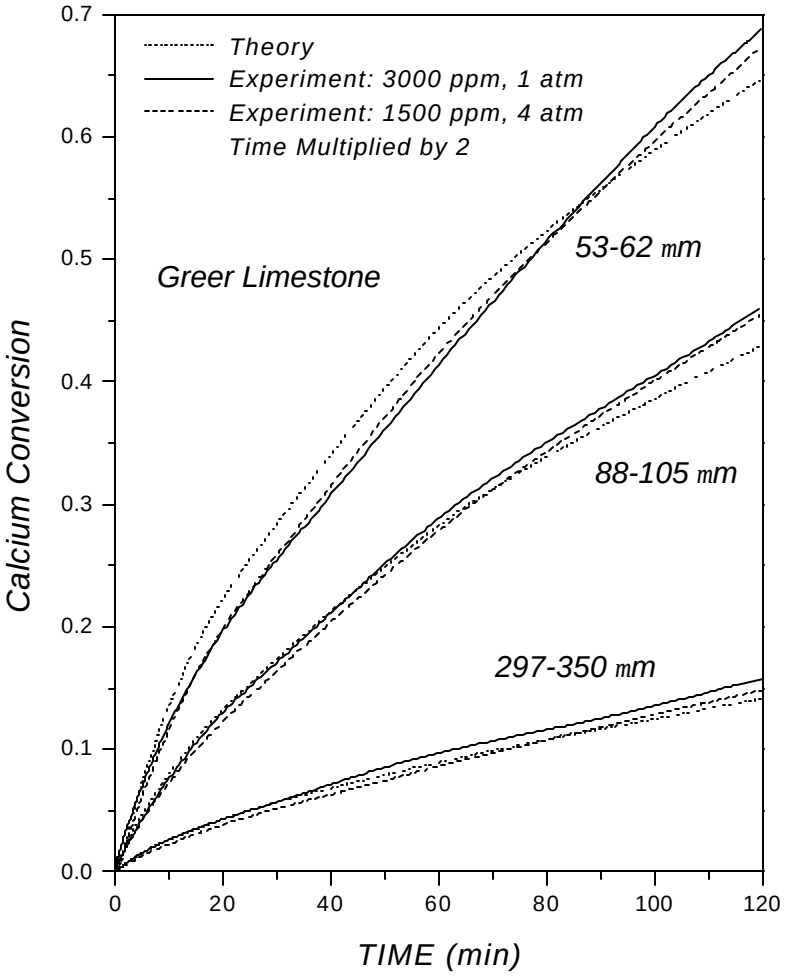

Figure 5.1. Dependence on the variation of the conversion with time for the Greer Limestone sample during direct sulfidation at 750 ^{o}C on the pressure, the H_2S concentration, and the particle size. For 4 atm pressure, the time has been multiplied by 2.

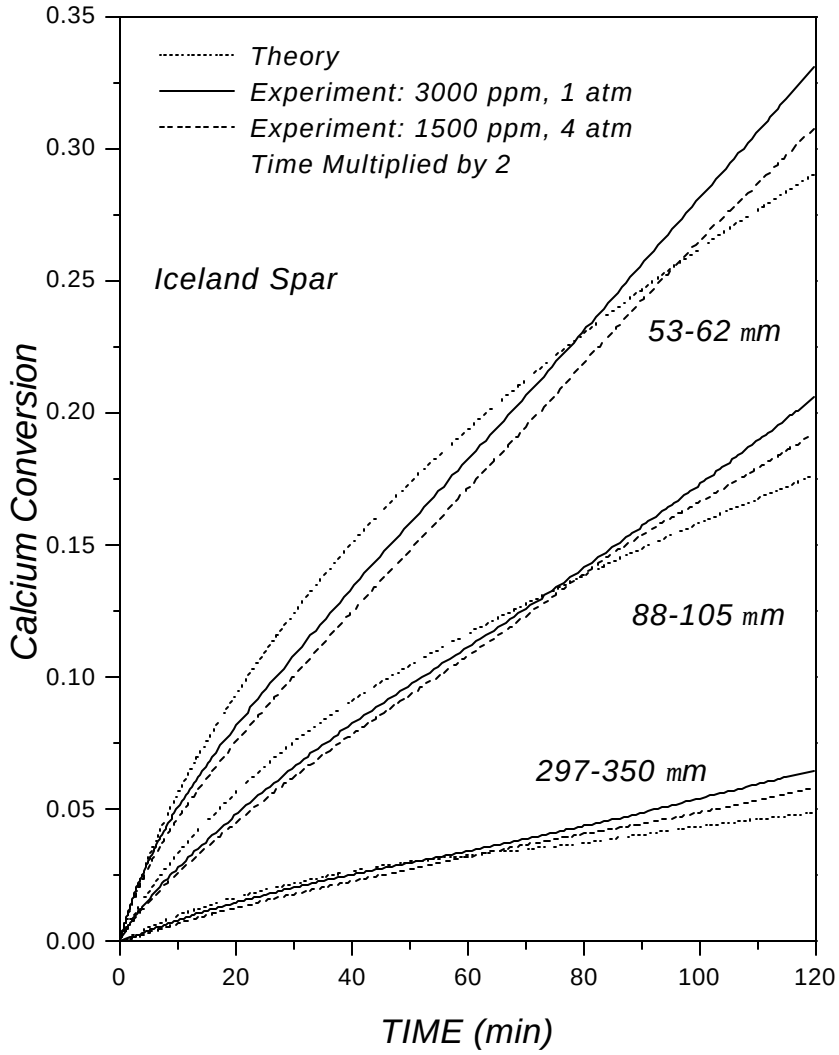

Figure 5.2. Dependence on the variation of the conversion with time for the Iceland Spar sample during direct sulfidation at 750 ^{o}C on the pressure, the H_2S concentration, and the particle size. For 4 atm pressure, the time has been multiplied by 2.

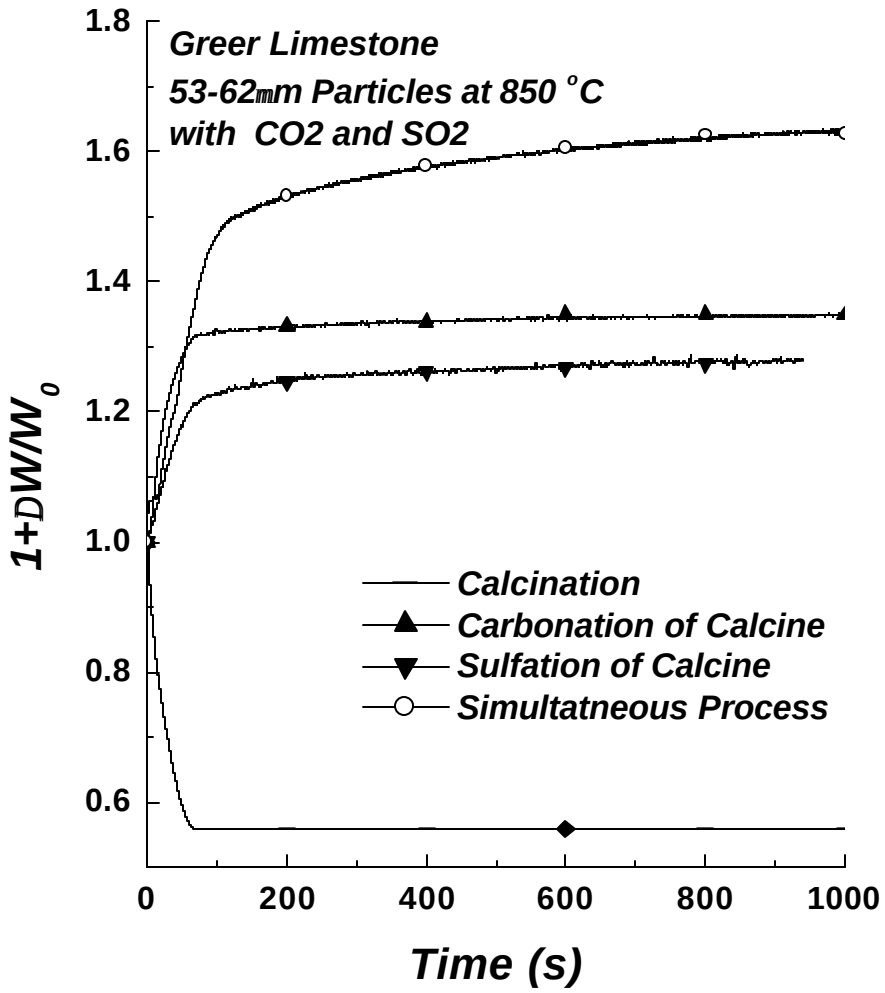

Figure 6.1. Variation of the conversion (weight of the solid sample) with time during calcination and subsequent carbonation, sulfation, or simultaneous carbonation and sulfation for 53-62 μm Greer Limestone particles at 850 °C.

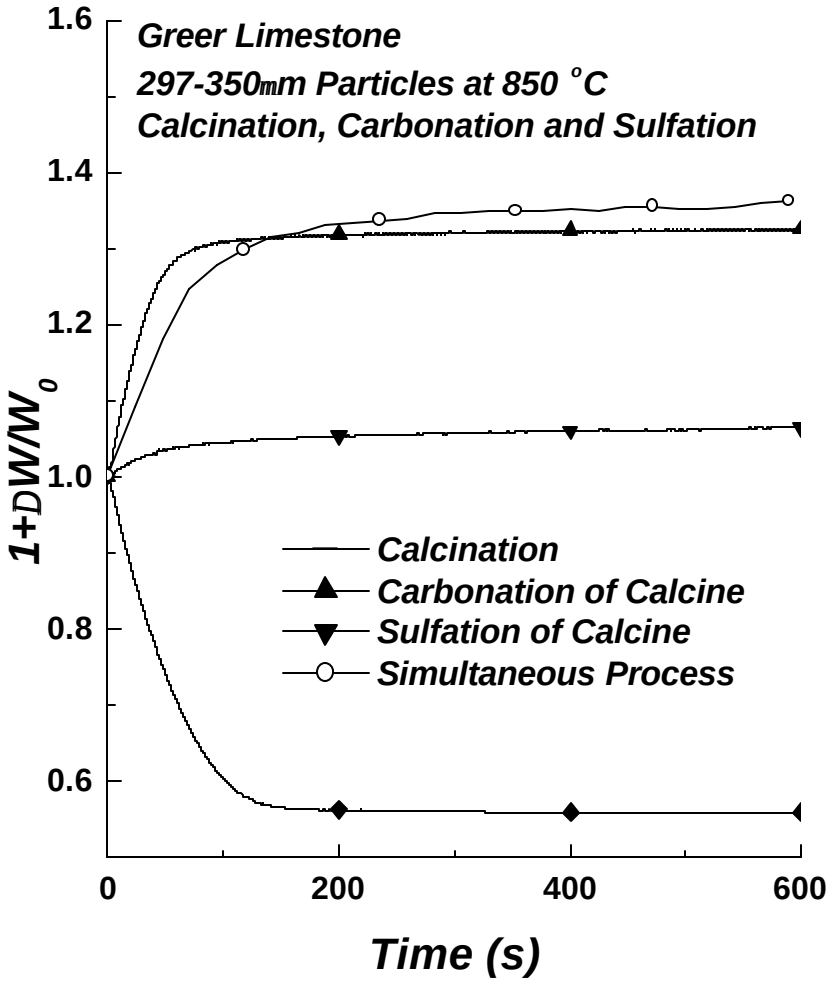

Figure 6.2. Variation of the conversion (weight of the solid sample) with time during calcination and subsequent carbonation, sulfation, or simultaneous carbonation and sulfation for 297-350 μm Greer Limestone particles at 850 °C.

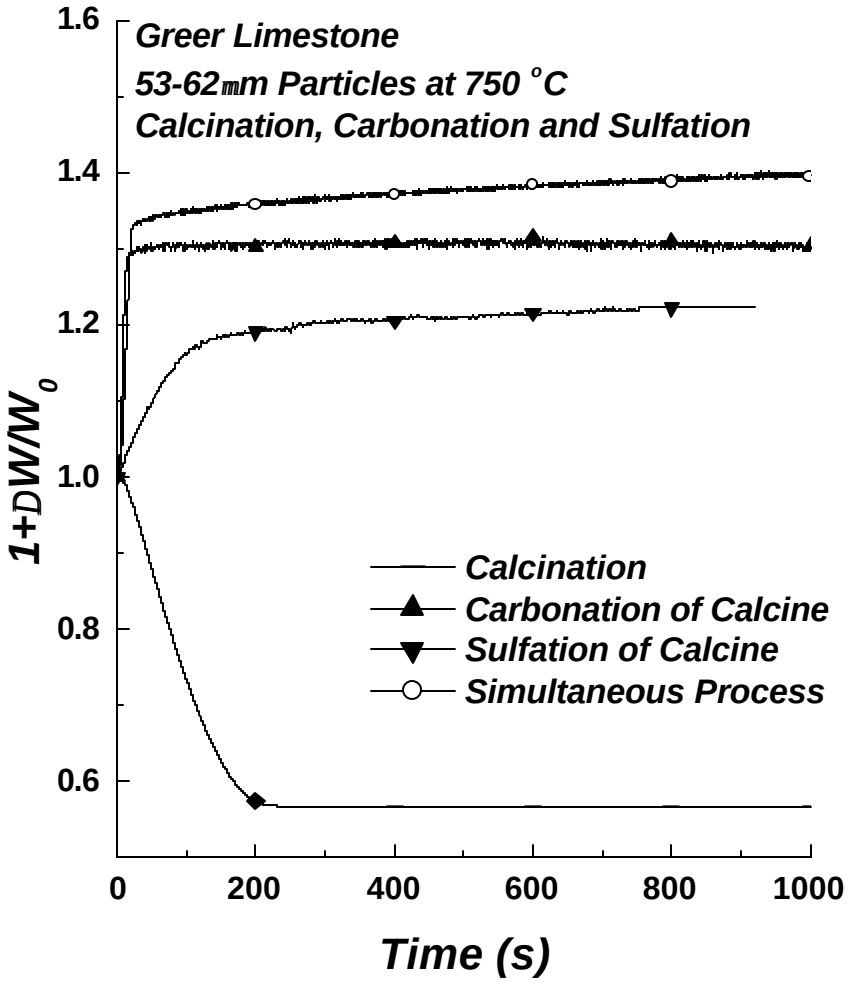

Figure 6.3. Variation of the conversion (weight of the solid sample) with time during calcination and subsequent carbonation, sulfation, or simultaneous carbonation and sulfation for 53-62 μm Greer Limestone particles at 750 °C.

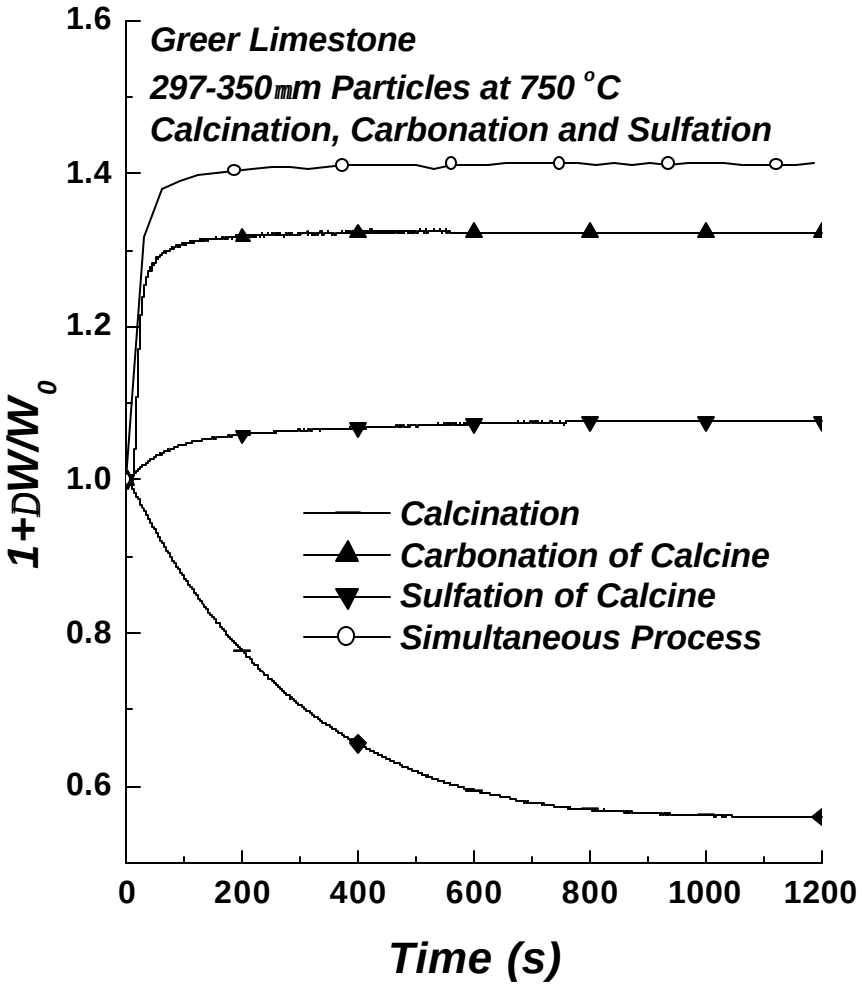

Figure 6.4. Variation of the conversion (weight of the solid sample) with time during calcination and subsequent carbonation, sulfation, or simultaneous carbonation and sulfation for 297-350 μm Greer Limestone particles at 750 °C.

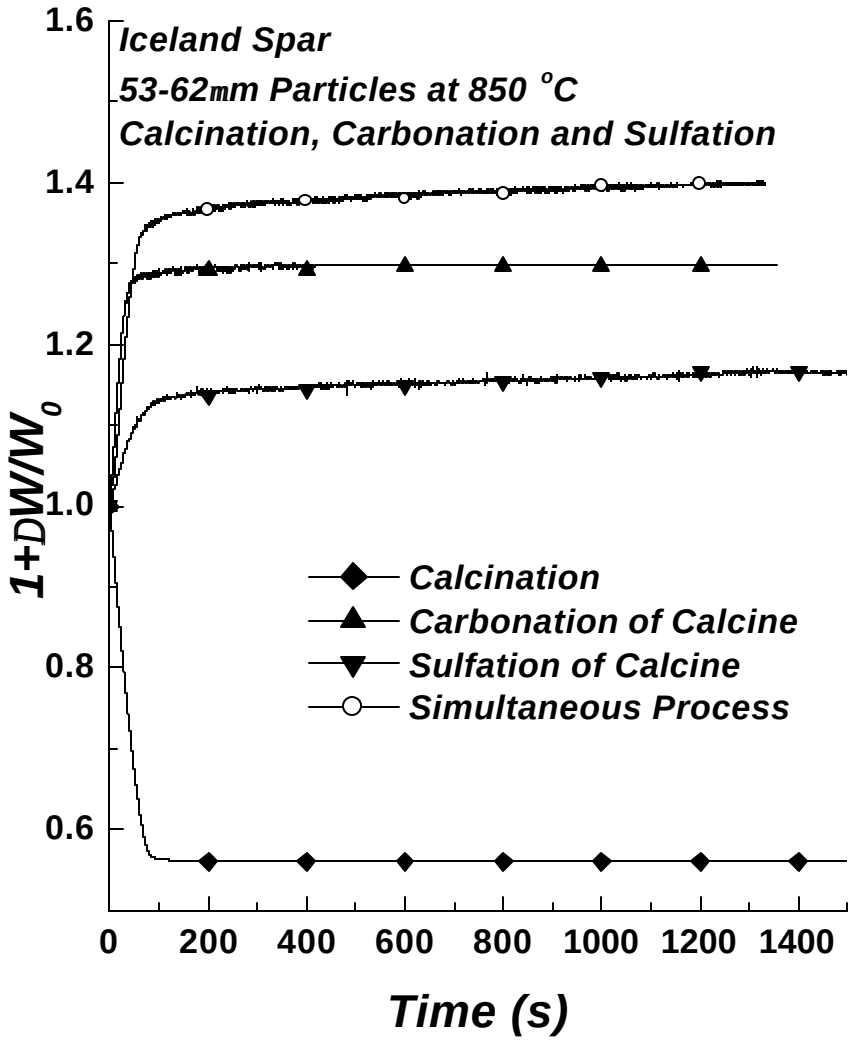

Figure 6.5. Variation of the conversion (weight of the solid sample) with time during calcination and subsequent carbonation, sulfation, or simultaneous carbonation and sulfation for 53-62 μm Iceland Spar particles at 850 °C.

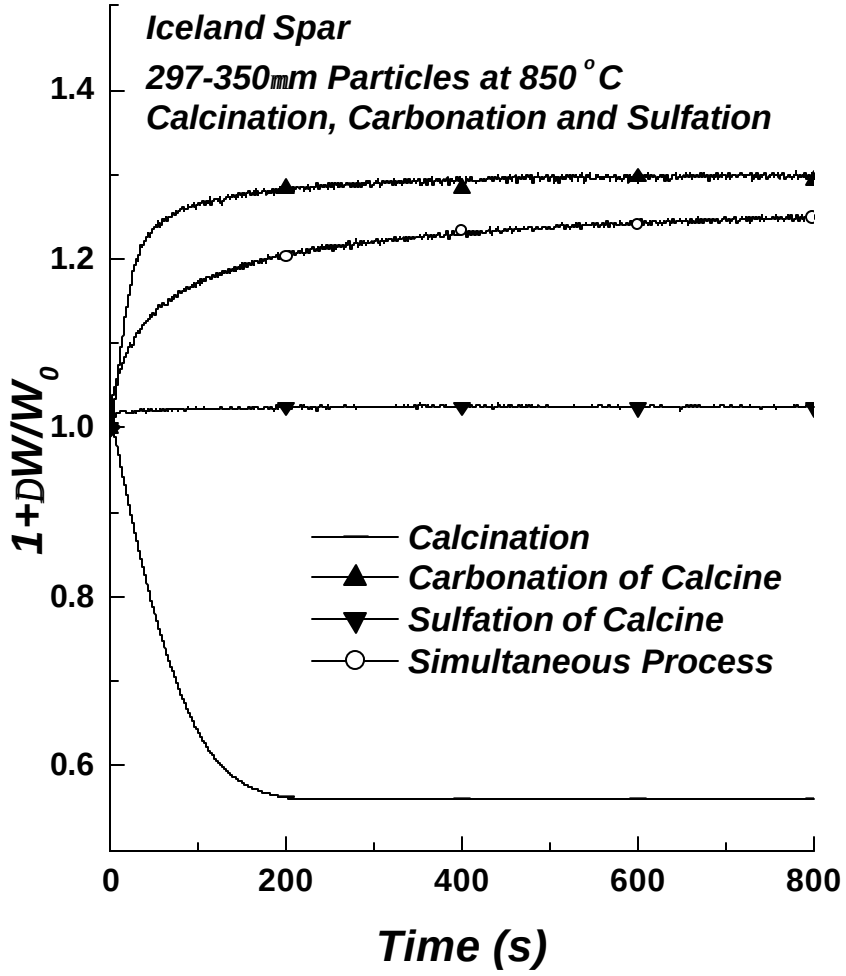

Figure 6.6. Variation of the conversion (weight of the solid sample) with time during calcination and subsequent carbonation, sulfation, or simultaneous carbonation and sulfation for 297-350 μm Iceland Spar particles at 850 °C.

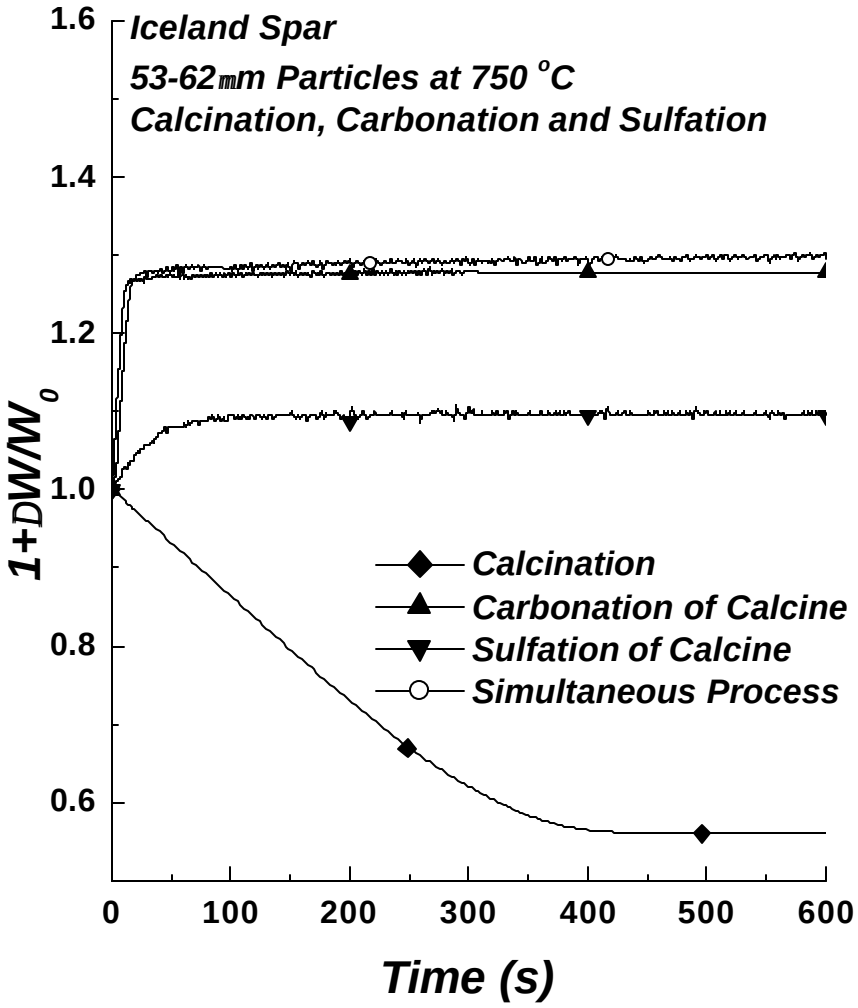

Figure 6.7. Variation of the conversion (weight of the solid sample) with time during calcination and subsequent carbonation, sulfation, or simultaneous carbonation and sulfation for 53-62 μm Iceland Spar particles at 750 °C.

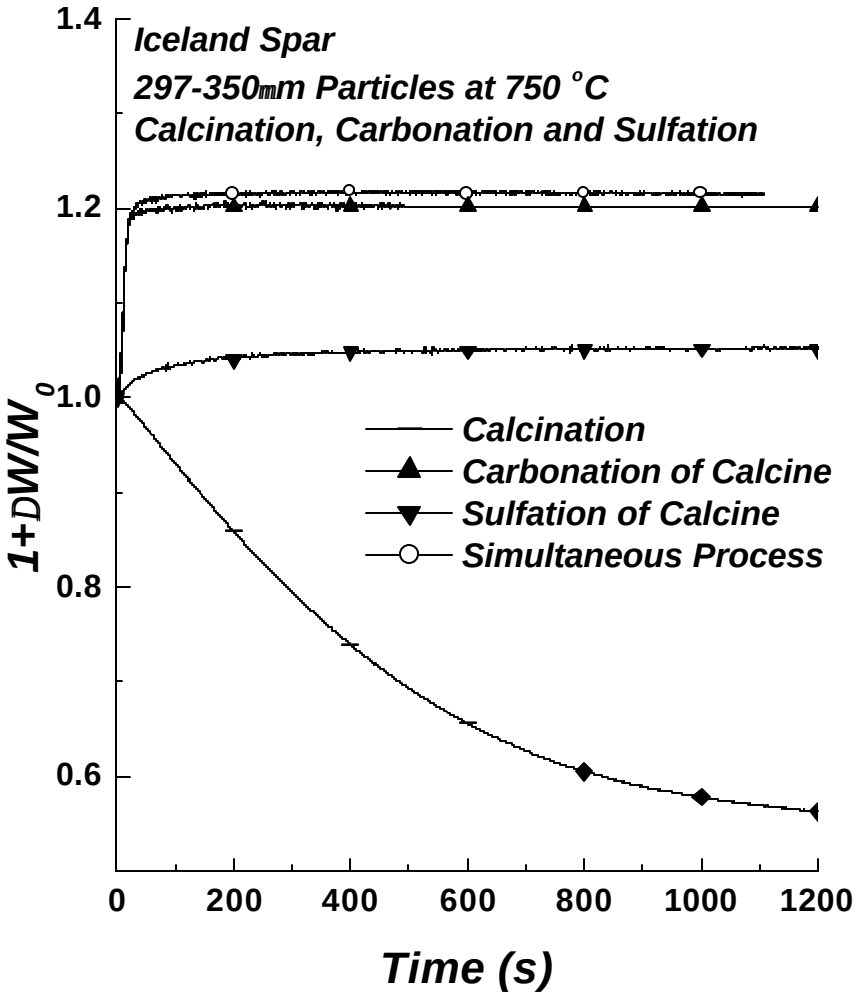

Figure 6.8. Variation of the conversion (weight of the solid sample) with time during calcination and subsequent carbonation, sulfation, or simultaneous carbonation and sulfation for 297-350 μm Iceland Spar particles at 750 °C.

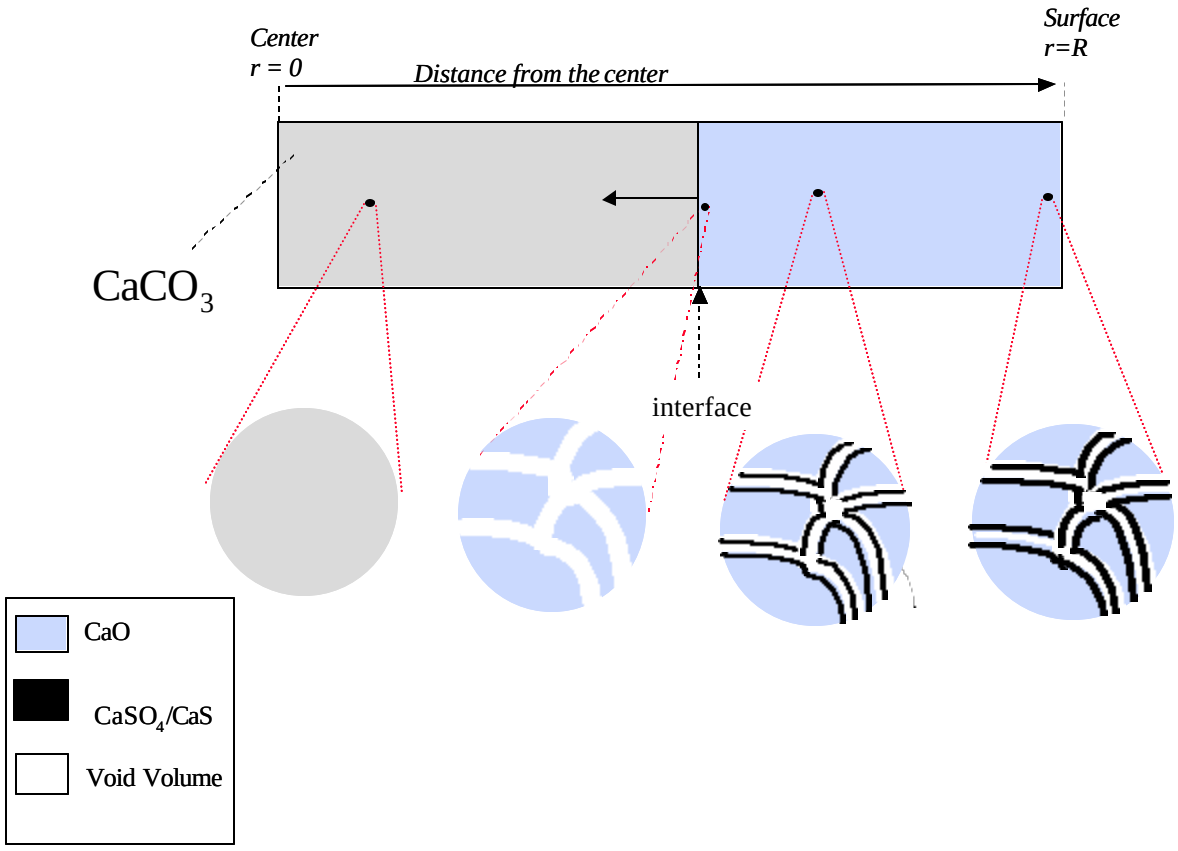

Figure 7.1. Schematic representation of the structure evolution of the solid during simultaneous calcination and sulfuration.